# MRI based Response Assessment and Diagnostics in Glioma

RENSKE GAHRMANN

# MRI based Response Assessment and Diagnostics in Glioma

RENSKE GAHRMANN

**Layout and Printing:** Optima Grafische Communicatie (www.ogc.nl)
**ISBN:** 978-94-6361-233-3

# MRI based response assessment and diagnostics in glioma

Verbetering van radiologische beoordeling van behandelrespons en andere uitdagingen in de beeldvorming van glioblastoma multiforme

Proefschrift

Ter verkrijging van de graad van doctor aan de
Erasmus Universiteit Rotterdam
op gezag van de
rector magnificus

Prof. Dr. R.C.M.E. Engels

en volgens het besluit van het College voor Promoties

de openbare verdediging zal plaatsvinden op
2 april 13:30
In het Erasmus MC, Queridozaal

**Renske Gahrmann**
Geboren te Leidschendam

**Erasmus University Rotterdam**

Erasmus

## PROMOTIECOMMISSIE

Promotoren:
Prof. Dr. M. Smits
Prof. Dr. M.J. van den Bent

Overige leden:
Prof. Dr. A. van der Lugt
Prof. Dr. A. Waldman
Dr. A.A. Jacobi-Postma

## TABLE OF CONTENTS

# Chapter 1

## General Introduction

## GLIOMAS

Gliomas are primary brain tumors in adults and are categorized by the World Health Organization (WHO) as grade I and II (low-grade gliomas), grade III (anaplastic) and IV (glioblastoma)[1]. Glioblastoma encompass 15% of all brain and central nervous system tumors and almost half of all primary brain tumors[2]. Astrocytoma and glioblastoma are categorized by the mutational status of the gene encoding for isocitrate dehydrogenase (*IDH*): *IDH*-mutant (*IDHmt*) and *IDH* wild-type (*IDHwt*). By definition, oligodendroglioma is both 1p19q codeleted and *IDHmt*[1]. While the exact diagnosis and tumor grade is determined by assessment of molecular markers and histology, Magnetic Resonance Imaging (MRI) can give information on the diagnosis as well. General features that can help predict glioma grade are presence or lack of contrast-enhancement and necrosis. More advanced measures such as Apparent Diffusion Coefficient (ADC) derived from Diffusion Weighted Imaging (DWI)[3,4] and regional cerebral blood volume (rCBV) from perfusion imaging can also have added value and are therefore often included in clinical glioma scanning protocols[5,6].

## MRI METHODS

MRI images are constructed by inducing alignment of hydrogen nuclei (protons) using a strong magnetic field (usually 1.5 or 3.0 tesla), after which the alignment is disturbed with a radiofrequency (RF) pulse. When the RF-pulse has ended, the protons realign themselves and emit signals while doing so. The exact location of every signal can be determined with the help of magnetic gradients and frequency encoding, which make sure that every voxel emits a slightly different signal. The signals are then processed to form an image.

The realignment signals are two-fold: there is the T1 signal (recovery of longitudinal relaxation) and the T2 signal (decay of transverse magnetization). The main MRI sequences are therefore T1-weighted and T2-weighted images. Differences in T1 and T2 relaxation times between different tissues allow distinction between tissues. Images can be reconstructed as well using more advanced techniques. For instance, when the water signal is nulled in a T2-weighted sequence, we are left with a T2-weighted FLuid Attenuation Inversion Recovery (FLAIR) image, which is a very useful image when looking at white matter abnormalities.

If a gadolinium-based contrast-agent is administered and a T1-weighted image is acquired, blood vessels and areas with a defective blood-brain-barrier (as is the case many tumors) enhance. Contrast-enhanced scanning can also be used for the evaluation of brain perfusion. There are several different methods to measure brain

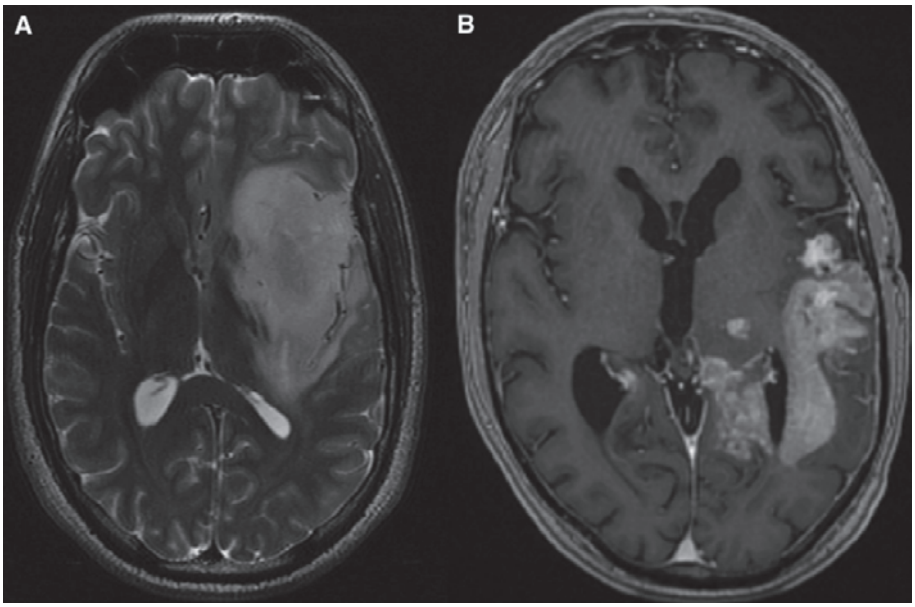


**Figure 1.** (**A**) Example of a low-grade glioma on a T2-weighted image. (**B**) Contrast enhancement of glioblastoma on a post-contrast T1-weighted image.

perfusion, and the method used in this thesis is Dynamic Susceptibility Contrast (DSC) MR perfusion, from which relative cerebral blood volume (rCBV) can be estimated. Examples of gliomas on structural imaging and perfusion imaging can be seen in ***figure 1*** and ***figure 2***.

Diffusion-weighted imaging (DWI) and diffusion tensor imaging (DTI) are MRI methods in which the degree of diffusion of water molecules within a voxel is measured. Certain tissues are more dense than others, affecting diffusion. Isotropic diffusion means that a water molecule can move freely in any direction, while anisotropic diffusion indicates one or more barriers preventing free diffusion. The anisotropy can also be used to determine the general direction of diffusion within a voxel and after linking voxels together, the general direction of white matter fibers can be determined[7].

Response assessment and follow-up of patients with brain tumors can include structural MRI (T1-weighted, T2-weighted and FLAIR images), advanced MRI (diffusion, perfusion and spectroscopy) and nuclear medicine imaging (Single-Photon Emission Computed Tomography or SPECT and Positron Emission Tomography or PET), and is described in more detail in ***chapter 3.1***.

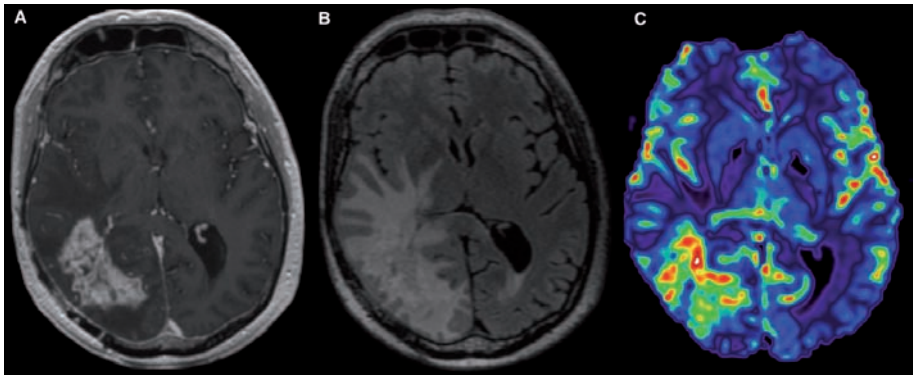


**Figure 2.** (**A**) Example of a recurrent glioblastoma with enhancement on the T1-weighted post-contrast image, (**B**) surrounding non-enhancing abnormalities on the FLAIR-image and (**C**) a DSC-perfusion-derived standardized and leakage-corrected rCBV map depicting increased rCBV in the enhancing tumor area.

## PRE-TREATMENT ASSESSMENT IN GLIOMAS

Before surgery, Diffusion Tensor Imaging (DTI) scans can be made for localization of important fiber tracts. Further post-processing of DTI-scans provides a variety of parameter maps, such as Mean Diffusivity (MD), Fractional Anisotropy (FA), pure isotropy (*p*) and anisotropy (*q*). The *p* and *q* maps have been used by Price et al.[8,9] to determine the extent of infiltrative growth of glioblastoma along white matter tracts in association with IDH-mutation status. In ***chapter 2***, Price's method is replicated and applied to non-enhancing gliomas (i.e. presumed low-grade) to see if it allows prediction of *IDH*-mutation status and 1p19q codeletion status in this specific patient group.

## POST-TREATMENT ASSESSMENT IN GLIOMAS

While ***chapter 2*** focuses on pre-treatment characteristics in non-enhancing gliomas, ***chapter 3*** focuses on response assessment after treatment. Treatment of glioma includes surgery, radiotherapy and chemotherapy at first diagnosis[10]. At recurrence, other and sometimes experimental treatment options are considered, including nitrosoureas, retreatment with temozolomide, and angiogenesis inhibitors. Tumors need a steady supply of nutrients and oxygen to grow. Normal blood vessels in the area of the tumor are insufficient to fulfill the demands of the tumor and so the tumor induces growth of new blood vessels: angiogenesis. Angiogenesis can be blocked by targeting endothelial cells directly or by inhibiting specific signal-mole-

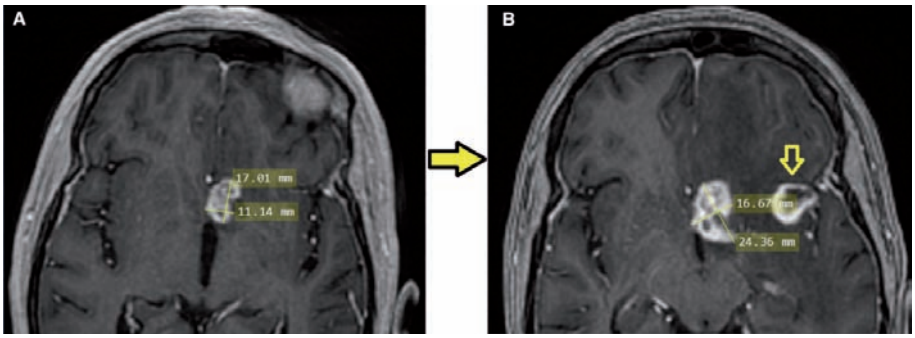


**Figure 3.** Example of 2D RANO measures in enhancing glioblastoma at baseline (**A**) and follow-up (**B**). There is progressive disease (PD) because the enhancing lesion has grown in size and a new enhancing lesion has appeared next to it.

cules released by the tumor. An important signal-molecule, produced in abundance by glioblastoma, is Vascular Endothelial Growth Factor (VEGF)[11]. The most commonly used angiogenesis inhibitor in glioblastoma is the VEGF- inhibitor bevacizumab (or Avastin®), which has been granted full approval by the United States Food and Drug Administration (FDA) in 2017 for second-line treatment in recurrent glioblastoma[12]. Bevacizumab is often given in combination with a chemotherapeutic agent.

Whether a recurrent glioblastoma is responding to treatment is based on MRI and clinical features. The Response Assessment in Neuro-Oncology (RANO) criteria include 2D measurements of enhancing tumor and an estimation of change in non-enhancing abnormalities. Additionally, the appearance of new lesions, steroid use and clinical status are taken into account[13] (see ***Figure 3***). There are two main problems when it comes to response assessment: 1) pseudo-response, and 2) pseudo-progression. Pseudo-progression is an increase in enhancement on the T1-weighted post-contrast scan caused by prior radiotherapy. It mimics actual tumor growth, while in fact is reflects radionecrosis. In ***chapter 3.1***, imaging of pseudo-progression is described in detail.

Pseudo-response is seen after treatment with angiogenesis inhibitors and describes the decrease in enhancement of the tumor and also a decrease in non-enhancing abnormalities without an actual decrease in tumor size. As the effect of pseudo-response is seen early after start of treatment, early radiological treatment response assessment can be a challenge. Early assessment is important because it provides valuable information on whether the tumor is responding to treatment or not. If a treatment is ineffective, there is no reason to continue, especially in the light of potential serious side effects. A different treatment might be considered in some patients. Additionally, radiological measures can provide information on the patient's prognosis. Measuring this early treatment response with the 2D RANO criteria in

those with pseudo-response is suboptimal at best and therefore we evaluated a variety of different methods for determining treatment response in this patient group.

It has been argued that volumetric measures are an improvement over 2D measures, especially in glioblastoma, because these heterogeneous tumors with asymmetrical growth could be measured more reliably with a volumetric approach, and also because semi-automated volumetric tumor segmentation was shown to have lower intra- and interrater variability than manual measures[14,15]. In ***chapter 3.2***, the 2D RANO criteria were compared with volumetric measures in recurrent glioblastoma treated with classical chemotherapy and/or bevacizumab. Change in tumor volume was measured between baseline (before treatment) and first/second follow-up. In ***chapter 3.3***, the quantitative approach to this volumetric response assessment is explored.

Measures other than tumor size might provide more information on treatment response (or lack thereof) in those treated with bevacizumab. Previous studies have shown that low values of Apparent Diffusion Coefficient (ADC) derived from DWI at baseline and after treatment (i.e. diffusion restriction) may be predictive for survival[16,17]. Studies that look at perfusion imaging derived, relative Cerebral Blood Volume (rCBV) find that an increase in rCBV from pre- to post-treatment decreases survival, while a decrease improves survival[18]. Early changes in diffusion after therapy in recurrent glioblastoma are discussed in ***chapter 3.4***.

## REFERENCES


1. Louis DN, Perry A, Reifenberger G, et al. The 2016 World Health Organization classification of tumors of the central nervous system: a summary. Acta Neuropathol 2016;131(6):803-820.
2. Ostrom QTG, Gittleman H, Fulop J, et al. CBTRUS statistical report: primary brain and central nervous system tumors diagnosed in the United States in 2008-2012. Neuro Oncol. 2015;17(suppl 4):iv1-iv62.
3. Kono K, Inoue Y, Nakayama K, et al. The role of diffusion-weighted imaging in patients with brain tumors. AJNR Am J Neuroradiol 2001;22(6):1081-1088.
4. Stadnik TW, Chaskis C, Michotte A, et al. Diffusion-weighted MR imaging of intracerebral masses: comparison with conventional MR imaging and histologic findings. AJNR Am J Neuroradiol 2001; 22(5):969-976.
5. Law M, Yang S, Wang H, et al. Glioma grading: sensitivity, specificity, and predictive values of perfusion MR imaging and proton MR spectroscopic imaging compared with conventional MR imaging. AJNR Am J Neuroradiol 2003;24(10):1989-1998.
6. Hakyemez B, Erdogan C, Ercan I, Ergin N, Uysal S, Atahan S. High-grade and low-grade gliomas: differentiation by using perfusion MR imaging. Clinical Radiology 2005;60(4):493-502.
7. Yousem DM, Grossman RI, (2010). 'Techniques in neuroimaging' in The requisites neuroradiology 3rd edition, Philadelphia, Mosby Inc, an affiliate of Elsevier Inc. p.4-11.
8. Price SJ, Allinson K, Liu H, et al. Less invasive phenotype found in isocitrate dehydrogenase-mutated glioblastomas than in isocitrate dehydrogenase wild-type glioblastomas: a diffusion-tensor imaging study. Radiology 2017;283(1):215-221.
9. Mohsen LA, Shi V, Jena R, Gillard JH, Price SJ. Diffusion tensor invasive phenotypes can predict progression-free survival in glioblastomas. Br J Neurosurg 2013;27(4):436-441.
10. Stupp RH, Hegi ME, Mason WP, et al. Effects of radiotherapy with concomitant and adjuvant temozolomide versus radiotherapy alone on survival in glioblastoma in a randomized phase III study: 5-year analysis of the EORTC-NCIC trial. Lancet Oncol. 2009;10(5):459-466.
11. El-Kenawi AE, El-Remessy AB. Angiogenesis inhibitors in cancer therapy: a mechanistic perspective on classification and treatment rationales. Br J Pharmacol 2013;170(4):712-729.
12. FDA Grants Genentech's Avastin Full Approval for Most Aggressive Form of Brain Cancer. Genentech. Accessed December 5, 2017. https://www.gene.com/media/press-releases/14695/2017-12-05/fda-grants-genentechs-avastin-full-appro.
13. Wen PY, Macdonald DR, Reardon DA, et al. Updated response assessment criteria for high-grade gliomas: response assessment in neuro-oncology working group. J Clin Oncol. 2010;28(11):1963-1972.
14. Chow DS, Qi J, Miloushev VZ, et al. Semiautomated volumetric measurement on postcontrast MR imaging for analysis of recurrent and residual disease in glioblastoma multiforme. AJNR Am J Neuroradiol 2014;35(3):498-503.
15. Sorensen AG, Patel S, Harmath C, et al. Comparison of diameter and perimeter methods for tumor volume calculation. J Clin Oncol 2001;19(2):551-557.
16. Rieger J, Bähr O, Müller K, Franz K, Steinbach J, Hattingen E. Bevacizumab-induced diffusion-restricted lesions in malignant glioma patients. J Neurooncol 2010;99(1):49-56.
17. Pope WB, Kim HJ, Huo J, et al. Recurrent glioblastoma multiforme: ADC histogram analysis predicts response to bevacizumab treatment. Radiology 2009;252(1):182-189.
18. Schmainda KM, Prah M, Connely J, et al. Dynamic-susceptibility contrast agent MRI measures of relative cerebral blood volume predict response to bevacizumab in recurrent high-grade glioma. Neuro Oncol 2014;16(6):880-888.

# Chapter 2

## Growth patterns of non-enhancing glioma assessed on DTI-derived isotropic and anisotropic maps are not associated with IDH mutation or 1p19q codeletion status

Renske Gahrmann
Jochem Spoor
Maarten Wijnenga
Sieger Leenstra
Arnaud Vincent
Marius de Groot
Pim French
Martin van den Bent
Marion Smits

SUBMITTED

## ABSTRACT

Background. Extent of mismatch between tumor delineations drawn on Diffusion Tensor Imaging (DTI) derived isotropic (*p*) and anisotropic (*q*) maps have been shown to distinguish isocitrate dehydrogenase (*IDH*) *wild-type* (*wt*) and *mutated* (*mt*) glioblastomas. We use this technique in non-enhancing gliomas to determine if an assessment of *IDH*-mutation as well as 1p19q codeletion status can be made.

Methods. All patients undergoing presurgical DTI for non-enhancing glioma between 2004 and 2013 from a single center were included (n=83). A targeted Next-Generation Sequencing panel (NGS) was used to determine the presence of *IDHmt* and 1p19q codeletion. A volume of interest (VOI) was drawn on the *p*-map and subsequently overlaid on the *q*-map to determine overlap with white matter tracts (>0.5cm) by 2 observers. Extent and pattern of mismatch was scored as: I) no indication of infiltration (i.e. no *p/q* mismatch), II) single focus of infiltration, III) multifocal infiltration, IV) expansion of lesion into white matter tracts, and V) infiltration following white matter tracts. Different patterns found in *IDHmt* versus *IDHwt* and 1p19q codeleted versus non-codeleted tumors were compared with a Mann-Whitney U test. Cohen's Kappa was calculated to assess interobserver agreement.

Results. Four of the non-enhancing gliomas were *IDHwt*, 29 were both *IDHmt* and 1p19q codeleted, and 50 *IDHmt* without 1p19q codeletion. The 4 *IDHwt* gliomas all had a different pattern of infiltrative growth (i.e. patterns II, III, IV, and V). These same patterns were also seen in the *IDHmt* glioma group. No significant differences between codeleted and non-codeleted tumors were found (Mann-Whitney U=714.0, p=.908). The interobserver agreement was moderate with a Kappa of 0.473 (SE=0.068) or 62.7%.

Conclusion. Because of overlap in growth patterns between *IDHwt* versus *IDHmt* and 1p19q codeleted versus non-codeleted gliomas and the suboptimal interobserver concordance, this DTI-derived technique does not allow for the distinction of possible different molecular subtypes in non-enhancing gliomas.

## Advances in knowledge

- Patterns of mismatch between DTI-derived isotropic and anisotropic maps do not predict *IDH*-mutation or 1p19q codeletion status in non-enhancing gliomas.
- While successfully applied in glioblastoma, this technique has moderate inter-rater agreement when used for assessment of non-enhancing glioma growth patterns.

## Implications for patient care

- Possible differences in growth pattern between non-enhancing glioma molecular subtypes could not be distinguished using *p/q* mapping and so we currently do not recommend using this technique for non-enhancing gliomas in a clinical setting.

## Summary statement

Previous research indicates that different molecular subtypes of glioblastoma (i.e. *IDH*-mutated versus *IDH* wild-type) can be discerned based on the extent/pattern of mismatch assessed on isotropic and anisotropic diffusion maps. Using this same technique in non-enhancing glioma, we found no differences in growth pattern between *IDH*-mutated versus *IDH* wild-type and 1p19q codeleted versus non-codeleted tumors.

## INTRODUCTION

The 2016 update of the WHO classification for central nervous system tumors presents a major change in the classification of gliomas: not only histological, but also molecular features now characterize different types of gliomas. The WHO 2016 classification distinguishes between two types of astrocytoma based on the mutational status of the gene encoding for isocitrate dehydrogenase (*IDH*) 1 or 2: *IDH*-mutant (*IDHmt*) and *IDH* wild-type (*IDHwt*) astrocytoma. Oligodendroglioma are characterized by the presence of a codeletion of chromosomal arms 1p and 19q and an *IDH1/2* mutation[1]. The incidence of *IDH* mutation in grade II and III gliomas (according to the WHO 2007 classification) is 60-80%, leaving a subset of lower-grade glioma to be *IDHwt*[2]. Many of these *IDHwt* tumors with grade II or III histological features present without enhancement on imaging. The prognosis of these patients is poor compared to that of patients with *IDHmt* gliomas especially in the presence of a TERT promotor mutation[3].

*IDHmt* gliomas with a 1p19q codeletion (oligodendrogliomas) have a better prognosis than those without a codeletion (astrocytoma, *IDHmt*). A non-invasive identification of the different molecular subtypes of non-enhancing gliomas can help discern a subgroup of more aggressive tumors from the more indolent ones. Not only will this lead to a more accurate prediction of molecular subtypes, but it may also aid in guiding treatment decisions.

The presence of enhancement is generally considered a sign of aggressiveness, however in its absence, other characteristics, such as growth patterns could be informative. Differences in glioma growth between subtypes of non-enhancing tumors (oligodendroglioma and *IDHmt* or *IDHwt* astrocytoma) have not been extensively explored. Infiltrative growth has been reported in both astrocytoma and oligodendroglioma, although in oligodendrogliomas areas with more compact infiltration can also be present[4]. Glioma infiltration occurs along perineuronal structures (also known as perineuronal satellitosis), subpial, and perivascular structures, as well as along white matter fibers. In extreme cases, the tumor infiltrates throughout the brain resulting in a gliomatosis cerebri pattern seen on imaging[5].

While displacement or destruction of white matter tracts is fairly easy to determine, infiltration of a tract is more difficult to assess[6]. With Diffusion Tensor Imaging (DTI) the microstructural properties of different tissues can be determined by measuring diffusion of water molecules. When water molecules are restricted in their diffusion, such as in the presence of white matter tracts, this is reflected in DTI-derived parameters of anisotropy ($q$) and isotropy ($p$)[7]. The use of $q$ eliminates the possible confounding effect of changes in the overall diffusion, as is the case when measuring the fractional anisotropy (FA). Combining anisotropic measures with isotropic

measures, such as Mean Diffusivity (MD), Apparent Diffusion Coefficient (ADC), and pure isotropy (*p*) can help determine tumor infiltration along white matter tracts. In enhancing/high-grade tumor it has been shown that in biopsy-proven areas of infiltration, *p* is abnormally high, while *q* is within a normal range[8-10]. The mismatch between *p* and *q* has been used by Price et al. to determine the extent of infiltrative growth along white matter tracts in *IDHmt* and *IDHwt* glioblastoma[11,12]. In IDHmt (and 8% of *IDHwt*) glioblastoma, a minimally invasive pattern was found, while in IDHwt glioblastoma, a locally invasive or diffusely invasive pattern was encountered[10]. These findings led us to apply this technique in the group of patients with presumed low-grade gliomas (i.e. non-enhancing tumors without necrosis).

We hypothesize that assessing the 'mismatch' between *p* and *q* could help visualize different growth patterns in non-enhancing gliomas and as such differentiate non-invasively between the molecularly defined glioma subtypes similar to previous findings in glioblastoma.

## METHODS

### Patients

Adult patients with suspected low-grade glioma (i.e. without enhancement and necrosis) that had undergone presurgical functional MRI (fMRI) and DTI between December 2004 and June 2014 in the Erasmus MC in Rotterdam (NL) were considered for retrospective analysis. Approximately 125 patients with suspected low-grade glioma were operated in this timeframe, 90 of whom had undergone presurgical DTI in preparation of awake-surgery. Targeted Next-Generation Sequencing panel (NGS) was performed on the archival tumor tissue to determine presence of *IDH1*- and *IDH2*-mutations and 1p19q codeletion and other molecular lesions characteristic of glioblastoma[13]. The institutional review board approved of the design of the study. Previously, Wijnenga et al.[3] reported on 65 of the 90 patients included in our study focusing on pre- and postoperative tumor volumes in relation to molecular information; DTI-data was not included in this prior analysis.

Tumors were categorized according to the presence or absence of an *IDH*-mutation (*IDHmt* respectively *IDHwt*) and 1p19q codeletion according to the WHO 2016 classification[1]. Patients with partial imbalance or loss of only one chromosomal arm were categorized as non-codeleted. Overall Survival (OS) was defined in years from the date of the preoperative DTI-scan until death.

## Data acquisition and processing

All scanning was performed at 1.5 or 3.0 tesla field strength (GE Healthcare, Milwaukee, IL, USA) with a matrix of 256x256 and an in-plane resolution of less than 1mm$^2$. All data were acquired with a minimum of 25 directions (all with b=1000 s/mm$^2$) and 1-4 b=0 s/mm$^2$ images. For more details see ***Supplementary Files table S1***.

DICOM files were converted to NIfTI format for processing in FSL (Oxford, UK)[14]. Images were reoriented and corrected for eddy currents using the b=0 s/mm$^2$ image as a reference. The brain was extracted using BET (Brain Extraction Tool)[15] with a threshold of 0.3. FSL-DTIFit was used to extract the eigenvectors, eigenvalues and mean diffusivity, which were then used to create a pure isotropic map (*p*) and an anisotropic map (*q*) with a custom script using FSLmaths according to equations from Price et al.[16]:

$$p = \sqrt{3D}$$

$$q = \sqrt{(\lambda_1 - D)^2 + (\lambda_2 - D)^2 + (\lambda_3 - D)^2}$$

Where *D* is the mean diffusivity and λ the eigenvalues:

$$D = (\lambda_1 + \lambda_2 + \lambda_3)/3$$

## Data analysis

A volume of interest (VOI) of the tumor area was drawn manually by one observer on the *p*-map using MRIcron (Chris Rorden, www.mricro.com, version 6.6.2013). Clearly recognizable blood vessels were excluded.

We overlaid the VOI from the *p*-map on the *q*-map to visually determine overlap with white matter tracts (i.e. high-intensity areas on the *q*-map). A VOI exceeding >0.5cm in three directions over such high intensity areas was considered to be a *p/q*-mismatch, indicating infiltration of the white matter tract[8] (***Figure 1***). The *p/q* mismatch was categorized by two independent observers (i.e. an experienced neuroradiologist and a radiology resident) as follows: I) no indication of infiltration (i.e. no *p/q* mismatch), II) single focus of infiltration, III) multifocal infiltration, IV) expansion of lesion into white matter tracts, and V) infiltration following white matter tracts (***Figure 2***). A combination of options was allowed. Both observers were blinded for histological and molecular tumor status. Interobserver agreement was determined by calculating Cohen's Kappa Coefficient. In case of discrepancy, the maps were reviewed again by the two observers together to assign the category in consensus, which was then used for further analyses. The difference in incidence within each *p/q* mismatch category between molecular tumor categories was compared using a Mann-Whitney U test.

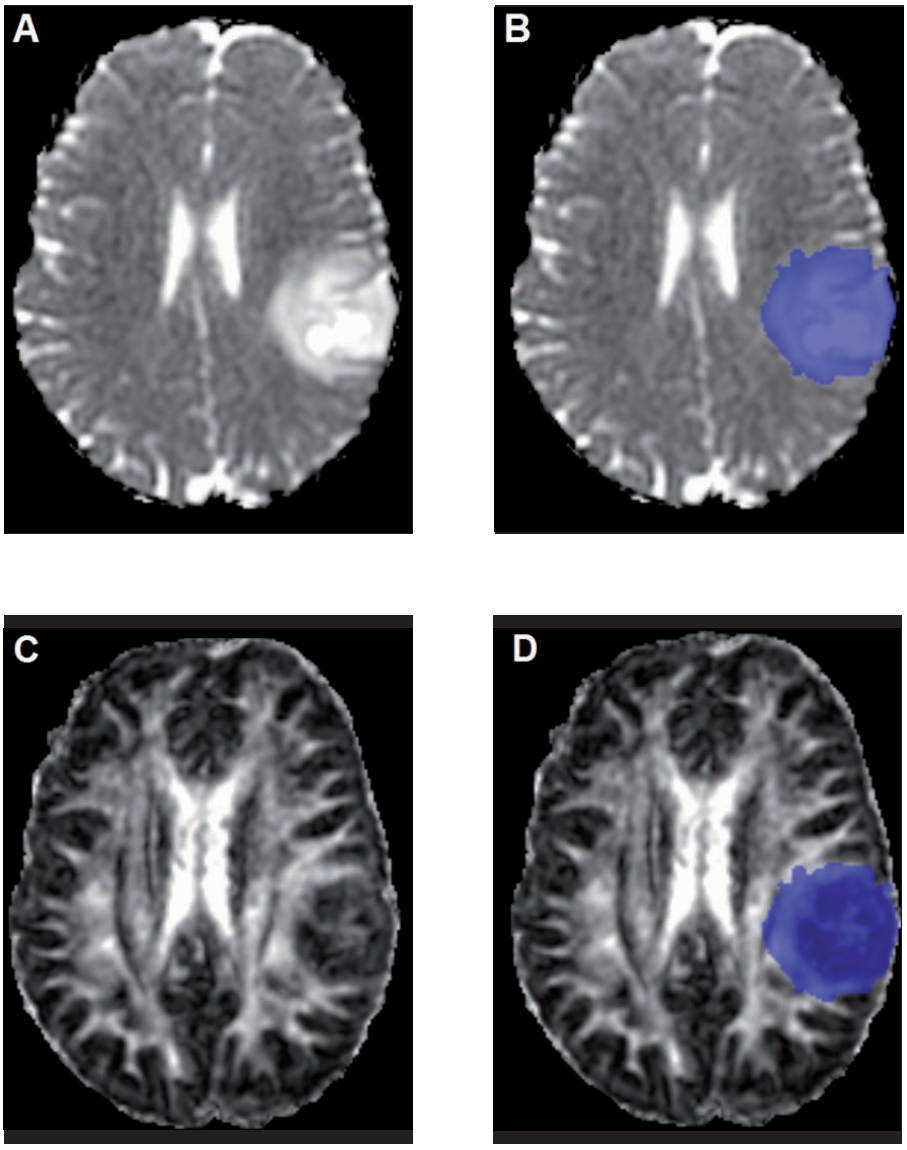


**Figure 1.** Example of a non-enhancing tumor with a peripheral localization, clearly visible on the *p*-map (**A**). Tumor segmentation was performed on the *p*-map (**B**) and subsequently overlaid on the *q*-map (**C**, **D**). An additional line drawn on image **D** shows the location of mismatch. This example was classified as 'expansion of lesion into white matter tracts'.

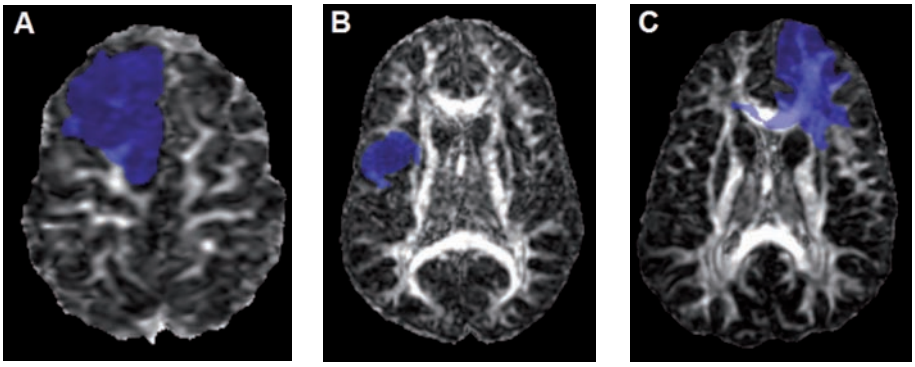


**Figure 2.** Examples of different *p/q* mismatch patterns: 'single focus of infiltration' (**A**), 'multifocal infiltration' (**B**), and 'infiltration following white matter tracts' (**C**). Additional lines have been drawn to show the location of mismatch.

## RESULTS

### Patients

In 7 patients NGS could not be performed since there was no tumor tissue available. The final analysis was performed on the remaining 83 patients (49 men and 34 women). Mean and median age was 39 years (range, 20 to 72 years). At the time of analysis, 29 patients had died with a median OS of 4.2 years (range, 0.9 to 9.2 years). Four (13.8%) of these patients had a 1p19q codeleted tumor.

Tumors were located in the frontal lobe in 41 (49.4%), the insula in 17 (20.5%), temporal lobe in 9 (10.8%), and parietal lobe in 4 (4.8%) patients. The remaining tumors were located in both the frontal and parietal lobes in 5 (6.0%), the parietal and temporal lobes in 5 (6.0%), and in more than 2 lobes in 2 (2.4%) patients. There was a left hemispheric predominance, with 69.9% (n=58) of tumors located in the left hemisphere.

### Molecular data

In 79 of 83 patients, an *IDH1* or *IDH2* mutation was found with the main subtype *IDH-R132H* found in 66 patients. Other subtypes found were *R132C* (n=4), R132G (n=3), *IDH1-R132S* (n=2), *IDH2-R172K* (n=3), and *IDH2-R172M* (n=1). Four patients with an *IDHwt* tumor were deceased at the time of analysis with a median OS of 2.0 years (range, 2.5 to 4.2 years). In the *IDHmt* tumor group, 25 (31.6%) patients had died with a median OS of 4.4 years (range, 0.9 to 9.2 years). Additional molecular information in the 4 *IDHwt* patients revealed TERT mutations (all 4), imbalance or loss of chromosome 7 and 10 (including PTEN; 3 patients), and EGFR amplification (2 patients), all corresponding with glioblastoma[13].

In the 79 *IDHmt* tumors, 29 (34.9%) were 1p19q codeleted, while 50 tumors were non-codeleted. The 2 tumors growing in more than 2 lobes were both *IDHmt* without a 1p19q codeletion.

## p/q assessment

A discrepancy between the initial ratings by the 2 observers was present in 31 (37.3%) cases. In the discrepant cases, consensus was reached by agreeing with observer 1 in 11 cases and with observer 2 in 14 cases. In the remaining 6 cases a new category was assigned. All final ratings are shown in ***Table 1***. The interobserver agreement was moderate with Kappa=0.473 (SE=0.068).

**Table 1.** Incidence of *p/q* mismatch categories (final assessment by 2 observers in consensus) in molecularly defined glioma subtypes. WM=white matter.

| p/q mismatch category | IDHmt (n=79) | IDHwt (n=4) | 1p19q codeleted (n=29) | 1p19q non-codeleted (n=50) |
|---|---|---|---|---|
| **I** No indication of infiltration | 2 (2.5%) | | - | 2 (4%) |
| **II** Single focus of infiltration | 4 (5.1%) | 1 (25%) | 1 (3.4%) | 3 (6%) |
| **III** Multifocal infiltration | 23 (29.1%) | 1 (25%) | 10 (34.5%) | 13 (26%) |
| **IV** Expansion of lesion into WM tracts | 25 (31.6%) | 1 (25%) | 9 (31%) | 16 (32%) |
| **V** Infiltration following WM tracts | 20 (25.3%) | 1 (25%) | 7 (24.1%) | 13 (26%) |
| **III** and **IV** | 3 (3.8%) | - | - | 3 (6%) |
| **IV** and **V** | 2 (2.5%) | - | 2 (6.9%) | - |

The predominant *p/q* mismatch categories in the *IDHmt* group were III) multifocal infiltration (29.1%), IV) expansion of lesion into white matter tracts (31.6%), and V) infiltration following white matter tracts (25.3%). The 4 patients with *IDHwt* tumor each showed a different category of *p/q* mismatch, i.e. II) single focus of infiltration, III) multifocal infiltration, IV) expansion of lesion into white matter tracts, and V) infiltration following white matter tracts, rendering these 4 *IDHwt* tumors indistinguishable from the *IDHmt* tumors.

In the 1p19q codeleted group (n=29) and non-codeleted group (n=50), the main *p/q* mismatch categories were III (34.5% respectively 26.0%), IV (31.0% respectively 32.0%), and V (24.1% respectively 26.0%). No significant difference in the incidence of *p/q* mismatch categories was found between these two groups: Mann-Whitney U=714.0, p=.91.

## DISCUSSION

Our study showed that the major groups of molecularly defined glioma subtypes (oligodendroglioma and *IDHmt* or *IDHwt* astrocytoma) in non-enhancing gliomas cannot be discerned based on infiltrative growth pattern assessed on DTI-derived isotropic and anisotropic maps. The 4 *IDHwt* tumors each showed a different pattern of tumor growth, while no differences in the various growth patterns between 1p19q codeleted and non-codeleted tumors were observed.

Glioma growth can lead to destruction, infiltration, edema or displacement of white matter tracts[6,17]. Destruction and tract displacement are easily recognized. A displaced tract can still be intact despite being compressed (sometimes increasing anisotropic values)[18]. Infiltration and edema of white matter tracts are more difficult to assess, as in both we see an increase in isotropic and a variable decrease in anisotropic values. In infiltrated white matter tracts the anisotropy is dependent on the amount of tumor infiltration and the degree to which the tracts are intact[18]. Different models looking at glioma growth find that anisotropic parameters are more suited to assess tumor infiltration than isotropic parameters[19-22].

Anisotropic values (*q* or FA), however, need to be looked at in context with isotropic values (*p* or MD or ADC). In the gross tumor, *p* or MD is increased and *q* or FA is reduced compared to normal tissue. But regions surrounding the tumor (high T2w signal) can consist of edema and/or infiltrating tumor, leading to abnormally high *p* or MD values, while *q* or FA values may be within normal range[8,9,23]. This mismatch between *p* and *q* has successfully been used to describe different infiltrative patterns in *IDHmt* and *IDHwt* glioblastoma by Price et al. They describe three different patterns of infiltration: a minimally invasive pattern, which is seen in all *IDHmt* and in 8% of *IDHwt* glioblastomas, a locally invasive pattern, and a diffusely invasive pattern seen in 23% and 69% of *IDHwt* glioblastomas respectively[10-12]. We used a slightly adapted categorization of these mismatch patterns to better capture the different growth patterns we encountered in non-enhancing gliomas. Categories I and II ('no indication of infiltration' and 'single focus of infiltration') are similar to Price et al.'s 'minimally invasive' pattern. In patients with more extensive white matter tract infiltration, however, we found both tumors that clearly followed white matter tracts and tumors that expanded into a large section of the tract. This distinction was felt not to be captured by simply categorizing both growth patterns as 'diffusely invasive', and thus further specified in our categorization.

Based on Price et al.'s findings in glioblastoma, we expected the non-enhancing *IDHwt* tumors (even if only present in 4 patients) to predominantly expand into or to infiltrate along white matter tracts and *IDHmt* tumors to express a less invasive growth pattern. Instead, we found that each of the 4 *IDHwt* tumors had a different

pattern of growth, ranging from minimally invasive (single focus of infiltration) to infiltration along white matter tracts. These same patterns were found in the *IDHmt* group. We were therefore unable to identify the *IDHwt* tumors based on their growth patterns as assessed with *p/q* mapping. Similarly, we were unable to distinguish 1p19q codeleted from non-codeleted tumors with this technique. Possible explanations for the lack of 'positive' findings are first that growth patterns between these molecular subtypes are in fact not significantly different, and second that potentially existing differences cannot be distinguished with *p/q* mapping.

Very little is known about growth patterns of non-enhancing glioma molecularly defined subtypes. Both codeleted (oligodendroglioma) and non-codeleted (astrocytoma) gliomas are known to infiltrate along white matter tracts, but this seems to be more common in astrocytoma[24,25]. It should be noted that these previous studies included both enhancing and non-enhancing tumors. While based on these studies on 1p19q codeletion and the study by Price et al. on *IDH*-mutation status in glioblastoma[10] differences in growth pattern between molecularly defined glioma subtypes are conceivable, it is possible that these findings can not be translated to the non-enhancing, lower grade (II/III) tumors and that in these tumors no significant differences in growth pattern are in fact present.

Alternatively, our 'negative' results may be related to the *p/q* mapping technique. We found that determining growth patterns in small and peripherally located tumors was problematic: in the peripheral, smaller tracts, the threshold for *p/q* mismatch of 0.5cm[10] was difficult to apply, because the lower anisotropy in the peripheral tracts hindered assessment of further reduction in anisotropy due to tumor infiltration. This likely contributed to the low agreement between the observers (62.7%). Price et al. reported an interobserver agreement of 90% (26), a difference that can be explained the study population (glioblastoma versus non-enhancing glioma) as well as the different number of categories (3 versus 5 categories).

The retrospective nature of this study introduced a selection bias towards patients who were eligible for awake-surgery, because preoperative DTI is only performed for these surgeries at our institution. These patients are generally in a better condition and of a younger age than those not selected for awake surgery and more often have a tumor located in the left hemisphere (for preservation of language function). This selection bias may also have resulted in the low number of only 4 *IDHwt* gliomas, since patients with *IDHwt* tumors tend to be older and thus less eligible for awake surgery. We furthermore only included non-enhancing gliomas, in which *IDHwt* is likely to be less frequent than in enhancing tumors. Despite this low number, it was clear that each of the *IDHwt* gliomas showed a different growth pattern that overlapped with patterns seen in *IDHmt* tumors. Our conclusion that *p/q* mapping in these patients does not distinguish between *IDHwt* and *IDHmt* thus remains valid.

In conclusion, we were unable to translate previous findings from glioblastoma, showing that *p/q* mapping can be used to discern different molecular subtypes, to non-enhancing glioma. Based on our findings, we do not recommend using this technique to determine molecular status in non-enhancing glioma.

## REFERENCES


1. Louis DN, Perry A, Reifenberger G, et al. The 2016 World Health Organization classification of tumors of the central nervous system: a summary. Acta Neuropathol 2016;131(6):803-820.
2. Hartmann C, Meyer J, Balss J, et al. Type and frequency of IDH1 and IDH2 mutations are related to astrocytic and oligodendroglial differentiation and age: a study of 1,010 diffuse gliomas. Acta Neuropathol 2009;118(4):469-474.
3. Wijnenga MMJ, French PJ, Dubbink HJ, et al. The impact of surgery in molecularly defined low-grade glioma: an integrated clinical, radiological and molecular analysis. Neuro Oncol 2017 sep 7 (Epub ahead of print).
4. Capper D, Weissert S, Balss J, et al. Characterization of R132H mutation-specific IDH1 antibody binding in brain tumors. Brain Pathol 2010;20(1):245-254.
5. Claes A, Idema AJ, and Wesseling P. Diffuse glioma growth: a guerilla war. Acta Neuropathol 2007; 114(5):443-458.
6. Yen PS, Teo BT, Chiu CH, Chen SC, Chiu TL, Su CF. White matter tract involvement in brain tumors: a diffusion tensor imaging analysis. Surg Neurol 2009;72(5):464-469.
7. Jones DK, Leemans A. Diffusion tensor imaging. Methods Mol Biol 2011;711:127-144.
8. Price SJ, Jena R, Burnet NG, et al. Improved delineation of glioma margins and regions of infiltration with the use of diffusion tensor imaging: an image-guided biopsy study. AJNR Am J Neuroradiol 2006;27(9):1969-1974.
9. Pena A, Green HA, Carpenter TA, Price SJ, Pickard JD, Gillard JH. Enhanced visualization and quantification of magnetic resonance diffusion tensor imaging using the p:q tensor decomposition. Br J Radiol 2006;79(938):101-109.
10. Price SJ, Jena R, Burnet NG, Carpenter TA, Pickard JD, Gillard JH. Predicting patterns of glioma recurrence using diffusion tensor imaging. Eur Radiol 2007;17(7):1675-1684.
11. Price SJ, Allinson K, Liu H, et al. Less invasive phenotype found in isocitrate dehydrogenase-mutated glioblastomas than in isocitrate dehydrogenase wild-type glioblastomas: a diffusion-tensor imaging study. Radiology 2017;283(1):215-221.
12. Mohsen LA, Shi V, Jena R, Gillard JH, Price SJ. Diffusion tensor invasive phenotypes can predict progression-free survival in glioblastomas. Br J Neurosurg 2013;27(4):436-441.
13. Dubbink HJ, Atmodimedjo PN, Kros JM, et al. Molecular classification of anaplastic oligodendroglioma using next-generation sequencing: a report of the prospective randomized EORTC Brain Tumor Group 26951 phase III trial. Neuro Oncol 2016;18(3):388-400.
14. Jenkinson M, Beckmann CF, Behrens TE, Woolrich MW, Smith SM. FSL. Neuroimage 2012;62(2): 782-790.
15. Smith SM. Fast robust automated brain extraction. Hum Brain Map 2002;17(3):143-155.
16. Price SJ, Pena A, Burnet NG, et al. Tissue signature characterization of diffusion tensor abnormalities in cerebral gliomas. Eur Radiol 2004;14(10):1909-1917.
17. Price SJ, Gillard JH. Imaging biomarkers of brain tumour margin and tumour invasion. Br J Radiol 2011;84 Spec No 2:S159-167.
18. Goebell E, Paustenbach S, Vaeterlein O, et al. Low-grade and anaplastic gliomas: differences in architecture evaluated with diffusion-tensor MR imaging. Radiology 2006;239(1):217-222.
19. Jbabdi S, Mandonnet E, Duffau H, et al. Simulation of anisotropic growth of low-grade gliomas using diffusion tensor imaging. Magn Reson Med 2005;54(3):616-624.
20. Painter KJ, Hillen T. Mathematical modeling of glioma growth: the use of Diffusion Tensor Imaging (DTI) data to predict the anisotropic pathways of cancer invasion. J Theor Biol 2013;323:25-39.

**21.** Schlüter M, Stieltjes B, Hahn HK, Rexillius J, Konrad-verse O, Peitgen HO. Detection of tumour infiltration in axonal fibre bundles using diffusion tensor imaging. Int J Med Robot 2005;1(3):80-86.

**22.** Stadlbauer A, Ganslandt O, Buslei R, et al. Gliomas: histopathological evaluation of changes in directionality and magnitude of water diffusion at diffusion tensor MR imaging. Radiology 2006; 240(3):803-810.

**23.** Wright AJ, Fellows G, Byrnes TJ, et al. Pattern recognition of MRSI data shows regions of glioma growth that agree with DTI markers of brain tumor infiltration. Magn Reson Med 2009;62(6):1646-1651.

**24.** Jenkinson MD, du Plessis DG, Smith TS, Joyce KA, Wamke PC, Walker C. Histological growth patterns and genotype in oligodendroglial tumours: correlation with MRI features. Brain 2006;129(Pt 7):1884-1891.

**25.** Chen S, Tanaka S, Giannini C, et al. Gliomatosis cerebri: clinical characteristics, management, and outcomes. J Neurooncol 2013;112(2):267-275.

**26.** Price SJ, Young AM, Scotton WJ, et al. Multimodal MRI can identify perfusion and metabolic changes in the invasive margin of glioblastomas. J Magn Reson Imaging 2016;43(2):487-494.

## SUPPLEMENTARY FILES

**Table S1.** number of patients scanned per type of scanner and corresponding settings, including the number of B=0 s/mm$^2$ and B=1000 s/mm$^2$ images (diffusion directions) scanned.

| Scanner (GE) | Number of patients | TR (ms) | TE (ms) | b=0/b=1000 (s/mm$^2$) | Slice thickness (mm) | Matrix | Pixel size (mm) |
|---|---|---|---|---|---|---|---|
| **SIGNA EXCITE** (3 tesla) | 44 | 14200** | 70-85 | 1-3/25 | 2.0 | 256x256 | 0.859 |
| **DISCOVERY MR450** (1.5 tesla) | 21 | 8000 | 81-85 | 1-3/25 | 2.0<br>5.0* | 256x256 | 0.977 |
| **SIGNA EXCITE** (1.5 tesla) | 13 | 8000 | 68-73 | 1-3/25 | 3.5 | 256x256 | 0.820 |
| **Signa HDxt** (3 tesla) | 4 | 16000 | 86 | 4/31 | 2.0 | 256x256 | 0.820 |
| **DISCOVERY MR750** (3 tesla) | 1 | 7925 | 88 | 4/32 | 2.5 | 256x256 | 0.938 |

* 5 patients were scanned with 5mm slice thickness.

** 4 deviations from protocol with TRs of 16000, 15525, 15450 and 15500

# Chapter 3.1

## Response evaluation and follow-up by imaging in brain tumours

**Chapter 26 in**
Imaging and interventional Radiology for Radiation Oncology

Renske Gahrmann
Javier Arbizu
Anne Laprie
Maribel Morales
Marion Smits

ACCEPTED

## ABSTRACT

Brain tumours, either primary or secondary, are frequent. Primary brain tumours include mainly glioma, lymphoma and meningioma. Secondary tumours, i.e. brain metastasis, are a frequent event during the disease course of patients with cancer. The evaluation of response to treatment is often difficult with structural imaging due to the interference of treatment effects. In this chapter, the role of advanced imaging for the differential diagnosis between pseudoprogression, radiation necrosis and tumour recurrence is described with perfusion and diffusion MR imaging, MR spectroscopy, and PET imaging with amino acid analogues, fluorodeoxiglucose and other tracers. Furthermore, the commonly used response criteria for various brain tumours are described. For glioma, these are those set out by the Response Assessment in Neuro-Oncology (RANO) group. For brain metastases the RANO-brain metastasis (RANO-BM) and RECIST criteria are commonly used. While conventional T1w post-contrast imaging is the mainstay imaging modality for basic response assessment, multimodal imaging is commonly necessary to evaluate the response to treatment of primary and secondary brain tumours.

## INTRODUCTION

Brain tumours can be either primary (gliomas, lymphomas, meningiomas) or secondary (metastases). They carry a substantial burden of severe symptoms and complications. Their treatment often includes radiotherapy. The evaluation of tumour response can be challenging particularly in gliomas with the issue of pseudoprogression. For all tumours, another challenge is to differentiate radiation necrosis from tumoural residue or recurrence. The use of advanced imaging modalities is commonly useful in these situations.

### Imaging methods

*Structural imaging*

Treatment response assessment of brain tumours is generally performed using structural magnetic resonance (MR) images, such as T2-weighted (T2w), T2w Fluid Attenuation Inversion Recovery (FLAIR), and pre- and post-contrast T1-weighted (T1w) imaging. Most tumours show enhancement on post-contrast T1w images and 2D measurements on this sequence remain the basis of treatment assessment.

Additional information on tumour pathophysiology can be obtained with advanced MR imaging techniques and nuclear medicine imaging.

*Advanced MR imaging*

*Diffusion weighted imaging* (DWI) and diffusion tensor imaging (DTI) can be considered as both structural and functional techniques. The amount of diffusion (or random motion) of water molecules is measured with DWI. In DTI, diffusion is measured in multiple directions (minimum of 6) to calculate the tensor or general direction of diffusion. Diffusion can be limited due to structures within the voxel. In tumour, high cellular density restricts diffusion, which is reflected in the DWI-derived Apparent Diffusion Coefficient (ADC)[1]. DTI-derived measures include fractional anisotropy (FA), which provides information on the degree of directional diffusion along the three main axes, and mean diffusivity (MD), which is similar to ADC[2]. It is important to note that ADC is not only influenced by extracellular space tortuosity, but also by membrane damage and perfusion[3].

Most commonly used for *perfusion imaging* is T2*-weighted dynamic susceptibility-weighted contrast-enhanced (DSC) imaging. When the blood-brain-barrier is breached, contrast-agent leaks from the vessels into the surrounding tissue, increasing T1w-signal intensity and decreasing the T2*-signal. This effect must be counteracted (either in advance or during post-processing) when maps of relative cerebral blood volume (rCBV) are calculated, but can also be used to calculate other parameters, such as the peak height (PH) and percentage signal intensity recovery (rPSR)[4]. Other

perfusion techniques include dynamic contrast enhanced (DCE) imaging and arterial spin labelling (ASL). DCE-derived measures include cerebral blood flow (CBF), capillary permeability ($K^{trans}$), and extravascular extracellular volume fraction ($V_e$)[5]. Where for both DSC- and DCE-imaging intravascular injection of contrast-agent is required, the blood itself forms the contrast in arterial spin labelling (ASL). ASL-derived CBF has been shown to correlate well with DSC-derived rCBV measures[6].

In *MR spectroscopy* different resonance frequencies of specific molecules and metabolites can be measured within different tissues, most commonly using protons ($^1$H-MRS). In brain tumours, N-acetyl aspartate (NAA), Choline (Cho), myo-Inositol (mI), lactate/lipid Lac), and Creatine (Cr) are commonly assessed, although many more may be measured[7].

*Chemical Exchange Saturation Transfer* (CEST) imaging is a more recent technique, which can be used to measure amides (-NH), amines (-$NH_2$), and hydroxyl (-OH) groups among others, but is still very much in the research arena[8].

*Nuclear medicine imaging*

Nuclear medicine techniques such as single photon tomography (SPECT) and positron emission tomography (PET) are being used worldwide for the characterisation, therapy planning and recurrence assessment of brain tumours. SPECT using cellular viability radiotracers like as 99mTechnetium- sestamibi (99mTc-MIBI) and 201Thallium were initially employed in clinical practice due to its high availability[9,10]. However, in recent years PET has been gradually introduced into the clinical practice instead of SPECT for the evaluation of brain tumours as a complementary and supplementary tool of standard MR imaging sequences. It is important to note that fusion images between structural (computed tomography (CT) and/or MR imaging) and PET or SPECT images are highly recommended to achieve better accuracy. Multimodality systems are now available that combine SPECT and PET scanners and structural imaging devices like CT (SPECT-CT and PET-CT) and more recently MR imaging (PET-MR imaging). Visual analysis of images is the most common method for scan evaluation in clinical practice. The study is classified as positive when the activity observed in the lesion exceeds the reference region (usually normal cortex). However, semiquantitative analysis of PET studies can also be performed using the standard uptake value (SUV), commonly calculated for quantifying systemic tumours. This parameter however has a limited role in the clinical interpretation of images in neuro-oncology. Instead, tumour or lesion to brain reference region ratios using mean or maximum SUV (TBR) are used to provide a measure of PET radiotracers uptake in brain tumours.

One of the hallmarks of PET is the variety of parameters that can be observed and measured in brain tumours by means of specific radiotracers. Some of the most commonly used in clinical practice are reviewed in this section.

*Glucose metabolism*

Brain 2-deoxy-2-[18F]-2-fluoro-2-deoxy-D-glucose (FDG) uptake is usually acquired 45 to 60 minutes after the injection of 185 MBq of FDG. Patients must be fasting for 4 hours prior to injection, and it is recommended to obtain a measurement of blood glucose prior to the exam: high blood glucose levels at the time of injection decreases uptake in tumour and healthy tissue, although it may not affect lesion detection detectability. In case sedation is required, this can be carried out 45-60 minutes after injection, just prior to the time of the acquisition[11].

FDG accumulates in the majority of tumours due to elevated glucose metabolism in response to increased energy demand. This technique has been applied to brain tumour imaging for many years. The relationship of FDG uptake to tumour glioma grade and prognosis has been reported in several studies[12]. However, FDG is in some way limited in neuro-oncology due to the high rate of glucose metabolism in normal brain parenchyma resulting in diminished signal-to-noise ratio for brain tumours. Another problem with FDG is the high uptake of this tracer in inflammatory cells, which can occur in a variety of disease processes and can be independent of tumour growth or response[13]. Consequently, as newer PET tracers have become available, the use of FDG for imaging in neuro-oncology has declined.

*Amino acid transport*

System L amino acid transport PET radiotracers ([11C-methyl]-methionine (-MET), O-(2-[18F]-fluoroethyl)-L-tyrosine (FET) and 3,4-dihydroxy-6-[18F]-fluoro-L-phenyl-alanine (FDOPA) are currently used in neuro-oncology. MET has been used since 1983[14], but is limited to centres with an on site cyclotron because it is labelled with $^{11}$Carbon, a radioisotope with a very short half-life (20 minutes). FET and FDOPA are labelled with $^{18}$Fluorine, a radioisotope with a longer half-life, which allows radio-tracer transportation from the manufacturing laboratory to the PET centre[12].

The uptake of radiolabelled amino acids observed in normal brain tissue as well as in brain lesions including tumours of many types is predominantly conditioned by the transmembrane active transport, which is responsible for the biological activity in tissues, including cell proliferation. The uptake by cerebral tumour tissue appears to be caused almost entirely by increased transport via the specific amino acid transport system L for large neutral amino acids[12]. The uptake is also influenced by passive diffusion in regions with blood-brain-barrier disruption, and by stagnation in regional vascular beds that depends on blood volume due to a large vascular bed[15]. In contrast to tumour, the uptake of radiolabelled amino acids in normal brain is very low resulting in a high contrast between tumour and normal brain tissue.

After a recommended period of 4 hours of fasting, 200 MBq of FET, 370-555 MBq of MET, or 185 MBq of FDOPA are injected and a static PET acquisition is performed

20 minutes later. In addition to static images, dynamic FET PET data can be acquired, which allows the characterisation of the temporal pattern of FET uptake by deriving a time-activity curve (TAC) in brain tumours[16,17]. It remains to be shown, however, whether dynamic MET and FDOPA can contribute significantly to the characterisation of brain tumours. The more widespread use of amino acid PET for the management of patients with brain tumours has been strongly recommended by the Response Assessment in Neuro-oncology (RANO) group[13,18].

*Somatostatine receptors*

The most common somatostatin receptor (SSTR) radioligands for PET imaging are 68Ga-DOTA-Tyr3-octreotide (68Ga-DOTATOC), 68Ga-DOTA-D-Phe1-Tyr3-octreotate (68Ga-DOTATATE) or 68Ga-DOTA-l-Nal3-octreotide (68Ga-DOTANOC). These radiotracers, frequently used for imaging of neuroendocrine tumours, have been introduced in neuro-oncology due the overexpression of SSTR subtype 2 in almost all meningiomas[19]. 68Ga has a physical half-life of 68 minutes and can be produced with a 68Ge/68Ga generator system, which enables in-house production without the need for an on-site cyclotron. PET ligands to SSTR provide high sensitivity with excellent target-to-background contrast due to low uptake in bone and healthy brain tissue[20].

There are no comparative studies of 68Ga-DOTATOC, 68Ga-DOTATATE and 68Ga-DOTANOC, but the uptake of all these tracers is relatively high compared to normal brain; thus, possible differences between these tracers are not really relevant. Procedure guidelines for PET imaging with 68Ga-DOTA-conjugated peptides have been published recently[21].

*Other radiotracers*

Several other radiotracers are used to image brain tumours. The *thymidine nucleoside analogue 3'-deoxy-3'-18F-fluorothymidine* (*FLT*) is a substrate for thymidine kinase-1 and reflects cell proliferation. Although previous studies suggest that FLT is a promising tool for glioma detection and grading[22] and is able to predict improved survival after bevacizumab therapy[22,23], the uptake of this tracer is dependent on disruption of the blood-brain barrier, thereby limiting its clinical value.

Hypoxia in brain tumours has been demonstrated with use of the PET tracer *18F-Fluoromisonidazole* (*FMISO*)[24]. FMISO enters tumour cells by passive diffusion and becomes trapped in cells with reduced tissue oxygen partial pressure by nitroreductase enzymes. This tracer thus allows the identification of hypoxic tumour areas, which are thought to be more resistant to irradiation[25], as well as a trigger for neoangiogenesis. Thus far, FMISO has predominantly been used in a preclinical setting.

Another interesting PET target is the *translocator protein* (*TSPO*), a mitochondrial membrane protein that has been used as biomarker for neuroinflammation. TSPO is

highly expressed in activated microglia, macrophages and neoplastic cells. Imaging with the TSPO ligand 11C-(R)PK11195 demonstrates increased binding in high-grade glioma compared to low-grade glioma and normal brain parenchyma[26]. More recently, the TSPO ligand 18F-DPA-714 labelled with 18F has been evaluated in glioma animal models[27].

Choline is a marker of phospholipid synthesis involved in the synthesis of cell membrane components. The *radiolabelled choline* (either $^{11}$Carbon and more recently $^{18}$Fluorine) is trapped by glioblastoma with a very high contrast to normal brain, whereas its role in lower grade gliomas is limited[28]. When compared with FDG, radiolabelled choline appears to be superior in terms of diagnostic performance in glioma and metastasis[29].

## TREATMENT RESPONSE

### Glioma

*Background*

Newly diagnosed anaplastic glioma and glioblastoma (GBM) are the most frequent primary brain tumours in adults. They are treated with the Stupp protocol, consisting of surgery, whole-brain radiotherapy (WBRT) and temozolomide (TMZ), followed by adjuvant TMZ. In diffuse low-grade gliomas the presence of certain negative prognostic factors can be considered a reason for adjuvant radiotherapy[30]. The effects of radiotherapy combined with TMZ positively influences patient survival in GBM, especially in those with a methylated $O^6$-methylguanine DNA methyltransferase (MGMT)[31,32].

*Radiological treatment assessment*

Radiological assessment of treatment response in glioma was traditionally based on the bidimensional measurement of the area of enhancement[33], but the introduction of angiogenesis inhibitors (such as bevacizumab) has led to the diagnostic challenge of pseudoresponse: enhancement decreases or disappears because the tumour vasculature normalises and is therefore no longer permeable, while the tumour itself may not be responding to treatment. The RANO criteria[34] therefore now includes the assessment of non-enhancing in addition to enhancing lesions, which also make them applicable to non-enhancing, commonly lower grade, glioma. The time between scans is generally 6-12 weeks, but is sometimes increased in case of stable disease. A summary of the RANO criteria for both GBM and lower grade glioma can be found in ***Table 1***.

**Table 1.** Summary of the RANO criteria for glioblastoma (GBM) and low-grade glioma (LGG)[34,37].

| Response | Criteria GBM | Criteria LGG |
|---|---|---|
| **CR** | *Requires all of the following*: complete disappearance of all enhancing (non-) measurable disease sustained for at least 4 weeks. No progression of non-enhancing disease. No new lesions. No corticosteroids. Stable or improved clinically. | *Requires all of the following*: complete disappearance of the lesion on T2w/ FLAIR images. No new lesions aside from radiation effects. No corticosteroids. Stable or improved clinically. |
| **PR** | *Requires all of the following*: ≥50% decrease in the sum of products of perpendicular diameters of all measurable enhancing lesions compared to baseline sustained for at least 4 weeks. No progression of non-enhancing disease. No new lesions. Stable or reduced corticosteroids. Stable or improved clinically. | *Requires all of the following*: ≥50% decrease in the sum of products of perpendicular diameters on Tw/FLAIR imaging compared to baseline sustained for at least 4 weeks. No new lesions aside from radiation effects. Stable or reduced corticosteroids. Stable or improved clinically. |
| **Minor response** | - | *Requires all of the following*: 25-50% decrease of non-enhancing lesion area on T2w/FLAIR images compared to baseline. No new lesions aside from radiation effects. Stable or reduced corticosteroids. Stable or improved clinically. |
| **SD** | Does not qualify for CR, PR or PD. Stable or reduced corticosteroids. Stable clinically. | Does not qualify for CR, PR, minor response or PD. No new lesions aside from radiation effects. Stable or reduced corticosteroids. Stable or improved clinically. |
| **PD** | *Requires any of the following*: ≥25% increase in the sum of products of perpendicular diameters of enhancing lesions compared to the smallest tumour measurement from earlier studies. Significant increase in non-enhancing lesions. Any new lesion. Clinical deterioration. | *Requires any of the following*: Development of new lesions or increase of enhancement. ≥25% increase of T2w/ FLAIR non-enhancing lesions while on stable or increasing steroid-dosage and not caused by radiotherapy or other. Clinical deterioration. |

*CR=complete response, PR=partial response, SD=stable disease, PD=progressive disease.

*Advanced methods of treatment assessment (MR imaging)*

In a pretreatment setting, *diffusion MR imaging* derived parameters, such as ADC and FA, can aid in grading gliomas and localising areas of high cellularity suitable for biopsy[35]. After treatment, however, these parameters no longer correlate with cellular density, as they are influenced by other factors such as cell swelling and necrosis[36]. At a group level, ADC values still tend to be higher in gliomas than in normal appearing white matter (NAWM), but at an individual level there is considerable overlap and they are therefore not useful for response assessment[37].

*Perfusion imaging* derived rCBV and CBF in both grey and white matter are decreased after radiotherapy and can remain low for up to 6 and 9 months respectively in high-dose areas[38,39]. High rCBV values (>2.0 times that of the contralateral NAWM) can be used to distinguish tumour from pseudo-progression or radiation necrosis with reported sensitivities of up to 82% and specificity of 78%[40,41]. In diffuse astrocytoma, an increase in rCBV indicates malignant transformation[37]. In oligodendroglioma rCBV tends to be moderately increased even when low grade, but a further increase indicates malignant transformation[37].

*MR spectroscopy* shows (transient) changes in molecules and metabolites in relation to treatment-related changes, such as neuronal dysfunction, oedema, damage to oligodendrocytes, demyelination, and inflammatory effects. Metabolites such as NAA, Cr, Cho and Lac change during and after radiation. For instance, a decrease in NAA occurs early after radiotherapy co-occurring with an increase in Cho, which can remain present for up to 6 months[42-44]. Due to the transient nature of metabolite changes, MR spectroscopy results need to be either interpreted in combination with other measures (MR imaging and/or PET) or with repeated measures in time.

*PET imaging*

A higher *FDG* uptake by glioma is correlated with higher tumour grade and worse prognosis[45-47]. With the exception of pilocytic astrocytomas, WHO grade I and II grade gliomas are typically negative on FDG PET (uptake similar to or less than white matter), and consequently this tracer is not suitable for response evaluation of low-grade glioma[13]. On the other hand, increased levels of FDG uptake in enhancing brain lesions are correlated with tumour recurrence in anaplastic glioma and glioblastoma.

In recurrent high-grade glioma, the uptake of FDG has been shown to be predictive of tumour metabolic response to TMZ versus TMZ plus radiotherapy[48], and for predicting survival following anti-angiogenic therapy with bevacizumab[45].

Current *amino acid* PET data suggest that both a reduction of amino acid uptake and/or a decrease of the metabolically active tumour volume are signs of treatment response associated with improved long-term outcome[13]. Moreover, the amount of residual tracer uptake in FET PET after surgery/prior to chemoradiation of glioblastoma (within 7-20 days after surgery) has a strong prognostic influence, even after adjustment by multivariate survival analyses for the effects of treatment, MGMT promoter methylation and other patient and tumour-related factors (***Figure 1***)[49]. The experience with amino acid PET for monitoring after treatment in patients with WHO grade II glioma is however limited.

The prognostic value of early changes of FET uptake 6-8 weeks after postoperative radiochemotherapy in glioblastoma patients has been evaluated prospectively[50,51]. PET responders with a decrease in the TBR of more than 10% had a significantly

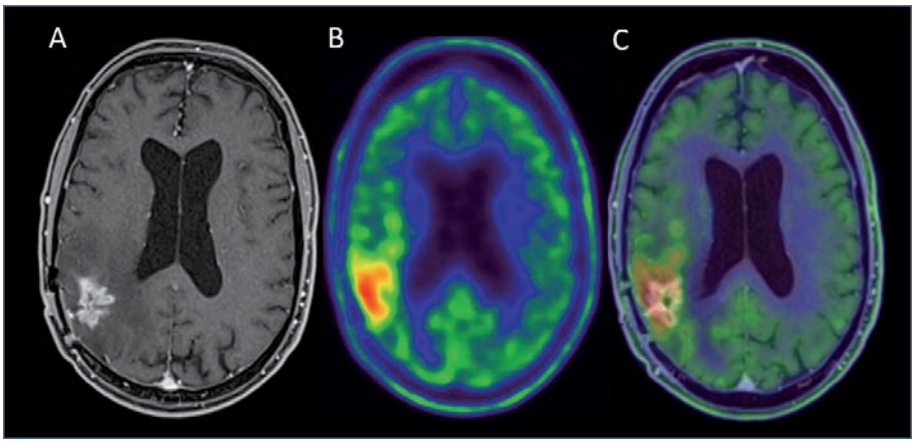


**Figure 1.** Neuroimaging studies of a patient with anaplastic astrocytoma performed 1 month after postoperative radiochemotherapy. An area of contrast enhancement on the T1w MR imaging sequence (**A**) is observed in the medial aspect of the residual surgical cavity. The MET-PET study (**B**) and MR imaging - PET fusion (**C**) show an absence of MET uptake in this part of the lesion ruling out the presence of tumour and indicating an area of pseudoprogression However, there is also an area of elevated MET uptake (TBR: 2.56) in the most lateral part of the lesion surrounding the area of pseudoprogression, suggesting the presence of infiltrative tumour relapse and as confirmed by biopsy.

longer disease-free and overall survival than patients with stable or increasing tracer uptake after radiochemotherapy. The kinetic analysis of FET uptake was not helpful in the evaluation of treatment effects to radiochemotherapy[50]. Patients with low-grade glioma evaluated 12 months after brachytherapy exhibit significantly reduced MET uptake[52,53]. For patients treated with alkylating chemotherapy, MET and FET PET may improve response assessment[54]. Reliable monitoring of temozolomide and nitrosourea-based chemotherapy (PCV scheme including procarbazine, CCNU and vincristine or CCNU monotherapy) has been demonstrated in patients with recurrent high-grade glioma[55]. Similarly, FET PET has been used to assess effects of TMZ according to the EORTC protocol 22033-26033 (application of 75 mg/m$^2$ TMZ per day over 21 days in a 28-day cycle)[56]. Additionally, a reduction of the metabolically active tumour volume after treatment initiation can be observed considerably earlier than volume reductions on FLAIR imaging[57]. Several studies suggest that treatment response and outcome in bevacizumab therapy can be assessed better with amino acid PET using 18F-FET and 18F-FDOPA than with MR imaging (see also ***section 4.2***)[58,59].

## Lymphoma

*Background*

The classification of central nervous system (CNS) lymphoma now corresponds with the WHO 2016 classifications of systemic haematopoietic/lymphoid disease[60]. A

distinction is made between primary CNS lymphoma (PCNSL) and secondary CNS lymphoma. Secondary CNS lymphoma generally arises from aggressive non-Hodgkin lymphoma and has commonly (2/3) a leptomeningeal, and less commonly (1/3) a parenchymal localisation. PCNSL almost invariably has a parenchymal localisation. Typically, single or multiple contrast-enhancing lesions are seen surrounding the ventricles or in the corpus callosum[61]. Patients are treated with WBRT and multiple chemotherapeutic agents (including methotrexate) given both systemically and intrathecally or intraventricularly. Additionally steroids are given.

*Radiological treatment assessment*

Conventional treatment response assessment of brain parenchymal lymphoma is by contrast-enhanced MR imaging with an average time between follow-up scans of 2 months during therapy. The International Primary CNS Lymphoma Collaborative Group has determined response criteria in 2005. Complete response (CR) is determined by a lack of contrast-enhancement on MR imaging, no steroid-treatment and

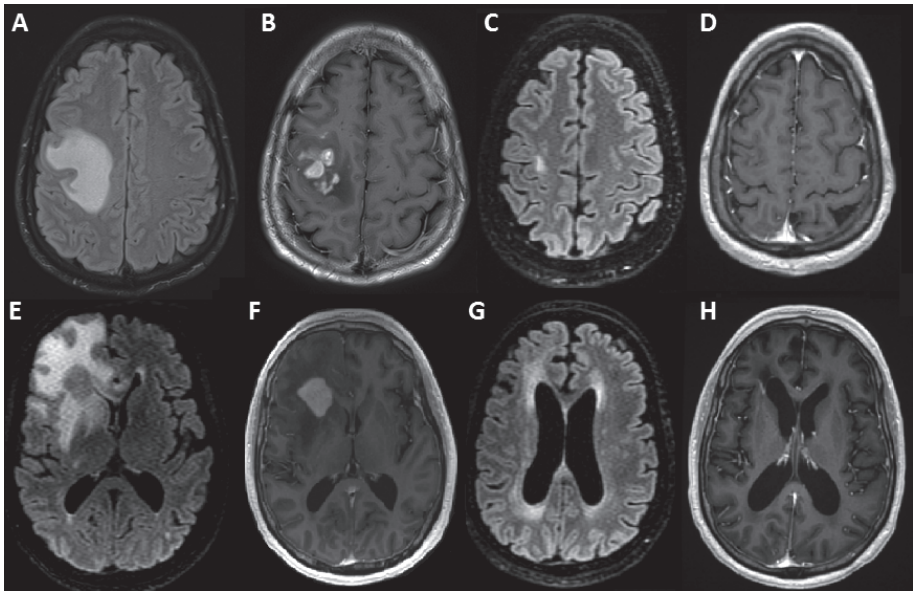


**Figure 2.** FLAIR and T1w post-contrast images in a 60-year old man with PCNSL in the right frontal lobe (**A** and **B**), treated with rituximab and MBVP followed by WBRT (30 Gy in 20 fractions) with resulting partial remission. Treatment continued with cytarabine and WBRT with SIB (30Gy in 20 fractions) and an additional boost on the tumour (10Gy in 20 fractions), resulting in complete remission with minimal white matter abnormalities considered to be a post-treatment effect (**C** and **D**). Recurrent disease four years later (**E** and **F**). After renewed treatment with MBVP and WBRT (20Gy in 5 fractions), a clear response was seen. Periventricular white-matter abnormalities and ex vacuo dilations of the ventricles is present as a post-treatment effect (**G** and **H**).

normal eye examination and cerebrospinal fluid (CSF) cytology. An unconfirmed complete response (CRu) is CR with minimal abnormalities on MR imaging and eye examination and/or any steroid use. Patients with a partial response (PR) have a 50% decrease of enhancing tumour without or only minor or decreasing eye disease with either negative or persistent/suspicious CSF cytology. Progressive disease (PD) is characterised by a ≥25% increase in enhancing lesions, new sites of disease, recurrent or new ocular disease and recurrent or positive CSF cytology[62]. Treatment response in parenchymal PCNSL is depicted in ***Figure 2***.

*PET imaging*

PCNSL often have high cellular density and consequently a markedly increased FDG uptake compared to other brain tumours, including glioblastoma and metastasis, and when compared to many infectious and inflammatory processes[13,63]. Cerebral infections such as toxoplasmosis and tuberculoma are a common differential diagnosis to PCNSL and exhibit a significantly lower uptake than patients with lymphoma, with no overlap of the uptake values (0.3-0.7 versus 1.7-3.1 respectively)[64,65].

There is no significant difference between MET PET and FDG PET in terms of sensitivity[66]. FDG PET has shown some clinical advantage in the differential diagnosis of lymphoma as most cerebral lymphomas have a high cell density and a high glucose metabolism, which is usually even higher than that of malignant gliomas and cerebral metastasis. In addition, FDG it is clinically more available and it can be performed as a whole-body scan for the assessment of systemic lymphoma involvement. Interestingly, FDG PET might also useful to demonstrate a response to chemotherapy in lymphoma patients very early after the initiation of therapy (***Figure 3***)[67].

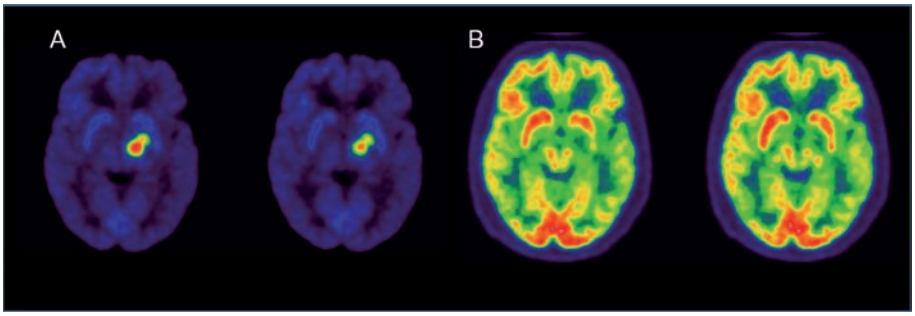


**Figure 3.** Brain FDG PET of primary CNS lymphoma at baseline (**A**), and 3 months after two cycles of chemotherapy (Carmustine, Methotrexate, Cytarabine, Rituximab according to the R-BAM scheme) and autologous hematopoietic stem cell transplantation (**B**) showing complete response.

## Metastasis

*Background*

The main primary sites of brain metastases are lung, breast, and skin (melanoma). About 80% of brain metastases are located in the supratentorial brain (mainly frontal lobes) and about half of all patients have more than one metastases at the time of diagnosis[68]. Treatment consists of WBRT and/or stereotactic radiosurgery (SRS) depending on the size and number of lesions. Larger metastases may be surgically removed[69].

*Radiological treatment assessment*

The RANO Brain Metastases (RANO-BM) working group created radiological criteria for treatment assessment in clinical trials, which can also be used in clinical practice[70]. The metastases are categorised as target and non-target lesions. Target lesions are parenchymal metastases of at least 10x5 $mm^2$ in size. Up to five target lesions can be

**Table 2.** Response assessment in brain metastases: target and non-target lesions according to the RANO-group, radiological characteristics only[70].

| | | |
|---|---|---|
| **Target lesions** | **CR** | *Requires all of the following:*<br>• Disappearance of all target lesions sustained for at least 4 weeks.<br>• No new lesions.<br>• No corticosteroids.<br>• Stable or improved clinically. |
| | **PR** | *Requires all of the following*<br>• ≥30% decrease in the sum of perpendicular diameters of target lesion size compared to the baseline sustained for at least 4 weeks.<br>• No new lesions.<br>• Stable or reduced corticosteroids.<br>• Stable or improved clinically |
| | **SD** | Does not qualify for CR, PR of PD. |
| | **PD** | *Requires all of the following:*<br>• ≥20% increase in the sum of longest diameters of target lesions compared to the smallest sum from earlier studies.<br>• At least one lesion has increased ≥5mm. |
| **Non-target lesions** | **CR** | *Requires all of the following:*<br>• Disappearance of all enhancing non-target lesions<br>• No new lesions. |
| | **PR/SD** | Persistence of one or more non-target lesions. |
| | **PD** | *Requires any of the following*:<br>• Unequivocal progression of existing enhancing non-target lesions.<br>• New lesions (except while on immunotherapy-based treatment*)<br>• Unequivocal progression of existing tumour-related non-enhancing (T2w/FLAIR) lesions. |

*In case of immunotherapy-based treatment, new lesions alone may not constitute PD.

**CR=complete response, PR=partial response, SD=stable disease, PD=progressive disease.

measured. Non-target lesions include smaller parenchymal lesions, but also dural, leptomeningeal, and cystic (or non-measurable) lesions. In case of a mixed response to treatment, lesions that increase in size are considered leading. Recommended time between scans is 6-12 weeks. Aside from radiological features, the RANO-BM also includes clinical status and steroid dosage. The RANO-BM criteria can be found in ***Table 2***. Other response assessment methods include the RECIST criteria, in which lesions are measured in a single direction (≥30% decrease in the sum of diameters of the target lesions constitutes partial response, and a ≥20% increase progressive disease) and the WHO criteria, which include bi-dimensional measures (≥50% decrease in in the sum of the product of the diameters constitutes partial response, and ≥25% increase progressive disease). The appearance of a new lesion always indicates progressive disease[71].

*PET imaging*

PET imaging in the context of treatment assessment of metastasis is mostly used to distinguish tumour recurrence from treatment effects (see ***section3***).

FDG PET can add to the specificity for enhancing lesions that are equivocal or suspicious for recurrent tumour based on contrast-enhanced MR imaging alone in patients with brain metastases treated with SRS[72].

## Meningioma

*Background*

The WHO classification distinguishes three grades of meningiomas: Grade I, or benign meningioma, constitute the vast majority (about 90%); Grade II (atypical) and grade III (malignant) meningiomas are considerably less common. Benign meningiomas can be eligible for (radio)surgery if the cause of symptoms. Radiotherapy can be considered in case of incomplete resection or at recurrence. Atypical and malignant meningiomas are surgically removed when possible and irradiated[60,73,74]. Both atypical and malignant meningiomas can metastasise to the lungs, liver and spine, although this is rare (0.1% of cases) and screening is therefore not routinely recommended[75].

*Radiological treatment assessment*

Meningiomas at risk for recurrence are those with pial invasion, and in the case of grade II and III meningioma when there is bone involvement or peritumoural oedema[76,77]. Meningiomas generally show intense homogeneous enhancement on post-contrast T1w images, and measurements are therefore performed on this sequence. Generally, the modified MacDonald criteria are used to determine treatment response, but it has been suggested that volumetric measures are more sensitive when it comes to

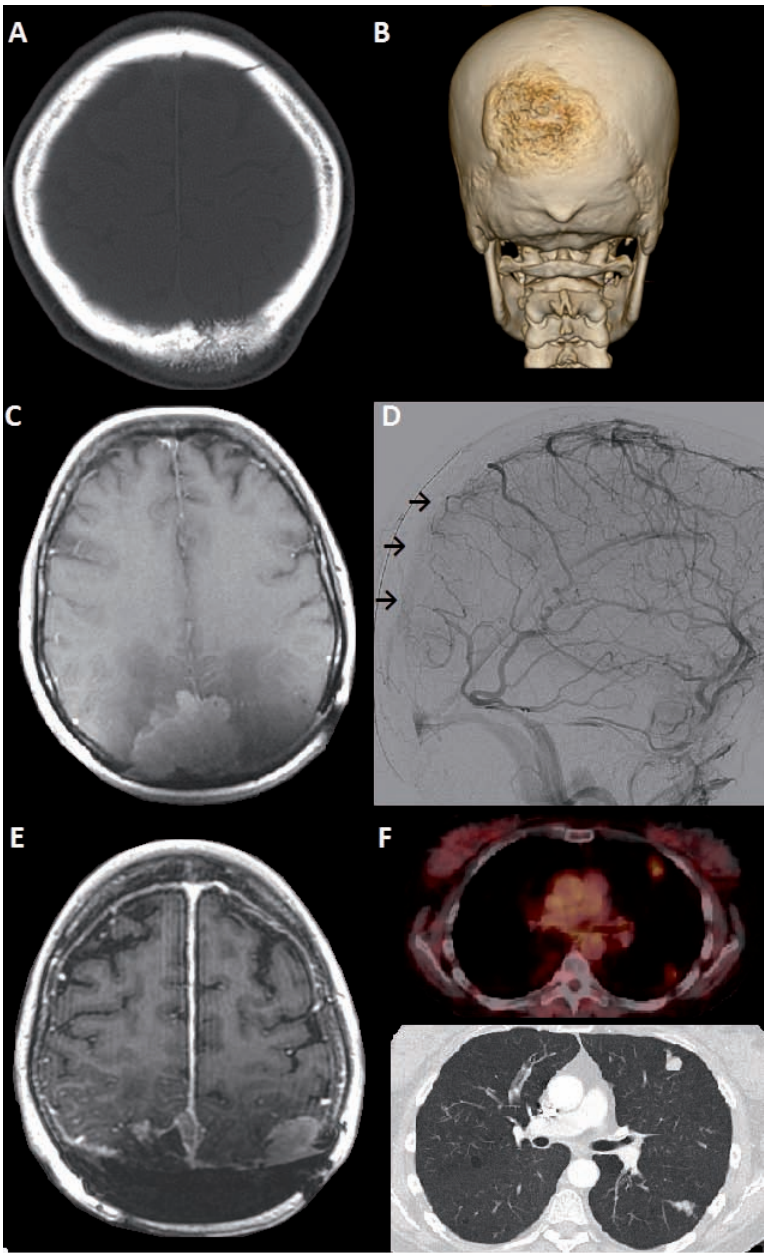


**Figure 4.** CT, MR imaging (T1w post-contrast), angiographic and FDG-PET images in a 40-year old woman with grade II meningioma primarily located in the skull (**A** and **B**). The tumour was resected and irradiated with 59.4Gy. Recurrent tumour growth appeared five years later intracranially (**C**) with compression of the superior sagittal sinus (**D**). Again, the tumour was resected. At second recurrence, multiple intracranial meningiomas appeared within the radiation field (**E**) and the patient was irradiated again (49.5Gy in 33 fractions). Aside from intracranial disease, the patient had histologically confirmed metastases in the lungs (**F**).

determining tumour growth due to the slow-growing nature of the tumours[78]. Additional meningiomas may appear in the course of time at other locations.

Early radiotherapy-related effects are tumour necrosis and oedema in the white matter[79]. Radiation-induced peritumoural changes occur in about 25% of patients, mainly in convexity, parasagittal and falx cerebri meningiomas after SRS[80]. Later radiotherapy-effects such as white matter abnormalities are often seen in high-dose areas and the periventricular white matter. An example of an irradiated patient with an atypical meningioma and its treatment course of depicted in ***Figure 4***.

*PET imaging*

The use of PET in meningioma patients is gradually increasing. Nevertheless, the usefulness of FDG PET is limited because meningiomas are mostly slow-growing and the metabolism of FDG is only elevated in atypical or anaplastic meningiomas[81].

MET PET scanning has been used to evaluate the effect of stereotactic high-energy proton beam treatment has been evaluated in a prospective study with 19 meningioma patients[82]. A reduction in the TBR was observed (even over several years) in the total patient group without a reduction in tumour size. Moreover, prior to the volume increase on MR imaging, MET uptake ratios were found to be increased, suggesting that treatment effects can be seen earlier than with CT or MR imaging[82].

Even though amino acid PET exhibits a better tumour-to-background contrast than FDG PET, the availability of specific SSTR ligands with even higher tumour-to-background contrast has led to a limited use of amino acid PET in meningioma assessment[54]. 68Ga-DOTA peptides PET have been shown more accurate than standard MR imaging to discriminate meningioma tissue from scar tissue related to pretreatment using both DOTATOC[83] and DOTATATE[20], even in transosseous extension of intracranial meningiomas[84]. Consequently, 68Ga-DOTA peptides may be useful in cases of unclear differential diagnosis between tumour progression and treatment-induced changes.

## TREATMENT EFFECTS

### Pseudo-progression and radiation necrosis

*Background*

Progressive disease can be mimicked by treatment-related toxicity from radiotherapy (pseudoprogression and radiation necrosis), immunotherapy, chemotherapy, and anti-epileptic drugs. Additional imaging techniques and sequential imaging combined with clinical characteristics may be needed to distinguish these entities from actual progressive disease[70,74]. Pseudoprogression occurs in a subacute setting after radiotherapy treatment combined with TMZ (within approximately 2-3

months after the start of treatment). Tumours with a methylated $O^6$-methylguanine DNA methyltransferase (MGMT) promotor respond best to TMZ. Initially it seemed that this group showed a higher incidence of pseudoprogression, but this has later been disputed[85]. Direct damage after radiotherapy is likely due to vasodilatation and increased capillary permeability, leading to disruption of the blood-brain-barrier and oedema. In case of pseudoprogression the response is excessive causing enhancement on post-contrast T1w images due to the damage to the blood-brain-barrier, and which is indistinguishable tumour progression[86.87].

Radiation necrosis is a chronic response to radiotherapy, which can occur from just months up to many years (median 1-2 years) after treatment; up to 90% occurs within the first 5 years posttreatment. There is endothelial damage**,** enzyme changes and immunological response leading tot necrosis. Radiation necrosis similar to pseudoprogression causes enhancement on post-contrast T1w images, mimicking tumour recurrence or progression[86,88].

The reported incidences of pseudoprogression and radiation necrosis vary widely, from 2% to 48%, depending on the source and the definition used. The incidence is influenced by radiation dose, field size, number of fractions, prior WBRT, chemotherapy (mainly cisplatin, carboplatin, doxorubicin, methotrexate, and temozolomide), immunotherapy, length of survival, age at time of radiotherapy, and diabetes mellitus[88].

*Standard structural imaging*

Distinguishing pseudoprogression and radiation necrosis from tumour residue or recurrence is challenging. Radiation-induced lesions can occur at the primary tumour site, but also at a distance, including the contralateral hemisphere, if included in the field of radiation. There is a predilection for white matter, especially the corpus callosum, because of the higher susceptibility of oligodendrocytes to radiation damage (compared to neurons) and relatively lower blood supply[89]. In patients with low-grade gliomas there is also a predilection for subependymal localisation[90]. The enhancing area is surrounded by oedema, which tends to be somewhat more extensive in radiation-induced lesions[91]. Different patterns of enhancement have been described, including nodular and rim enhancement with either regular or irregular margins and combined nodular and linear enhancing foci that create a mosaic-like appearance[88,92], but no reliable distinctive characteristics have been found. Radiation-induced lesions more often contain haemorrhagic lesions visible on T2*-weighted images, although these can also occur in glioma and metastases (especially malignant melanoma)[88]. To complicate things further, lesions containing both radiation damage and tumour commonly occur. Patients with multiple lesions can show a mixed response, which can indicate the presence of pseudoprogression or radiation necrosis. More advanced imaging techniques, follow-up and sometimes histopathological assessment are generally necessary to make the final diagnosis.

*Advanced MR imaging*

With *diffusion MR imaging*, ADC values tend to be lower in recurrent tumour compared to radiation necrosis at the group level, likely due to increased cellularity, but at the individual level these values overlap[93]. Comparing ADC measures from the enhancing and non-enhancing areas can be helpful: in case of tumour, the ADC values taken from the non-enhancing area tend to be significantly higher than those from the enhancing area, while in radiation necrosis ADC values from both enhancing and non-enhancing areas are similar[88]. DTI-derived FA values in enhancing areas tend to be higher in recurrent tumour than in radiation necrosis[94].

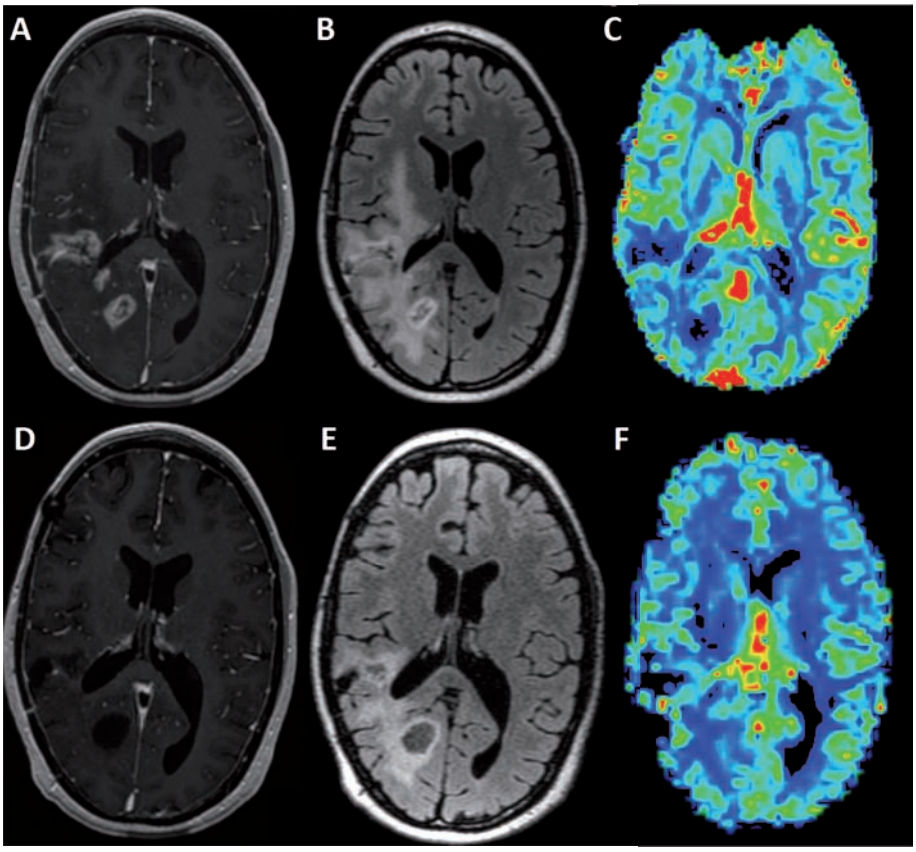


**Figure 5.** T1w post-contrast, FLAIR and DSC-perfusion rCBV maps in a glioblastoma patient with new enhancing lesions (**A**) and surrounding oedema (**B**) after prior treatment by the Stupp protocol. The rCBV map (**C**) shows low perfusion in the enhancing areas. The patient was enrolled in a clinical trial and treated with both bevacizumab and lomustine. At 6 weeks' follow-up the enhancement had disappeared (**D**) and the surrounding oedema was decreased (**E**). A small artefact is present on the rCBV map (**F**), but there is no evidence of increase in perfusion.

*Perfusion-imaging* derived rCBV is commonly assessed as a ratio of the area of interest over the normal appearing white matter (NAWM) in the contralateral hemisphere. In high-grade tumours and metastases the rCBV ratio is high, whereas in radiation necrosis/pseudoprogression the rCBV ratio is low. The proposed cut-off value lies between 1.5 and 2.6[40,41]. In about 8% of cases results are false-negative, as tumours can have rCBV ratios <1.5. Radiation necrosis can be safely diagnosed when the ratio is <0.6 (***Figure 5***)[41,95]. In current clinically used software it is easy to measure rCBV in multiple regions of interest (ROIs), but the interrater variability is quite large when it comes to deciding ROI size and placement. Other methods for measuring perfusion, such as using a different contrast-agent than gadolinium like ferumoxytol and using a different technique such as ASL are under investigation, showing promising results[96.97].

*MR spectroscopy* shows different metabolite concentrations in radiation necrosis from those measured in tumour. Reductions in individual metabolites Cho, Cr, and NAA indicate tissue damage and thus radiation necrosis. Favouring tumour are high ratios of Cho/Cr and Cho/NAA and low ratios of NAA/Cr and Lac/Cho. In order to distinguish tumour from radiation necrosis different cut-off values for these ratios have been proposed: Cho/Cr >1.5-1.8, Cho/NAA >1-1.8, and Lac/Cho <0.75-1.05[43,98,99]. Single voxel MR spectroscopy techniques requires precise placement of the voxel to be measured. In the presence of mixed tumour and radiation necrosis within the same voxel, tumour signal can be obscured because the metabolite concentration is averaged and then tends to suggest inflammatory changes[43]. Such partial volume effects can be reduced with multivoxel MRS, in which multiple small voxels are placed. It is sometimes also important to look at changes over time, because of certain transient changes in metabolite concentrations: Cho for instance can be temporality increased in radiation necrosis, falsely indicating tumour presence[99].

A relatively new method of measuring metabolites is *CEST*, which can potentially also be used to distinguish radiation damage from tumour: Amide proton transfer (APT), for instance, is found to be increased in tumour tissue[8]. CEST studies to date are still scarce and the true clinical value remains to be determined.

*PET imaging*

After radiation therapy, *FDG* can be used to distinguish radiation necrosis from recurrent glioma. Although different rates of diagnostic accuracy has been have been reported in the literature, FDG seems to be less sensitive than amino acid radiotracers with lower inter-observer agreement[100,101]. However, diagnostic accuracy increases when FDG is evaluated in combination with MR imaging (***Figure 6***)[102]. *Amino acid* PET radiotracers are useful for the differentiation between treatment related changes

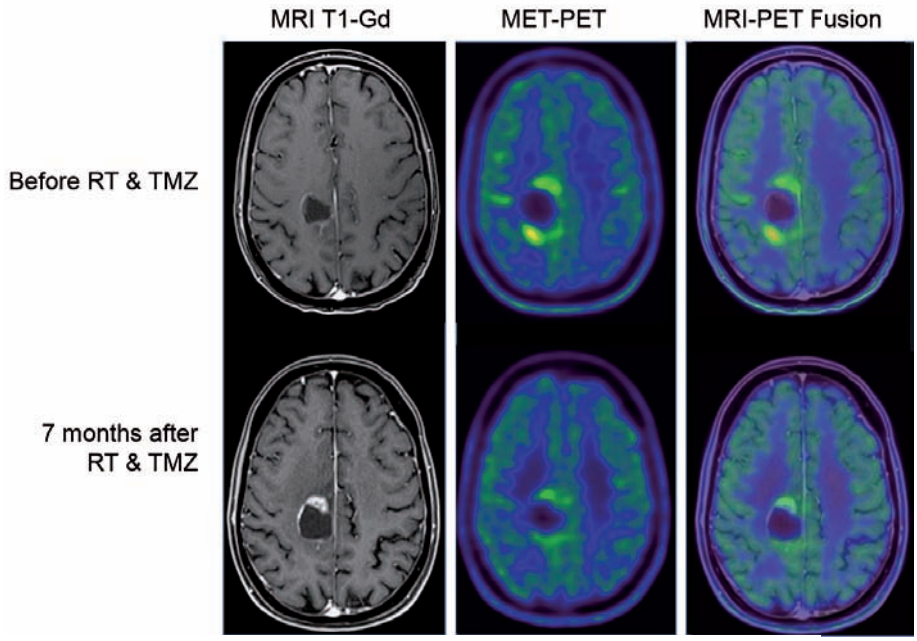


**Figure 6.** Patient with GBM studied before and after treatment (radiotherapy with concomitant temozolomide, and additional 6 cycles of temozolomide). An area of contrast enhancement on the T1w MR imaging sequence is observed in the anterior part of the cavity; there is only mild MET uptake (TBR=1.7; significantly lower than initial residual tumour with TBR= 2.6), consistent with radiation necrosis.

and true progression with higher diagnostic accuracy than standard MR imaging. [13] Recent studies with a larger glioblastoma patient cohort reported a diagnostic accuracy of FET PET of at least 85% for differentiating both typical (within 12 weeks) and late (> 12 weeks) pseudoprogression after radiochemotherapy completion from true tumour progression (***Figure 1***)[54].

Pseudoprogression after immunotherapy has been reported using FET PET in a small retrospective pilot study in patients with malignant melanoma brain metastasis treated with ipilimumab or nivolumab[103].

TBR, uptake kinetics and tumour volumes using FET PET have been evaluated for their value in monitoring stereotactic brachytherapy using iodine-125 seeds[104]. FET PET correctly differentiated with a high diagnostic accuracy late posttherapeutic effects after 6 months from local tumour progression in patients with recurrent high-grade glioma.

*Comparison/combination of methods*

Perfusion-derived and PET-derived measures are considered the most reliable when it comes to discerning tumour from radiation necrosis. ASL may be preferable over

DSC-perfusion imaging because it does not suffer from T1 leakage effects and it allows for quantitative measurement of CBF[97].

In clinical practice a combination of MR imaging sequences are used and they can be complementary. When the diagnosis is unclear based on MR imaging alone, PET-imaging can be considered. An ideal situation would be to use hybrid PET-MR imaging. Information on tissue perfusion, cellularity, integrity of neurons, anaerobic glycolysis during hypoxia, status of cellular membranes and metabolic pathways can then be acquired in one setting[5].

## Angiogenesis inhibitors and pseudoresponse

*Background*

Angiogenesis inhibitors, such as the VEGF-inhibitor bevacizumab, are now used in variety of tumours including (recurrent) glioblastoma and meningioma. In addition, bevacizumab is now used to alleviate oedema surrounding the tumour, but also oedema due to radiation necrosis. Due to vascular normalisation 'leaky' tumour vasculature is normalised and new vessel growth is inhibited. This not only reduces oedema but also reduces or even complete dissolution of tumour enhancement. This phenomenon is known as pseudoresponse because the tumour may still present[107].

With radiation necrosis already difficult to distinguish from residual or recurrent tumour, the addition of angiogenesis inhibitors further complicates image interpretation as it can mask the tumour as well as reduce radiation necrosis effects. Varying or mixed response to the treatment between patients further plays a confounding role[108,109]. In the context of treatment for radiation necrosis, patients responding to bevacizumab treatment only infrequently show recurrence or progression of radiation necrosis after discontinuation[110].

*PET imaging*

The problem of accurately identifying non-enhancing tumour (pseudoresponse) has been investigated using amino acid PET to assess treatment response to antiangiogenic therapy[111]. Recent studies and case reports indicate that FET and FDOPA PET are useful in the context of pseudoresponse both detecting and ruling out the presence of tumour[54]. FET and FDOPA PET have also been used to predict a favourable outcome in responders to bevacizumab[54].

A cost effectiveness analysis of FET PET for therapy monitoring of antiangiogenic therapy suggests that the combined use of MR imaging and FET PET in the management of these patients have the potential to avoid overtreatment and corresponding costs, as well as unnecessary patient side effect[112].

## LATE EFFECTS OF RADIOTHERAPY

In addition to radiation necrosis, radiotherapy has other late effects on the brain parenchyma, including demyelination, vascular abnormalities and atrophy. Radiation-induced tumours and malignant transformation have also been reported[87,113]. The extent of these effects is related to total radiation dose, field size, number of fractions and frequency, chemotherapy and other medication (methotrexate, corticosteroids, anti-epileptic drugs), patient survival and age at the time of radiation therapy[87].

### White matter abnormalities

White matter is rich in glial cells, such as oligodendrocytes, which are more sensitive to radiation than neurons[43]. White matter damage is a common finding in irradiated patients and includes reactive gliosis, inflammation, oedema, demyelination, atrophy, coagulative necrosis, cavitation/cysts and calcification[87,114]. These different entities are difficult to distinguish on histological data and practically impossible to differentiate with MR imaging. White matter damage is visible as atrophy and/or T2w/FLAIR hyperintensity, also known as leukoencephalopathy[87,92]. The damage can be limited to small discrete lesions or there can be large confluent areas.

Radiation-induced damage to the white matter starts to appear on T2w/FLAIR images just months after treatment and is generally more severe in older patients[113]. Areas with limited blood supply, such as the periventricular white matter, are affected more than for instance the arcuate fasciculus which also receives cortical arterial supply[88,89]. Before abnormalities are visible on the T2w/FLAIR images, DTI can already pick up changes in white matter, using parameters such as MD, FA, and diffusivity perpendicular and parallel to the white matter fibres[115]. It has been postulated that some of these observed changes may be reversible[116].

### Grey matter abnormalities

Because neurons are less sensitive to radiation than glial cells the grey matter is generally less affected than white matter. Effects that occur are cortical thinning, irregularity within the cortex (visible as T2w-hyperintensity) and blurring of the grey matter white matter junction[92,117]. Both grey and white matter damage can result in cognitive decline with deficits in learning, working memory and executive functions. Symptoms are more prominent when specific areas, such as the hippocampus and corpus callosum, are damaged[118].

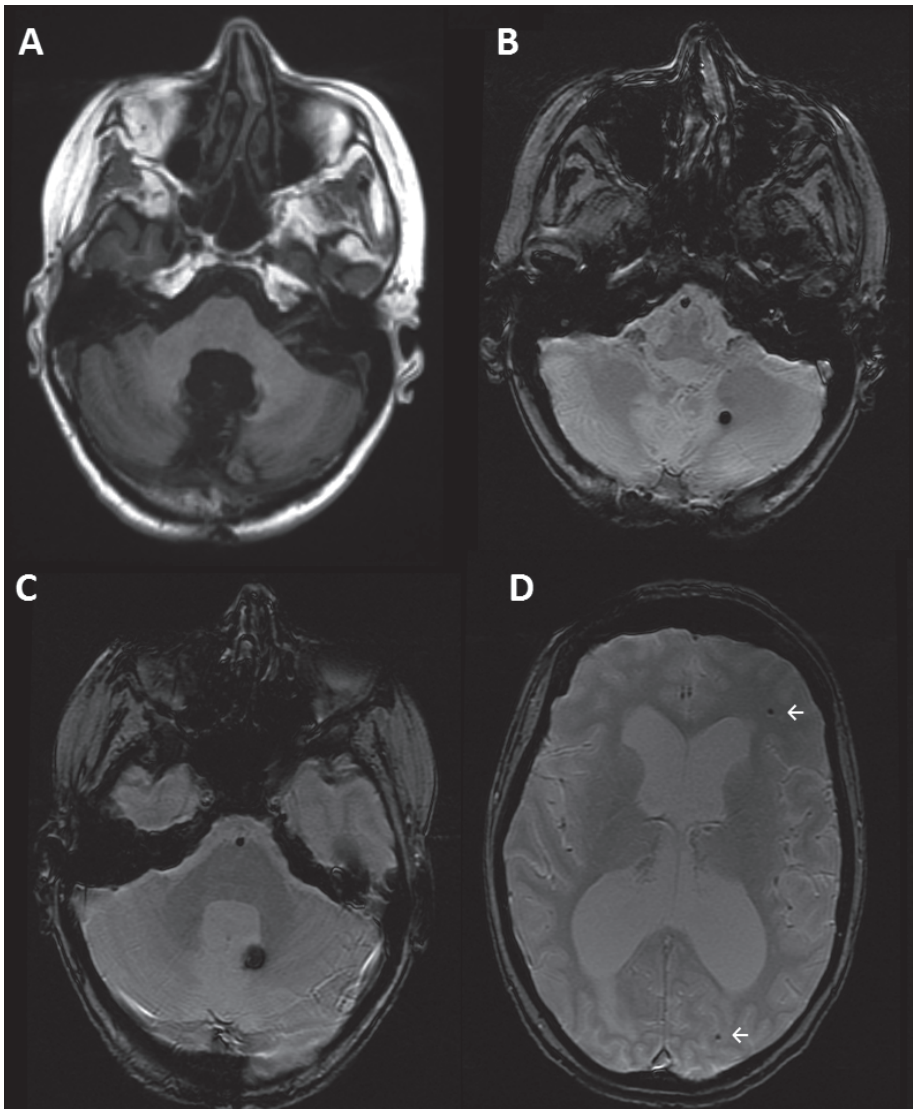


**Figure 7.** 35-year old woman treated for medulloblastoma 14 years ago. After subtotal resection, the tumour was irradiated (57.5Gy) and there has been no recurrent disease. T1w-image shows post-operative effects in the posterior fossa (**A**). The T2* (gradient echo) sequence shows multiple lesions with signal loss infra- and supratentorially (**B**, **C**, and **D**), consistent with cavernomas.

## Vascular changes

Direct damage to endothelial cells leads to an increase in permeability, vasogenic oedema, ischemia and hypoxia. Complications that develop after four months include lacunar infarcts, microbleeds, large-vessel occlusions with moya-moya syndrome, (capillary) teleangiectasias, cavernomas (***Figure 7***), and stroke[86].

A rare late complication after radiotherapy is the so-called SMART syndrome: Stroke-like Migraine Attacks after Radiation Therapy (***Figure 8***). Patients have transient clinical symptoms and radiological findings suggestive of tumour recurrence such as unilateral enhancement of the cortex and T2w-hyperintense white matter. The posterior regions of the brain is predominantly involved. The effects are reversible[119].

## Radiation-induced tumours and malignant transformation

A radiation-induced tumour is a new tumour that grows within the radiation field and different histology from the original tumour. Tumours most often encountered are meningiomas, followed by glioma and sarcoma[87,113]. The reported incidence of radiation-induced tumours is 2.6% in irradiated children. In adults however, the incidence is much lower[87,120].

Malignant transformation of meningioma due to irradiation is disputed. The reported incidence is 2.2%, but since malignant transformation of meningioma can also occur in the absence of radiotherapy, the true incidence is probably lower. Vestibular schwannoma has been reported to undergo malignant transformation due to radiation therapy in 0.3% of cases[73,121].

## PET imaging

Treatment effects may decrease FDG uptake in the treatment area as well as in brain regions that receive synaptic input from the treated area.

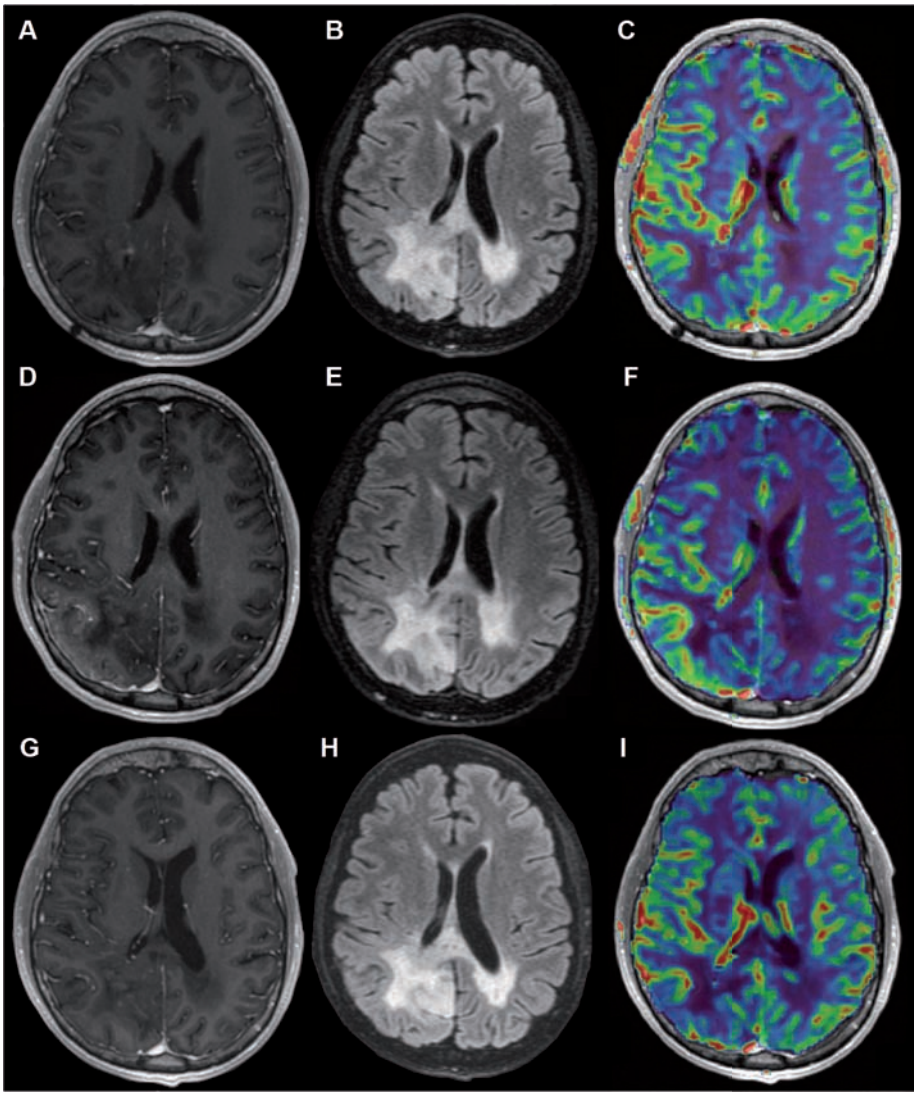


**Figure 8.** 43-year old male with oligodendroglioma initially treated with radiotherapy (50.4Gy) 6 years previously and with chemotherapy at progression 4 years later. T1w post-contrast (**A**), FLAIR (**B**), and rCBV (**C**) after therapy show stable residual abnormalities. The patient subsequently developed headaches and disorientation. On the T1w post-contrast image there is enhancement of the cortex (**D**) adjacent to the FLAIR hyperintense area (**E**). rCBV is increased in the enhancing area (**F**). At 2 months' follow-up imaging findings had regressed (**G**, **H**, **I**). Symptoms and imaging findings were consistent with SMART-syndrome.

## REFERENCES


1. Symms M, Jager H, Schmierer M, Yousry T. A review of structural magnetic resonance neuroimaging. J Neurol Neurosurg Psychiatry 2004;75(9):1235-1244.
2. Soares JM, Marques P, Alves V, Sousa N. A hitchhiker's guide to diffusion tensor imaging. Fron Neurosci 2013;7:31.
3. Shim WH, Kim HS, Choi C-G, Kim SJ. Comparison of apparent diffusion coefficient and intravoxel incoherent motion for differentiating among glioblastoma, metastasis, and lymphoma focusing on diffusion-related parameter. PLoS One 2015;10(7):e134761.
4. Paulson ES, Schmainda KM. Comparison of dynamic susceptibility-weighted contrast-enhanced MR methods: recommendations for measuring relative cerebral blood volume in brain tumors. Radiology 2008;249(2):601-613.
5. Ferda J, Ferdova E, Hes O, Mracek J, Kreuzberg B, Baxa J. PET/MRI: multiparametric imaging of brain tumors. Eur J Radiol 2017;94:A14-A25.
6. Cebeci H, Aydin O, Ozturk-Isik E, et al. Assessment of perfusion in glial tumors with arterial spin labelling; comparison with dynamic susceptibility contrast method. Eur J Radiol 2014;83(10):1914-1919.
7. Horska A, Barker PB. Imaging of brain tumors: MR spectroscopy and metabolic imaging. Neuroimaging Clin N Am 2010;20(3):293-310.
8. Kogan F, Hariharan H, Reddy R. Chemical exchange saturation transfer (CEST) imaging: description of technique and potential clinical applications. Curr Radiol Rep 2013;1(2):102-114.
9. Sugo N, Yokota K, Kondo K, et al. Early dynamic 201TI SPECT in the evaluation of brain tumours. Nuclear Medicine Communications 2006;27(2):143-149.
10. Prigent-Le Jeune F, Dubois F, Perez S, Blond S, Steinling M. Technetium-99m sestamibi brain SPECT in the follow-up of glioma for evaluation of response to chemotherapy: first results. Eur J Nucl Med Mol Imaging 2004;31(5):714-719.
11. Varrone A, Asenbaum S, van der Borght T, et al. EANM procedure guidelines for PET brain imaging using [18F]FDG, version 2. Eur J Nucl Med Mol Imaging 2009;36(12):2103-2110.
12. Herholz K, Langen KJ, Schiepers C, Mountz JM. Brain tumors. Semin Nucl Med 2012;42(6):356-370.
13. Albert NL, Weller M, Suchorska B, et al. Response Assessment in Neuro-Oncology working group and European Association for Neuro-Oncology recommendations for the clinical use of PET imaging in gliomas. Neuro Oncol 2016;18(9):1199-1208.
14. Bergström M, Collins VP, Ehrin E, et al. Discrepancies in brain tumor extent as shown by computed tomography and positron emission tomography using [68Ga]EDTA, [11C]glucose, and [11C]methionine. J Comput Assist Tomogr 1983;7(6):1062-1066.
15. Aki T, Nakayama N, Yonezawa S, et al. Evaluation of brain tumors using dynamic 11C-methionine-PET. J Neurooncol 2012;109(1):115-122.
16. Calcagni NL, Galli G, Giordano A, et al. Dynamic O-(2-[18F]fluorethyl)-L-tyrosine (F-18 FET) PET for glioma grading: assessment of individual probability of malignancy. Clin Nucl Med 2011;36(10): 841-847.
17. Ceccon G, Lohmann P, Stoffels G, et al. Dynamic O-(2-18F-fluorethyl)-L-tyrosine positron emission tomography differentiates brain metastasis recurrence from radiation injury after radiotherapy. Neuro Oncol 2017;19(2):281-288.
18. Langen KJ, Watts C. Neuro-oncology: amino acid PET for brain tumours – ready for the clinic? Nat Rev Neurol 2016;12(7):375-376.

**19.** Dutour A, Kumar U, Panetta R, et al. Expression of somatostatin receptor subtypes in human brain tumors. Int J Cancer 1998;76(5):620-627.

**20.** Rachinger W, Stoecklein VM, Terpolilli NA, et al. Increased 68Ga-DOTATATE uptake in PET imaging discriminates meningioma and tumor-free tissue. J Nucl Med 2015;56(3):347-353.

**21.** Galldiks N, Albert NL, Sommerauer M, et al. PET imaging in patients with meningioma-report of the RANO/PET group. Neuro oncol 2017;19(12):1576-1587.

**22.** Chen W, Delaloye S, Silverman DH, et al. Predicting treatment response of malignant gliomas to bevacizumab and irinotecan by imaging proliferation with [18F] fluorothymidine positron emission tomography: a pilot study. J Clin oncol 2007;25(30):4714-4721.

**23.** Wardak M, Schiepers C, Cloughesy TF, Dahlbom M, Phelps ME, Huang SC. $^{18}$F-FLT and $^{18}$F-FDOPA PET kinetics in recurrent brain tumors. Eur J Nucl Med Mol Imaging 2014;41(6):1199-1209.

**24.** Lee ST, Scott AM. Hypoxia positron emission tomography imaging with 18f-fluoromisonidazole. Semin Nucl Med 2007;37(6):451-461.

**25.** Spence AM, Muzi M, Swanson KR, et al. Regional hypoxia in glioblastoma multiforme quantified with [18F]fluoromisonidazole positron emission tomography before radiotherapy: correlation with time to progression and survival. Clin Cancer Res 2008;14(9):2623-2630.

**26.** Su Z, Roncaroli F, Durrenberger PF, et al. The 18-kDa mitochondrial translocator protein in human gliomas: an 11C-(R):PK11195 PET imaging and neuropathology study. J Nucl Med 2015;56(4):512-517.

**27.** Awde AR, Bolsgard R, Theze B, et al. The translocator protein radioligand 18F-DPA-714 monitors antitumor effect of erufosine in a rat 9L intracranial glioma model. J Nucl Med 2013;54(12):2125-2131.

**28.** Gomez-Rio M, Testart Dardel N, Santiago Chinchilla A, et al. $^{18}$F-Fluorocholine PET/CT as a complementary tool in the follow-up of low-grade glioma: diagnostic accuracy and clinical utility. Eur J Nucl Med Mol Imaging 2015;42(6):886-895.

**29.** Rottenburger C, Hentschel M, Kelly T, et al. Comparison of C-11 methionine and C-11 choline for PET imaging of brain metastases: a prospective pilot study. Clin Nucl Med 2011;36(8):639-642.

**30.** Stupp R, Brada M, van den Bent MJ, et al. High-grade glioma: ESMO Clinical Practice Guidelines for diagnosis, treatment and follow-up. Ann Oncol 2014;25 Suppl 3:iii93-101.

**31.** Nifterik van KA, van den Berg J, Stalpers LJ, et al. Differential radiosensitizing potential of temozolomide in MGMT promotor methylated glioblastoma multiforme cell lines. Int J Radiat Oncol Biol Phys 2007;69(4):1246-1253.

**32.** Chalmers AJ, Ruff EM, Martindale C, Lovegrove N, Short SC. Cytotoxic effects of temozolomide and radiation are additive- and schedule-dependent. Int J Radiat Oncol Phys 2009;75(5):1511-1519.

**33.** Macdonald DR, Cascino TL, Schold SC Jr, Cairncross JG. Response criteria for phase II studies of supratentorial malignant glioma. J Clin Oncol 1990;8(7):1277-1280.

**34.** Wen PY, Macdonald DR, Reardon DA, et al. Updated response assessment criteria for high-grade gliomas: response assessment in neuro-oncology working group. J Clin Oncol 2010;28(11):1963-1972.

**35.** Inoue T, Ogasawara K, Beppu T, Ogawa A, Kabasawa H. Diffusion tensor imaging for preoperative evaluation of tumor grade in gliomas. Clin Neurol Neurosurg 2005;107(3):174-180.

**36.** Tsien C, Cao Y, Chenevert T. Clinical applications for diffusion magnetic resonance imaging in radiotherapy. Semin Radiat Oncol 2014;24(3):218-226.

**37.** Bent van den MJ, Wefel JS, Schiff D, et al. Response assessment in neuro-oncology (a report of the RANO group): assessment of outcome in trials of diffuse low-grade gliomas. Lancet Oncol 2011; 12(6):583-593.

**38.** Fuss M, Wenz F, Scholdei R, et al. Radiation-induced regional cerebral blood volume (rCBV) changes in normal brain and low-grade astrocytomas: quantification and time and dose-dependent occurrence. Int J Radiat Oncol Biol Phys 2000;48(1):53-58.

**39.** Petr J, Platzek I, Seiditz A, et al. Early and late effects of radiochemotherapy on cerebral blood flow in glioblastoma patients measured with non-invasive perfusion MRI. Radiother oncol 2016;118(1): 24-28.

**40.** Kong DS, Kim ST, Kim EH, et al. Diagnostic dilemma of pseudoprogression in the treatment of newly diagnosed glioblastomas: the role of assessing relative cerebral blood flow volume and oxygen-6-methylguanine-DNA-methyltransferase promotor methylation status. AJNR Am J Neuroradiol 2011;32(2):382-387.

**41.** Sugahara T, Korogi Y, Tomiguschi S, et al. Posttherapeutic intraaxial brain tumor: the value of perfusion-sensitive contrast-enhanced MR imaging for differentiating tumor recurrence from nonneoplastic contrast-enhancing tissue. AJNR Am J Neuroradiol 2000;21(5):901-909.

**42.** Peca C, Pacelli R, Elefante A, et al. Early clinical and neuroradiological worsening after radiotherapy and concomitant temozolomide in patients with glioblastoma: tumour progression or radionecrosis? Clin Neuro Neurosurg 2009;111(4):331-334.

**43.** Sundgren PC. MR spectroscopy in radiation injury. AJNR Am J Neuroradiol 2009;30(8):1469-1476.

**44.** Walecki J, Sokol M, Pieniazek P, et al. Role of short TE 1H-MR spectroscopy in monitoring of postoperation irradiated patients. Eur J Radiol 1999;30(2):154-161.

**45.** Colavolpe C, Chinot O, Metellus P, et al. FDG-PET predicts survival in recurrent high-grade gliomas treated with bevacizumab and irinotecan. Neuro Oncol 2012;14(5):649-657.

**46.** Dunet V, Pomoni A, Hottinger A, Nicod-Lalonde M, Prior JO. Performance of 18F-FET versus 18F-FDG-PET for the diagnosis and grading of brain tumors: systematic review and meta-analysis. Neuro Oncol 2016;18(3):426-434.

**47.** Mertens K, Acou M, van Hauwe J, et al. Validation of 18F-FDG PET at conventional and delayed intervals for the discrimination of high-grade from low-grade gliomas: a stereotactic PET and MRI study. Clin Nucl Med 2013;38(7):495-500.

**48.** Charnley N, West CM, Barnett CM, et al. Early change in glucose metabolic rate measured using FDG-PET in patients with high-grade glioma predicts response to temozolomide but not temozolomide plus radiotherapy. Int J Radiat Oncol Biol Phys 2006;66(2):331-338.

**49.** Suchorska B, Jansen NL, Linn J, et al. Biological tumor volume in 18FET-PET before radiochemotherapy correlated with survival in GBM. Neurology 2015;84(7):710-719.

**50.** Piroth MD, Pinkawa M, Holy R, et al. Prognostic value of early [18F]fluoroethyltyrosine positron emission tomography after radiochemotherapy in glioblastoma multiforme. Int J Radiat Oncol Biol Phys 2011;80(1):176-184.

**51.** Galdiks N, Langen KJ, Holy R, et al. Assessment of treatment response in patients with glioblastoma using O-(2-18F-fluoroethyl)-L-tyrosine PET in comparison to MRI. J Nucl Med 2012;53(7): 1048-1057.

**52.** Voges J, Herholz K, Hölzer T, et al. 11C-methionine and 18F-2-fluorodeoxyglucose positron emission tomography: a tool for diagnosis of cerebral glioma and monitoring after brachytherapy with 125I seeds. Stereotact Funct Neurosurg 1997;69(1-4 Pt2):129-135.

**53.** Würker M, Herholz K, Voges J, et al. Glucose consumption and methionine uptake in low-grade gliomas after iodine-125 brachytherapy. Eur J Nucl Med 1996;23(5):583-586.

**54.** Galdiks N, Law I, Pope WB, Arbizu J, Langen KJ. The use of amino acid PET and conventional MRI for monitoring of brain tumor therapy. Neuroimage Clin 2016;13:386-394.

**55.** Galdiks N, Kracht LW, Burghaus L, et al. Use of 11C-methionine PET to monitor the effects of temozolomide chemotherapy in malignant gliomas. Eur J Nucl Med Mol Imaging 2006;33(5):516-524.

**56.** Wyss M, Hofer S, Bruehlmeier M, et al. Early metabolic responses in temozolomide treated low-grade glioma patients. J Neuroncol 2009;95(1):87-93.

**57.** Roelcke U, Wyss M, Nowosielski M, et al. Amino acid positron emission tomography in monitor chemotherapy response and predict seizure control and progression-free survival in WHO grade II gliomas. Neuro Oncol 2016;18(5):744-751.

**58.** Galdiks N, Rapp M, Stoffels G, et al. Response assessment of bevacizumab in patients with recurrent malignant glioma using [18F]Fluoroehtyl-L-tyrosine PET in comparison to MRI. Eur J Nucl Med Mol Imaging 2013;40(1):22-33.

**59.** Schwarzenberg J, Czernin J, Cloughesy TF, et al. Treatment response evaluation using 18F-FDOPA PET in patients with recurrent malignant glioma on bevacizumab therapy. Clin Cancer Res 2014; 20(13):3550-3559.

**60.** Louis DN, Perry A, Reifenberger G, et al. The 2016 World Health Organization Classification of Tumor of the Central Nervous System: a summary. Acta Neuropathol 2016;131(6):803-820.

**61.** Haldorsen IS, Espeland A, Larsson EM. Central nervous system lymphoma: characteristic findings on traditional and advanced imaging. AJNR Am J Neuroradiol 2011;32(6):984-892.

**62.** Abrey LE, Batchelor TT, Ferreri AJ, et al. Report of an international workshop to standardize baseline evaluation and response criteria for primary CNS lymphoma. J Clin Oncol 2005;23(22): 5034-5043.

**63.** Makino K, Hirai T, Nakamura H, et al. Does adding FDG-PET to MRI improve the differentiation between primary cerebral lymphoma and glioblastoma? Observer performance study. Ann Nucl Med 2011;25(6):432-438.

**64.** Hoffman JM, Waskin HA, Schifter T, et al. FDG-PET in differentiating lymphoma from nonmalignant central nervous system lesions in patients with AIDS. J Nucl Med 1993;34(4):567-575.

**65.** Sathekge M, Goethals I, Maes A, van de Wiele C. Positron emission tomography in patients suffering from HIV-1 infection. Eur J Nucl Med Mol Imaging 2009;36(7):1176-1184.

**66.** Kawase Y, Yamamoto Y, Kameyama R, Kawai N, Kudomi N, Nishiyama Y. Comparison of 11C-methionine PET and 18F-FDG PET in patients with primary central nervous system lymphoma. Mol Imaging Biol 2011;13(6):1284-1289.

**67.** Kawai N, Miyake K, Yamamoto Y, Nishiyama Y, Tamiya T. 18F-FDG PET in the diagnosis and treatment of primary central nervous system lymphoma. Biomed Res Int 2013;2013:247152.

**68.** Nussbaum ES, Djalillian HR, Cho KH, Hall WA. Brain metastases. Histology, multiplicity, surgery, and survival. Cancer 1996;78(8):1781-1788.

**69.** Lippitz B, Lindquist C, Paddick I, Peterson D, O'Neill K, Beaney R. Stereotactic radiosurgery in the treatment of brain metastases: the current evidence. Cancer Treat Rev 2014;40(1):48-59.

**70.** Lin NU, Lee EQ, Aoyama H, et al. Response assessment criteria for brain metastases: proposal from the RANO group. Lancet Oncol 2015;16(6):e270-278.

**71.** Lin NU, Lee EQ, Aoyama H, et al. Challenges relating to solid tumour brain metastases in clinical trials, part 1: patient population, response, and progression. A report from the RANO group. Lancet Oncol 2013;14(10):e396-406.

**72.** Belohlavek O, Simonova G, Kantorova I, Novotny J Jr, Liscak R. Brain metastases after stereotactic radiosurgery using the Leksell gamma knife: can FDG PET help to differentiate radionecrosis from tumour progression? Eur J Nucl Med Mol Imaging 2003;30(1):96-100.

**73.** Rogers L, Barani I, Chamberlain M, et al. Meningiomas: knowledge base, treatment outcomes, and uncertainties. A RANO review. J Neurosurg 2015;122(1):4-23.

**74.** Alexiou GA, Gogou P, Markoula S, Kyritsis AP. Management of meninigomas. Clin Neurol Neurosurg 2010;112(3):177-182.

**75.** Kessler RA, Garzon-Muvdi T, Yang W, et al. Metastatic atypical and anaplastic meningioma: a case series and review of the literature. World Neurosurg 2017;101:47-56.

**76.** Nowak A, Dziedzic T, Krych P, Czernicki T, Kunert P, Marchel A. Benign versus atypical meningiomas: risk factors predicting recurrence. Neurol Neurochir Pol 2015;49(1):1-10.

**77.** Gabeau-Lacet D, Aghi M, Betensky RA, Barker FG, Loeffler JS, Louis DN. Bone involvement predicts poor outcome in atypical meningioma. J Neurosurg 2009;111(3):464-471.

**78.** Quant EC, Wen PY. Response assessment in neuro-oncology. Curr Oncol Rep 2011;13(1):5056.

**79.** Lee SR, Yang KA, Kim SK, Kim SH. Radiation-induced intratumoral necrosis and peritumoral edema after gamma knife radiosurgery for intracranial meningiomas. J Korean Neurosurg Soc 2012;52(2): 98-102.

**80.** Chang JH, Chang JW, Chol JY, Park YG, Chung SS. Complications after gamma knife radiosurgery for benign meningiomas. J Neurol Neurosurg Psychiatry 2003;74(2):226-230.

**81.** Cremerius U, Bares R, Weis J, et al. Fasting improves discrimination of grade 1 and atypical or malignant meningioma in FDG-PET. J Nucl Med 1997;38(1):26-30.

**82.** Ryttlefors M, Danfors T, Latini F, Montelius A, Blomquist E, Gudjonsson O. Long-term evaluation of the effect of hypofractionated high-energy proton treatment of benign meningiomas by means of (11)C-L-methionine positron emission tomography. Eur J Nucl Med Mol Imaging 2016;43(8): 1432-1443.

**83.** Afshar-Oromieh A, Giesel FL, Linhart HG, et al. Detection of cranial meningiomas: comparison of $^{88}$Ga-DOTATOC PET/CT and contrast-enhanced MRI. Eur J Nucl Med Mol Imaging 2012;39(9): 1409-1415.

**84.** Kunz WG, Jungblut LM, Kazmierczak PM, et al. Improved detection of transosseous meningioma using 66Ga-DOTATATE PET/CT compared with constrast-enhanced MRI. J Nucl Med 2017;58(10): 1580-1587.

**85.** Wick W, Chinot OL, Bendszus M, et al. Evaluation of pseudoprogression rates and tumor progression patterns in a phase III trial of bevacizumab plus radiotherapy/temozolomide for newly diagnosed glioblastoma. Neuro Oncol 2016;18(10):1434-1441.

**86.** Brandsma D, Stalpers L, Taal W, Sminia P, van den Bent MJ. Clinical features, mechanisms, and management of pseudoprogression in malignant gliomas. Lancet Oncol 2008;9(5):453-461.

**87.** Martino A, Krainik A, Pasteris C, et al. Neurological imaging of brain damages after radiotherapy and/or chimiotherapy. J Neuroradiol 2014;41(1):52-70.

**88.** Raimbault A, Cazals X, Lauvin MA, Destrieux C, Chapet S, Cottier JP. Radionecrosis of malignant glioma and cerebral metastasis: a diagnostic challenge in MRI. Diagn Interv Imaging 2014;95(10): 985-1000.

**89.** Kumar AJ, Leed NE, Fuller GN, et al. Malignant gliomas: MR imaging spectrum of radiation therapy- and chemotherapy-induced necrosis of the brain after treatment. Radiology 2000;217(2):377-384.

**90.** West van SE, de Bruin HG, van de Langerijt B, Swaak-Kragten AT, van den Bent MJ, Taal W. Incidence of pseudoprogression in low-grade gliomas treated with radiotherapy. Neuro Oncol 2017; 19(5):719-725.

**91.** Leeman JE, Clump DA, Flickinger JC, Mintz AH, Burton SA, Heron DE. Extent of perilesional edema differentiated radionecrosis from tumor recurrence following stereotactic radiosurgery for brain metastases. Neuro Oncol 2013;15(12):1732-1738.

**92.** Chan YL, Leung SF, King AD, Choi PH, Metreweli C. Late radiation injury to the temporal lobes: morphologic evaluation at MR imaging. Radiology 1999;213(3):800-807.

**93.** Castillo M, Smith JK, Kwock L, Wilber K. Apparent diffusion coefficients in the evaluation of high-grade cerebral gliomas. AJNR Am J Neuroradiol 2001;22(1):60-64.

**94.** Xu JL, Li YL, Lian JM, et al. Distinction between postoperative recurrent glioma and radiation injury using MR diffusion tensor imaging. Neuroradiology 2010;52(12):1193-1199.

**95.** Hu LS, Baxter LC, Smith KA, et al. Relative cerebral blood volume values to differentiate high-grade glioma recurrence from posttreatment radiation effect: direct correlation between image-guided tissue histopathology and localized dynamic susceptibility-weighted contrast-enhanced perfusion MR imaging measurements. AJNR Am J Neuroradiol 2009;30(3):552-558.

**96.** Gahramanov S, Raslan AM, Muldoon LL, et al. Potential for differentiation of pseudoprogression from true tumor progression with dynamic susceptibility-weighted contrast-enhanced magnetic resonance imaging using ferumoxytol vs. gadoteridol: a pilot study. Int J Radiat Oncol Biol Phys 2011;79(2):514-523.

**97.** Ozsunar Y, Mullins ME, Kwong K, et al. Glioma recurrence versus radiation necrosis? A pilot comparison of arterial spin-labeled dynamic susceptibility contrast enhanced MRI, and FDG-PET imaging. Acad Radiol 2010;17(3):282-290.

**98.** Elias AE, Carlos RC, Smith EA, et al. MR spectroscopy using normalized and non-normalized metabolite ratios for differentiating recurrent brain tumor from radiation injury. Acad Radiol 2011; 18(9):1101-1108.

**99.** Nakajima T, Kumabe T, Kanamori M, et al. Differential diagnosis between radiation necrosis and glioma progression using sequential proton magnetic resonance spectroscopy and methionine positron emission tomography. Neurol Med Chr (Tokyo) 2009;49(9):394-401.

**100.** Dankbaar JW, Snijders TJ, Robe PA, et al. The use of $^{18}$F-FDG PET to differentiate progressive disease from treatment induced necrosis in high grade glioma. J Neurooncol 2015;125(1):167-175.

**101.** Laere van K, Ceyssens S, van Calenbergh F, et al. Direct comparison of 18F-FDG and 11C-methionine PET in suspected recurrence of glioma: sensitivity, inter-observer variability and prognostic value. Eur J Nucl Med Mol Imaging 2005;32(1):39-51.

**102.** Santra A, Kumar R, Sharma P, et al. F-18 FDG PET-CT in patients with recurrent glioma: comparison with contrast enhanced MRI. Eur J Radiol 2012;81(3):508-513.

**103.** Kebir S, Rauschenbach L, Galldiks N, et al. Dynamic O-(2-[18F]fluoroethyl)-L-tyrosine PET imaging for the detection of checkpoint inhibitor-related pseudoprogression in melanoma brain metastases. Neuro Oncol 2016;18(10):1462-1464.

**104.** Jansen NL, Suchorska B, Schwarz SB, et al. [18F]fluoroethyltyrosine-positron emission tomography-based therapy monitoring after stereotactic iodine-125 brachytherapy in patients with recurrent high-grade glioma. Mol Imaging 2013;12(3):137-147.

**105.** Brandsma D, van den Bent MJ. Pseudoprogression and pseudoresponse in the treatment of gliomas. Curr Opin Neurol 2009;22(6):633-638.

**106.** Norden AD, Young GS, Setayesh K, et al. Bevacizumab for recurrent malignant gliomas: efficacy, toxicity, and patterns of recurrence. Neurology 2008;70(10):779-787.

**107.** Nayak L, Iwamoto FM, Rudnick JD, et al. Atypical and anaplastic meninigomas treated with bevacizumab. J Neurooncol 2012;109(1):187-193.

**108.** Gonzalez J, Kumar AJ, Conrad CA, Levin VA. Effect of bevacizumab on radiation necrosis of the brain. Int J Radiat Oncol Biol Phys 2007;67(2):232-236.

**109.** Sanborn MR, Danish SF, Rosenfeld MR, O'Rourke D, Lee JY. Treatment of steroid refractory, Gamma Knife related radiation necrosis with bevacizumab: case report and review of the literature. Clin Neurol Neurosurg 2011;113(9):798-802.

**110.** Levin VA, Bidaut L, Hou P, et al. Randomized double-blind placebo-controlled trial of bevacizumab therapy for radiation necrosis of the central nervous system. Int J Radiat Oncol Biol Phys 2011; 79(5):1487-1495.

**111.** Reithmeier T, Lopez WO, Spehl TS, et al. Bevacizumab as salvage therapy for progressive brain stem gliomas. Clin Neurol Neurosurg 2013;115(2):165-169.

**112.** Heinzel A, Müller D, Langen KJ, et al. The use of O-(2-18F-fluoroethyl)-L-tyrosine PET for treatment management of bevacizumab and irinotecan in patients with recurrent high-grade glioma: a cost-effectiveness analysis. J Nucl Med 2013;54(8):1217-1222.

**113.** Johannesen TB, Lien HH, Hole KH, Lote K. Radiological and clinical assessment of long-term brain tumour survivors after radiotherapy. Radiother Oncol 2003;69(2):169-176.

**114.** Schultheiss TE, Kun LE, Ang KK, Stephens LC. Radiation response of the central nervous system. Int J Radiat Oncol Biol Phys 1995;31(5):1093-1112.

**115.** Nagesh V, Tsien CI, Chenevert TL, et al. Radiation-induced changes in normal-appearing white matter in patients with cerebral tumors: a diffusion tensor imaging study. Int J Radiat Oncol Biol Phys 2008;70(4):1002-1010.

**116.** Tsui EY, Chan JH, Ramsey RG, et al. Late temporal lobe necrosis in patients with nasopharyngeal carcinoma: evaluation with combined multi-section diffusion weighted and perfusion weighted MR imaging. Eur J Radiol 2001;39(3):133-138.

**117.** Seibert TM, Karunamuni R, Kaifi S, et al. Cerebral cortex regions selectively vulnerable to radiation dose-dependent atrophy. Int J Radiat Oncol Biol Phys 2017;97(5):910-918.

**118.** Saad S, Wang TJ. Neurocognitive deficits after radiation therapy for brain malignancies. Am J Clin Oncol 2015;38(6):634-640.

**119.** Zheng Q, Yang L, Tan L-M, Qin L-X, Wang C-Y, Zhang H-N. Stroke-like migraine attacks after radiation therapy syndrome. Chin Med J (Engl) 2015;128)15):2097-2101.

**120.** Pollocl BE, Link MJ, Stafford SL, Parney IF, Garces YI, Foote RL. The risk of radiation-induced tumors or malignant transformation after single-fraction intracranial radiosurgery: results based on a 25-year experience. Int J Radiat Oncol Biol Phys 2017;97(5):919-923.

**121.** Al-Mefty O, Kadri PA, Pravdenkova S, Sawyer JR, Strangeby C, Husain M. Malignant progression in meningioma: documentation of a series and analysis of cytogenetic findings. J Neurosurg 2004; 101(2):210-218.

# Chapter 3.2

## Comparison of 2D (RANO) and volumetric methods for assessment of recurrent glioblastoma treated with bevacizumab – a report from the BELOB trial.

Renske Gahrmann
Martin van den Bent
Bronno van der Holt
René Vernhout
Walter Taal
Maaike Vos
Jan Cees de Groot
Laurens Beerepoot
Jan Buter
Zwenneke Flach
Monique Hanse
Bas Jasperse
Marion Smits

*NEURO ONCOL 2017;19(6)853-861.*

## ABSTRACT

Background. The current method for assessing progressive disease (PD) in glioblastoma is according to the Response Assessment in Neuro-Oncology (RANO) criteria. Bevacizumab-treated patients may show pseudo-response on post-contrast T1w, and a more infiltrative non-enhancing growth pattern on T2w/FLAIR-images. We investigated whether the RANO criteria remain the method of choice for assessing bevacizumab-treated recurrent glioblastoma when compared to various volumetric methods.

Methods. Patients with assessable MRI-data from the BELOB-trial (n=148) were included. Patients were treated with bevacizumab, lomustine, or both. At first and second radiological follow-up (6 and 12 weeks) PD was determined using the 2D RANO criteria and various volumetric methods based on enhancing tumor only and enhancing plus non-enhancing tumor. Differences in overall survival (OS) between PD and non-PD patients were assessed with the log-rank test and a cox-model. Hazard ratios (HR) and their 95% confidence-intervals were determined.

Results. For all patients together, all methods (except subtraction of non-enhancing from enhancing volume at first follow-up) showed significant differences in OS between PD and non-PD patients ($p<.001$). The largest risk-increase for death in case of PD at both first and second follow-up was found with the RANO criteria: HR = 2.81 (95% CI, 1.92-4.10) and HR = 2.80 (95% CI, 1.75-4.49) respectively. In the bevacizumab-treated patients, all methods assessed showed significant differences in OS between PD and non-PD patients. There were no significant differences between methods.

Conclusions. In the first 12 weeks, volumetric methods did not provide significant improvement over the RANO criteria as a post-treatment prognostic marker.

## Keywords

Recurrent glioblastoma, bevacizumab, RANO, volumetry

## Importance of study

Currently, the 2D RANO criteria are the method of choice for assessing progressive disease in glioblastoma. However, those treated with bevacizumab may show pseudo-response on post contrast T1w-images and non-enhancing tumor growth on T2w/FLAIR-images upon progression that may not optimally be captured with the 2D RANO criteria. We compared the 2D RANO criteria with various volumetric methods based on enhancement, subtraction and T2w/FLAIR abnormalities in this distinct patient group. The risk increase for death was determined based on the presence of progressive disease upon follow-up. The largest hazard ratios (HR) at first and second follow-up were found with the 2D RANO criteria: HR = 2.81 (95% CI, 1.92-4.10) and HR = 2.80 (95% CI, 1.75-4.49) respectively. We found no clear differences in prediction of overall survival between the 2D RANO and volumetric methods. The routine use of volumetric methods in clinical trials in recurrent glioblastoma is therefore not warranted.

## INTRODUCTION

Glioblastoma is the most common malignant primary brain tumor, comprising 15% of all primary brain and central nervous system tumors and almost half of all primary malignant brain tumors. The 5-year survival rate is only about 5% despite treatment of newly diagnosed patients with surgery, radiotherapy and concomitant and adjuvant temozolomide[1,2].

In 2009, the United States Food and Drug Administration (FDA) approved bevacizumab (Avastin®, Genentech, San Francisco) for second-line treatment in patients with recurrent glioblastoma based on the observed response rates from phase 2 trials with bevacizumab and irinotecan[3,4]. Bevacizumab is a humanized monoclonal antibody directed against Vascular Endothelial Growth Factor (VEGF), which inhibits angiogenesis and normalizes abnormally permeable tumor blood vessels[5,6]. This may also lead to a decrease (or complete disappearance) of enhancing tumor on post-contrast T1w-images without actual changes in tumor size. Due to this phenomenon of pseudo-responses the conventional MacDonald assessment criteria[6], that rely primarily on the assessment of enhancing lesions, were no longer sufficient and have been replaced by the Response Assessment in Neuro-Oncology or RANO criteria[7]. These have become the standard in clinical neuro-oncology and include the assessment of T2w/FLAIR (non-enhancing) abnormalities in addition to enhancing lesions. Progressive disease (PD) is defined as a ≥25% increase in the sum of the products of perpendicular diameters of enhancing tumor, a significant increase in non-enhancing tumor, the appearance of new lesions, or clinical deterioration. It has been shown that adding non-enhancing abnormalities based on T2w/FLAIR imaging to the response assessment in recurrent glioblastoma treated with bevacizumab may lead to earlier detection of PD[8].

Despite the inclusion of T2w/FLAIR assessment into the RANO criteria, the main focus of response evaluation remains on enhancing tumor. The observed initial decrease of enhancing tumor and increase in T2w/FLAIR abnormalities at progression[9,10] in patients treated with bevacizumab suggests that more advanced methods of assessment, such as volumetry, might improve prediction of overall survival (OS). This is particularly relevant to the assessment of T2w/FLAIR abnormalities, since it is defined as a qualitative, and not a quantitative change in volume. Volumetric assessments are likely to increase precision of measurements of enhancement in irregularly shaped tumors, such as glioblastoma, and T2w/FLAIR abnormalities are likely to be more reliably assessed quantitatively with volumetry.

The occurrence of pseudo-response, i.e. the decrease of tumor enhancement due to vascular normalization rather than a true anti-tumor effect in glioblastoma patients treated with VEGF inhibitors, has now been well documented and questions

arise whether further improvement of the RANO criteria is needed. Several studies have investigated the evaluation of tumor response using volumetric measures from both enhancing and non-enhancing recurrent glioblastoma treated with bevacizumab[9,11,12]. Boxerman et al[13] also directly compared 2D with volumetric methods in this specific patient group but did not assess the full RANO criteria. Ultimately, to be a reliable surrogate endpoint in phase I and II studies, response should reflect OS, the gold standard in oncology trials. Our aim was to determine whether in bevacizumab-treated recurrent glioblastoma volumetric methods are superior to the 2D RANO criteria in determining PD in association with OS.

For this purpose we used data from the BELOB-trial, which is the first randomized and properly controlled phase 2 trial in recurrent glioblastoma, comparing single-agent bevacizumab or lomustine with bevacizumab plus lomustine[14].

## METHODS

### Patients

A total of 148 eligible patients with first recurrence of glioblastoma were included in the BELOB-trial, a randomized controlled phase 2 trial in which patients received bevacizumab (Avastin®) (n=50), lomustine (n=46) or both (n=52). Patients were recruited between December 2009 and October 2011 from 5 University hospitals and 9 community hospitals in the Netherlands. Patients were at least 18 years of age and had received no prior treatment with anti-VEGF or nitrosoureas. All patients provided written informed consent according to national regulations. A more detailed description of the study and its findings can be found in Taal et al. 2014[14].

The primary endpoint of the BELOB trial was 9-month OS. Additional outcome measures were median progression-free survival (PFS), PFS at 6 and 12 months, median OS, OS at 6 and 12 months, and proportion of patients with objective response. In the current radiological analysis, OS was used as the endpoint.

### Scanning procedure

Patients underwent standardized MRI scanning at baseline and follow-up with approximately 6-week intervals, i.e. a follow-up scan was made after every treatment cycle. The standardized MRI protocol can be found in the ***Supplementary Files***. Imaging was performed at 1.5T and 3.0T scanners. During the study, MRI quality assessment was performed. Unfortunately, some patients still had incomplete imaging datasets as specified in the results section.

## PD assessment

The presence of PD was determined with the 2D RANO method (method 1) and 4 volumetric methods: total contrast-enhancing (CE) volume measured on T1w post-contrast images only (method 2), total CE volume measured on subtraction (post-contrast minus pre-contrast) images only (method 3), total CE volume (as measured on T1w post-contrast images) complemented with non-enhancing volume measured on FLAIR images (method 4), and total CE volume as measured on subtraction images complemented with non-enhancing volume (method 5).

RANO assessment to establish PD was performed centrally (pre- and post-contrast T1w- and T2w/FLAIR-images) by 2 independent reviewers (MB, MS). In case of disagreement, PD was decided by an adjudicator (BJ).

Volumes of enhancing areas and non-enhancing (FLAIR) abnormalities were measured on 3D T1w post-contrast and 3D FLAIR images, respectively, by a single rater (RG) using a semi-automated technique in BrainLab I-Plan 4.0 Cranial (BrainLab, Feldkirchen, Germany) software. This technique involves the manual placement of 'inclusion' and 'exclusion' points (***Figure 1***), after which an algorithm is used to render a volume of interest (VOI). All VOIs were visually checked in three directions and adjusted if needed.

In each scan, in case of more lesions all lesions were measured separately and summed for the current analysis to obtain a single volumetric measure of both the enhancing tumor and one of FLAIR abnormalities. Blood vessels, dura and necrotic areas were excluded. Enhancing areas were included in the FLAIR VOIs, because these areas are also hyperintense on FLAIR. The commonly T2w-hyperintese cortical

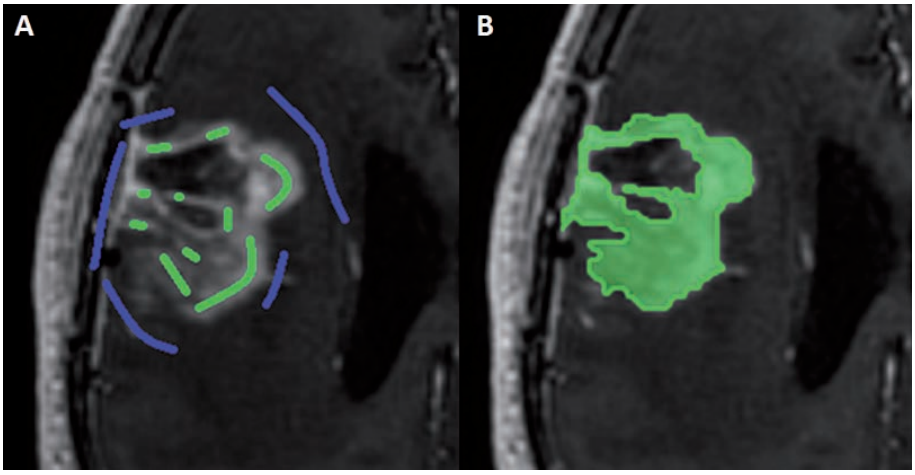


**Figure 1.** Example of segmentation in BrainLab I-Plan 4.0 Cranial using inclusion (green) and exclusion (blue) lines/points in the axial plane (**A**) and the resulting segmentation (**B**).

ribbon was excluded. Lesions clearly of vascular origin and periventricular apical capping (i.e. not continuous with FLAIR lesions and remaining unchanged in time) were excluded, as well as the septum pellucidem. FLAIR abnormalities when present in both left- and right hemispheres were measured separately when possible.

Subtraction images were created with FSL-FLIRT (FMRIB Software Library, Oxford, England) with custom scripts in AFNI (National Institute of Mental Health, Bethesda) created by Ellingson et al[15]. VOIs of resulting enhancing tumor areas were drawn manually in MRIcron (Chris Rorden, www.mrico.com, version 6.6.2013) by a single rater (RG). Necrotic areas, blood vessels and dura were excluded.

PD was defined according to the 2D RANO criteria (as described earlier) for method 1. For the volumetric methods (methods 2-5), PD was defined as ≥40% increase in enhancing/subtraction volume, which was the most commonly used threshold in previous literature[16-18], ≥25% increase of FLAIR volume[19], or the appearance of new lesions, whether enhancing or non-enhancing. The 40% threshold for volumetric assessment is based on an extrapolation from the ≥25% increase in the sum of perpendicular diameters of a 2D lesion to a 3D sphere-shape and the assumption that all increase in size is equal in every direction. Setting the threshold this high will ensure that only patients showing clear PD are categorized as such.

## Statistical analysis

Patients were classified as to PD or non-PD according to each of the 5 methods at both first and second follow-up scans. For each of the follow-up moments separately, OS was determined from the date of the scan to death from any cause. Patients still alive at last contact were censored. Kaplan-Meier survival curves were drawn from each follow-up time points for all patients from all treatments groups, as well as for patients treated either with bevacizumab (with/without lomustine) or lomustine separately. A log-rank test was used to determine the difference in OS between the PD and non-PD patients as established by each of the methods. To determine whether there were significant differences between methods in predicting OS, hazard ratios (HR) and their corresponding 95% confidence intervals (CI) were determined by means of a cox regression analysis per method, using each method as a single covariate. The HR was determined for all patients together and for the different treatment groups per method. The overlap of the corresponding 95% CIs was determined and conclusions were drawn based on the extent of overlap. Statistical analysis was performed using SPSS Statistics for Windows (IBM Corp. 2012, Version21.0, Armonk, NY).

A post-hoc power analysis (G*Power[20]) was performed for all patients together and for the two different treatment groups per method at both first and second follow-up to evaluate the validity of the results.

## RESULTS

### Patients

148 patients were included in the BELOB-trial. At first follow-up 10 patients were excluded from the analysis due to a lack of follow-up and missing data required for 2D RANO assessment. Some further patients had missing 3D T1w pre- and/or post-contrast or 3D FLAIR images, resulting in the following numbers of patients available for analysis at first follow-up: n=138 for method 1, n=121 for method 2, n=86 for method 3, n=109 for method 4, and n=89 for method 5. At second follow-up, at which time patients with prior PD or death had dropped out, the following numbers of patients with adequate imaging were available for analysis: n=83 for method 1, n=78 for method 2, n=71 for method 3, n=71 for method 4, and n=67 for method 5.

### Assessment of all patients from all treatment groups

Significant differences in OS (***Figures 2 and 3***) were found between all patients with PD and non-PD as determined with methods 1, 2, 4 and 5 at first follow-up, and with all 5 methods at second follow-up (***Table 1***). At first follow-up the highest risk increase for death was found for PD as determined with method 1, i.e. the RANO criteria, with an HR of 2.81 (95% CI, 1.92 – 4.10). In comparing the methods, the extent of overlap in CIs (>50%) indicates that there are no significant differences in HR. At second follow-up the highest risk increase was again found for PD determined with the RANO criteria (method 1), with an HR of 2.80 (95% CI, 1.75 – 4.49). Again, no significant differences were observed between methods as determined by the extent of overlap in CIs. For a graphic depiction of the direct comparison between the HRs and 95% CI we refer to the ***Supplementary Files (figure S1)***.

**Table 1.** Hazard ratios of each of the methods for all patients at first and second follow-up (FU1 and FU2).

| Method | HR (95% CI) FU1 | p-value | HR (95% CI) FU2 | p-value |
|---|---|---|---|---|
| 1. 2D RANO | 2.81 (1.92 – 4.10) | < .001 | 2.80 (1.75 – 4.49) | < .001 |
| 2. Contrast enhancing volume | 1.99 (1.29 – 3.05) | .002 | 2.17 (1.27 – 3.71) | .004 |
| 3. Subtraction volume | 1.80 (0.99 – 3.26) | .054 | 2.16 (1.27 – 3.68) | .005 |
| 4. Contrast enhancing + FLAIR volume | 2.45 (1.60 – 3.74) | <.001 | 2.57 (1.53 – 4.31) | <.001 |
| 5. Subtraction + FLAIR volume | 2.66 (1.61 – 4.38) | <.001 | 2.48 (1.47 – 4.18) | .001 |

### Assessment per treatment group

The post-hoc power analysis showed that power in the lomustine-only patient group was well below 80%, precluding meaningful analysis. Within the bevacizumab-treated group, power was also insufficient for a meaningful analysis at first follow-up for method 3 and at second follow-up for methods 2, 3 and 5. Differences in

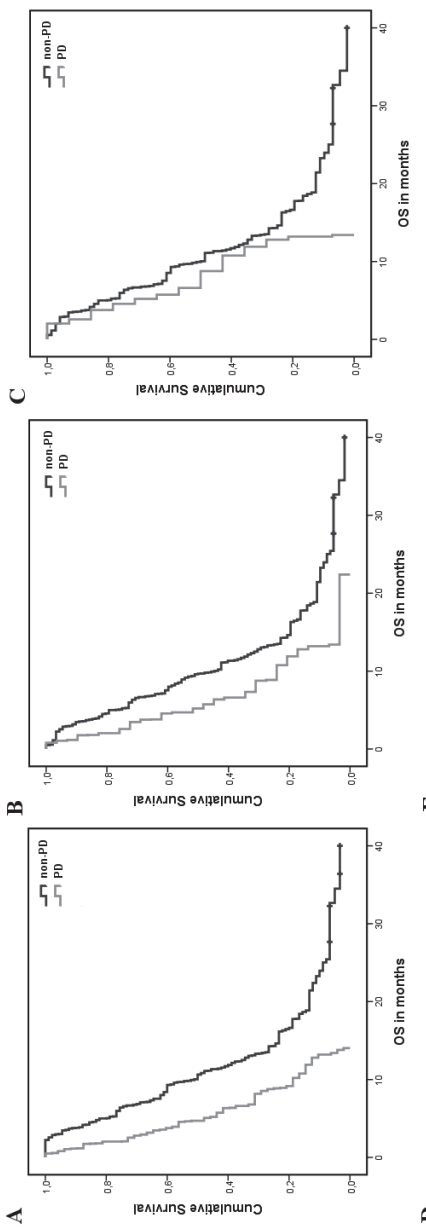


**Figure 2.** Kaplan-Meier curves of all progressive (PD) versus non-progressive (non-PD) patients for each of the methods at first follow-up. (**A**) 2D RANO, (**B**) Contrast enhancing volume, (**C**) Subtraction volume, (**D**) Contrast enhancing + FLAIR volume, and (**E**) Subtraction + FLAIR volume. OS = overall survival.

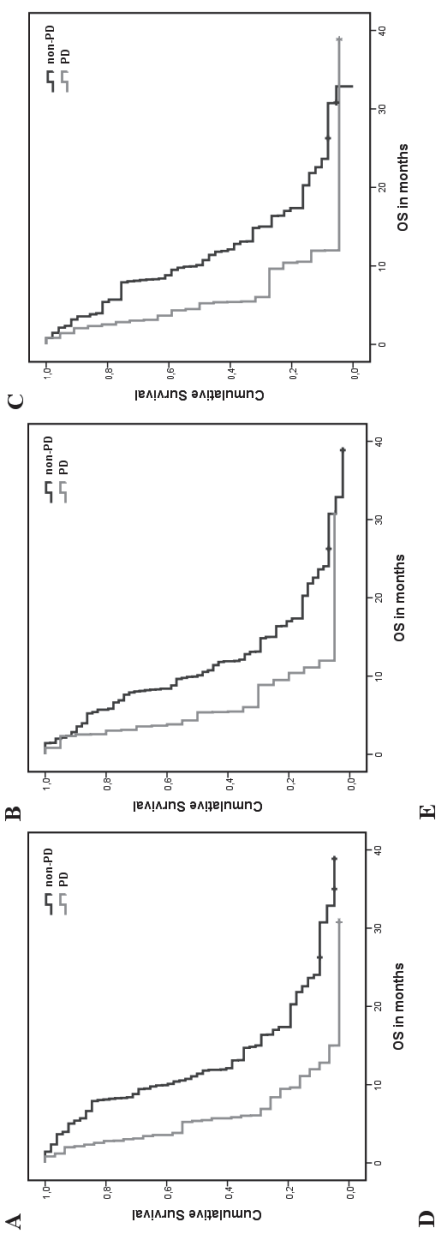


**Figure 3.** Kaplan-Meier curves of all progressive (PD) versus non-progressive (non-PD) patients for each of the methods at second follow-up. (**A**) 2D RANO, (**B**) Contrast enhancing volume, (**C**) Subtraction volume, (**D**) Contrast enhancing + FLAIR volume, and (**E**) Subtraction + FLAIR volume. OS = overall survival.

power between methods can be attributed to a difference in the number of patients available for analysis per method as well as differences in the number of patients classified as PD and non-PD.

In the bevacizumab-treated group significant differences in OS (***Figure 4***) were found between patients with PD and non-PD as determined with methods 1, 2, 4 and 5 at first follow-up, and with methods 1 and 4 at second follow-up (***Table 2***). The highest risk increase at first follow-up was found for PD as determined with method 2 (i.e. CE volume), with an HR of 7.21 (95% CI, 3.20 – 16.22). This was however not significantly different from other methods. At second follow-up only the results from methods 1 (i.e. RANO criteria) and 4 (i.e. combined analysis of CE and FLAIR volume) were deemed reliable (i.e. power >80%), with HRs of 2.44 (95% CI, 1.46 – 4.08) and 2.08 (95% CI, 1.16 – 3.73) respectively. These were not significantly different from each other. For a graphic depiction of the direct comparison between the HRs and 95% CI we refer to the ***Supplementary Files (Figure S1)***.

## Concordance between methods

Concordance rates between method 1 (2D RANO) and the volumetric methods (2-5) at first follow-up in all patients together and in the bevacizumab-treated group varied between 81.3% and 87.4%. For a more detailed report and individual examples we refer to the ***Supplementary Files (table S1 and Figures S2 and S3)***. There are several underlying reasons for discrepancies between methods in individual cases. The main reasons were: a) PD based on the increase of FLAIR abnormalities, which was not picked up using methods 2 and 3 (enhancing/subtraction volume), b) PD determined in 2D RANO based on mixed response, not picked up with volumetric methods because change in total (non-) enhancing volume was analyzed, c) lesions that did not reach the threshold for PD in volumetry (≥40% increase), while having reached the threshold for PD in 2D RANO (≥25% increase), and d) significant increase in FLAIR volume in volumetry (≥25% increase), not scored as significant in 2D RANO (no threshold).

**Table 2.** Hazard ratios of methods with sufficient power (>80%) for bevacizumab-treated patients only at first and second follow-up (FU1 and FU2).

| Method | HR (95% CI) FU1 | p-value | HR (95% CI) FU2 | p-value |
|---|---|---|---|---|
| 1. 2D RANO | 5.53 (3.12 – 9.80) | <.001 | 2.44 (1.46 – 4.08) | .001 |
| 2. Contrast enhancing volume | 7.21 (3.20 – 16.22) | <.001 | | |
| 4. Contrast enhancing + FLAIR volume | 5.94 (3.06 – 11.53) | <.001 | 2.35 (1.32 – 4.19) | .004 |
| 5. Subtraction + FLAIR volume | 5.63 (2.66 – 11.93) | <.001 | | |

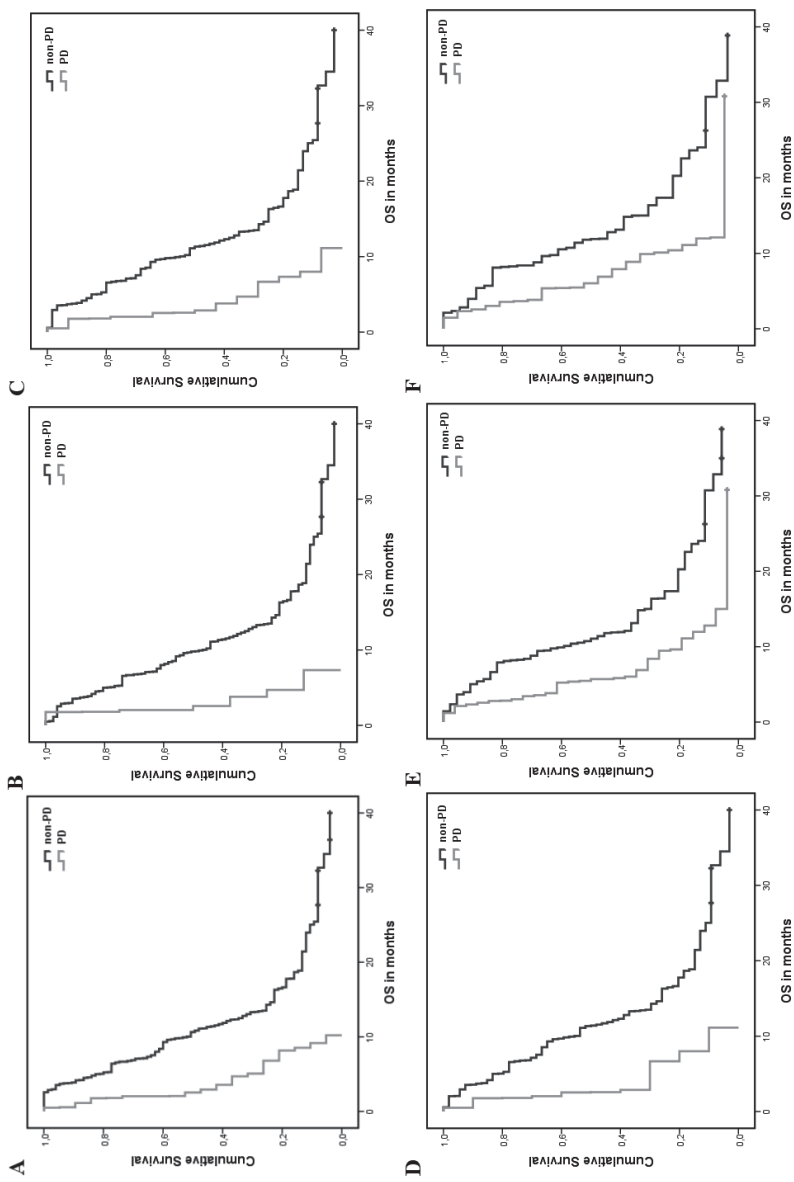


**Figure 4.** Kaplan-Meier curves of progressive (PD) versus non-progressive (non-PD) bevacizumab-treated patients only for methods with sufficient power (>80%) at first follow-up. (**A**) 2D RANO, (**B**) Contrast enhancing volume, (**C**) Contrast enhancing + FLAIR volume, and (**D**) Subtraction + FLAIR volume. And at second follow-up **E**) 2D RANO, and **F**) Contrast enhancing + FLAIR volume. OS = overall survival.

## DISCUSSION

We investigated whether PD, as determined with various MRI-based methods, was associated with OS, the gold standard in oncology studies, in order to identify the optimal method for radiological treatment response assessment, in particular in the context of anti-angiogenic treatment of recurrent glioblastoma. Currently, the 2D RANO criteria are the established method of choice for determining PD in studies on glioblastoma. We found that in patients with recurrent glioblastoma treated with bevacizumab determining PD with volumetric methods, with or without subtraction, did not provide significant improvement as a post-treatment prognostic marker at 6 and 12 weeks follow-up. The volumetric methods assessed were based on enhancing lesions only (methods 2 and 3) or on the combined analyses of enhancing and FLAIR lesions (methods 4 and 5). The volumetric methods were also not significantly different from each other. In the past, several studies on the added value of volumetry in recurrent glioblastoma in determining OS have been performed[11, 21,22], most notably by Boxerman et al.[13], in which a direct comparison is made between 2D and volumetric methods. We analyzed all patients together and the bevacizumab-treated patients separately. Both these analyses failed to show significant differences between methods. The lomustine-only group comprised one-third of all patients, but because this group was too small to draw reliable conclusions from separate analysis, its influence on the analysis of all patients together is unclear. This is however of less importance, since our main goal was to look at the added value of volumetry (and subtraction) in bevacizumab-treated patients. A larger dataset would be required to draw definitive conclusions about lomustine treated patients.

Comparisons between 2D (and other linear) and volumetric measures have been investigated extensively in a whole range of different tumors[23-25], including glioma, with contradictory results. Dempsey et al. compared 1D, 2D and volumetric measurements of enhancing volume of high-grade gliomas and found only volumetry to be predictive for OS[26]. Shah et al. on the other hand compared linear measures with volumetry and found these comparable when correlated with median progression-free survival (mPFS), but found linear methods superior when correlated with OS[24]. Galanis et al. compared 1D, 2D, area, and volume-measures of enhancing (and non-enhancing) newly diagnosed gliomas and found with a time-dependent Cox model that PD measured by all four methods was predictive of OS in enhancing tumors[27]. Boxerman et al. compared 2D and volumetric measurements of enhancement and the added value of non-enhancing volume in recurrent glioblastoma treated with bevacizumab plus a chemotherapeutic agent and found that 2D and volumetric measurements were equally good at predicting OS based on PD at 8 and 16 weeks[13]. Our results are in accordance with these findings. The main differences between their

and our studies are that we compared the current golden standard, i.e. the 2D RANO criteria, with various volumetric methods including subtraction, and that our study had three different treatment arms. It must be noted that the 2D (RANO) assessment of our study was performed by raters with extensive clinical experience, i.e. a neuro-oncologist and two neuro-radiologists. This may have had a positive influence on the performance of the 2D method in predicting OS. Semi-automated volumetric assessment was performed by a single rater. Previous studies have however shown inter- and intra-rater variability to be lower in computer-assisted (volumetric) methods when compared to (non-automated) diameter methods[17,28].

Aside from an early pseudo-response, bevacizumab-treated glioblastoma patients have also shown an increase of T2w/FLAIR abnormalities at progression[9,29]. This non-enhancing tumor progression is likely due to the cooption of blood vessels by tumor cells, along which the tumor infiltrates to more distant areas[30]. The 2D RANO criteria adopted a subjective approach for assessing T2w/FLAIR abnormalities. Volumetric methods assessing T2w/FLAIR are potentially better suited to quantify these abnormalities, especially in view of the often complex shape of glioblastoma. We assessed the added value of volumetric FLAIR measures to the enhancement (and subtraction) measures and found no differences with the 2D RANO criteria. We did not assess FLAIR volume separately, because previous research suggests that volumetric FLAIR measures alone are insufficient for predicting OS. Ellingson et al. for instance found that FLAIR volume (initial, residual, and change) was not predictive of either PFS or OS[11]. Similarly, Schaub et al. determined that PD on FLAIR measures alone was not predictive of OS[22]. Huang et al. found a correlation between post-treatment T2w/FLAIR volume and OS, but this correlation disappeared when corrected for enhancing volume[20].

In addition to measuring enhancing tumor volume on T1w post-contrast and non-enhancing tumor volume on FLAIR images, we measured enhancing tumor volume on subtraction images. Patients treated with bevacizumab may develop T1 hyperintense lesions in a previously enhancing area with a reported prevalence between 20 and 80%[15,31-33]. These lesions likely represent calcifications[31]. The presence of T1 hyperintensities might hinder assessment of residual enhancement. Also, enhancement may become more vague, interfering with measurement. Ellingson et al. found that subtraction images improved visualization, tumor volume quantification and prediction of OS in patients with recurrent glioblastoma treated with bevacizumab in comparison to T1w post-contrast images[15]. We found that prediction of OS by assessing PD on subtraction (method 3) and subtraction plus FLAIR volumes (method 5) was similar to that with methods not using subtraction techniques. It must be noted that the number of scans suitable for this analysis was limited due to the multicenter study designs with hospitals using scanners from different vendors,

with varying data quality and protocol violations. This was especially problematic for subtraction methods, because matching 3D pre- and post-contrast T1w images were commonly not available. Unfortunately, this meant that not all subtraction-based methods could be reliably assessed in the bevacizumab-treated patient group. These technical shortcomings unfortunately resemble the real life conditions under which clinical trials are being conducted. The recently published standardized MRI brain tumor imaging protocol should overcome some of these technical difficulties[34].

There are several important considerations when designing novel ways to assess outcome in phase I and phase II trials. First and foremost, they must correlate with the final endpoint used in phase III trials, they must be reliable, and they must be feasible in large multicenter trials. A new method must bring either a clear benefit in being more accurate, or it must bring an advantage in being simpler but with a similar precision. Volumetric assessment is more precise in irregularly shaped tumors, but labor intensive, time-consuming and more complex, also in the case of semi-automated techniques. It is also not readily available in many institutions. Our data suggest volumetric assessment is not better as compared to classical 2D assessment. Therefore, there seems to be no rationale at this point to start using volumetric assessment in trials on recurrent glioblastoma.

There are some limitations to consider in this retrospective study. As previously mentioned, rater-experience may have positively influenced the 2D RANO assessment. The interrater variability for assessment according to the 2D RANO from this trial will be reported separately. It must also be noted that the volumetry measurements were performed by a single observer. Secondly, our data was analyzed at first and second follow-up and presence of PD was determined at these time points only. Later follow-up data was not included in this study, because there were not enough patients that had not yet shown PD left to obtain reliable results.

Our future efforts are aimed at exploring more advanced imaging techniques, such as diffusion imaging-derived apparent diffusion coefficient (ADC) as well as relative cerebral blood volume (rCBV) values from enhancing and T2w/FLAIR lesions in bevacizumab-treated patients. Additionally, in future exploratory analyses different volumetric thresholds for determining PD and a combination of enhancing volume plus qualitative FLAIR assessment will be investigated to provide more insight in the added value of volumetry in this patient group and that of FLAIR in particular.

We conclude that the current, widely used and easily applicable, 2D RANO criteria remain valid for response evaluation in patients with recurrent glioblastoma treated with bevacizumab. Volumetric and subtraction evaluation methods failed to yield a superior correlation with OS in the first 12 weeks in this patient group. Our data therefore do not support their routine use in clinical trials.

## REFERENCES


1. Ostrom QTG, Gittleman H, Fulop J, et al. CBTRUS statistical report: primary brain and central nervous system tumors diagnosed in the United States in 2008-2012. Neuro Oncol. 2015;17(suppl 4):iv1-iv62.
2. Stupp RH, Hegi ME, Mason WP, et al. Effects of radiotherapy with concomitant and adjuvant temozolomide versus radiotherapy alone on survival in glioblastoma in a randomized phase III study: 5-year analysis of the EORTC-NCIC trial. Lancet Oncol. 2009;10(5):459-466.
3. Friedman HS, Prados MD, Wen PY, et al. Bevacizumab alone and in combination with irinotecan in recurrent glioblastoma. J Clin Oncol. 2009;27(28):4733-4740.
4. Kreisl TN, Kim L, Moore K, et al. Phase II trial of single-agent bevacizumab followed by bevacizumab plus irinotecan at tumor progression in recurrent glioblastoma. J Clin Oncol. 2009;27(5):740-745.
5. Jain RK. Normalization of tumor vasculature: an emerging concept in antiangiogenic therapy. Science. 2005;307(5706):58-62.
6. Macdonald DR, Cascino TL, Schold SC Jr, et al. Response criteria for phase II studies of supratentorial malignant glioma. J Clin Oncol. 1990;8(7):1277-1280.
7. Wen PY, Macdonald DR, Reardon DA, et al. Updated response assessment criteria for high-grade gliomas: response assessment in neuro-oncology working group. J Clin Oncol. 2010;28(11):1963-1972.
8. Gállego Pérez-Larraya J, Lahutte M, Petirena G, et al. Response assessment in recurrent glioblastoma treated with irinotecan-bevacizumab: comparative analysis of the Macdonald, RECIST, RANO, and RECIST + F criteria. Neuro Oncol. 2012;14(5):667-673.
9. Norden AD, Young GS, Setayesh K, et al. Bevacizumab for recurrent malignant gliomas: efficacy, toxicity, and patterns of recurrence. Neurology. 2008;70(10):779-787.
10. Iwamoto FM, Abrey LE, Beal K, et al. Patterns of relapse and prognosis after bevacizumab failure in recurrent glioblastoma. Neurology. 2009;73(15):1200-1206.
11. Ellingson BM, Cloughesy TF, Lai A, et al. Quantitative volumetric analysis of conventional MRI response in recurrent glioblastoma treated with bevacizumab. Neuro Oncol. 2011;13(4):401-409.
12. Ananthnarayan SB, Bahng J, Roring J, et al. Time course of imaging changes of GBM during extended bevacizumab treatment. J Neurooncol. 2008;88(3):339-347.
13. Boxerman JL, Zhang Z, Safriel Y et al. Early post-bevacizumab progression on contrast-enhanced MRI as a prognostic marker for overall survival in recurrent glioblastoma: results from the ACRIN 6677/RTOG 0625 Central Reader Study. Neuro-Oncology. 2013;15(7):945-954.
14. Taal W, Oosterkamp HM, Walenkamp AM, et al. Single-agent bevacizumab or lomustine versus a combination of bevacizumab plus lomustine in patients with recurrent glioblastoma (BELOB trial): a randomized controlled phase 2 trial. Lancet Oncol. 2014;15(9):943-953.
15. Ellingson BM, Kim HJ, Woodworth DC, et al. Recurrent glioblastoma treated with bevacizumab: contrast-enhanced T1-weighted subtraction maps improve tumor delineation and aid prediction of survival in a multicenter clinical trial. Radiology. 2014;271(1):200-210.
16. Pichler J, Pachinger C, Pelz M, et al. MRI assessment of relapsed glioblastoma during treatment with bevacizumab: volumetric measurement of enhanced and FLAIR lesions for evaluation of response and progression - a pilot study. Eur J Radiol. 2013;82(5):240-245.
17. Chow DS, Qi J, Miloushev VZ, et al. Semiautomated volumetric measurement on postcontrast MR imaging for analysis of recurrent and residual disease in glioblastoma multiforme. AJNR Am J Neuroradiol. 2014;35(3):498-503.

**18.** Wang MY, Cheng JL, Han YH, et al. Measurement of tumor size in adult glioblastoma: classical cross-sectional criteria on 2D MRI or volumetric criteria on high resolution 3D MRI? Eur J Radiol. 2012;81(9):2370-2374.

**19.** Gerstner ER, Chen PJ, Wen PY, et al. Infiltrative patterns of glioblastoma spread detected via diffusion MRI after treatment with cediranib. Neuro Oncol. 2010;12(5):466-472.

**20.** Faul F, Erdfelder E, Lang AG, et al. G*Power 3: a flexible statistical power analysis program for the social, behavioral, and biomedical sciences. Behav Res Methods. 2007;39(2):175-191.

**21.** Huang RY, Rahman R, Hamdan A, et al. Recurrent glioblastoma: volumetric assessment and stratification of patient survival with early posttreatment magnetic resonance imaging in patients treated with bevacizumab. Cancer. 2013;119(19):3479-3488.

**22.** Schaub C, Greschus S, Seifert M, et al. FLAIR-only progression in bevacizumab-treated relapsing glioblastoma does not predict short survival. Oncology. 2013;85(3):191-195.

**23.** Tran LN, Brown MS, Goldin JG, et al. Comparison of treatment response classifications between unidimensional, bidimensional, and volumetric measurements of metastatic lung lesions on chest computed tomography. Acad Radiol. 2004;11(12):1355-1360.

**24.** Shah GD, Kesari S, Xu R, et al. Comparison of linear and volumetric criteria in assessing tumor response in adult high-grade gliomas. Neuro Oncol. 2006;8(1):38-46.

**25.** Sohaib SA, Turner B, Hanson JA, et al. CT assessment of tumour response to treatment: comparison of linear, cross-sectional and volumetric measures of tumour size. Br J Radiol. 2000;73(875): 1178-1184.

**26.** Dempsey MF, Condon BR, Hadley DM. Measurement of tumor “size” in recurrent malignant glioma: 1D, 2D, or 3D? AJNR Am J Neuroradiol. 2005;26(4):770-776.

**27.** Galanis E, Buckner JC, Maurer MJ, et al. Validation of neuroradiologic response assessment in gliomas: measurement by RECIST, two-dimensional computer-assisted tumor area, and computer-assisted tumor volume methods. Neuro Oncol. 2006;8(2):156-165.

**28.** Sorensen AG, Patel S, Harmath C, et al. Comparison of diameter and perimeter methods for tumor volume calculation. J Clin Oncol. 2001;19(2):551-557.

**29.** Zuniga RM, Torcuator R, Jain R, et al. Efficacy, safety and patterns of response and recurrence in patients recurrent high-grade gliomas treated with bevacizumab plus irinotecan. J Neurooncol. 2009;91(3):329-336.

**30.** Rubenstein JL, Kim J, Ozawa T, et al. Anti-VEGF antibody treatment of glioblastoma prolongs survival but results in increased vascular cooption. Neoplasia. 2000;2(4):306-314.

**31.** Bähr O, Hattingen E, Rieger J, et al. Bevacizumab-induced tumor calcifications as a surrogate marker of outcome in patients with glioblastoma. Neuro Oncol. 2011;13(9): 1020-1029.

**32.** Bähr O, Harter PN, Weise LM, et al. Sustained focal antitumor activity of bevacizumab in recurrent glioblastoma. Neurology. 2014;83(3):227-234.

**33.** Mong S, Ellingson BM, Nghiemphu PL, et al. Persistent diffusion-restricted lesions in bevacizumab-treated malignant gliomas are associated with improved survival compared with matched controls. AJNR Am J Neuroradiol. 2012;33(9):1763-1770.

**34.** Ellingson BM, Bendszus M, Boxerman J, et al. Consensus recommendations for a standardized brain tumor imaging protocol in clinical trials. Neuro Oncol. 2015;17(9):1188-1198.

## SUPPLEMENTARY FILES

MRI protocol.

The standardized MRI protocol consisted of the following sequences with full brain coverage:

- Pre-contrast three-dimensional (3D) T1-weighted (T1w) IR FSPGR images with slice thickness and in-plane resolution ≤1mm.
- Transverse diffusion weighted image (DWI) with slice thickness 3mm (no gap), an in-plane resolution of 2mm, and b=0 and b=1000 s/mm$^2$.
- 3D T2-weighted (T2w) fluid attenuation inversion recovery (FLAIR) with slice thickness and in-plane resolution ≤1mm and fat-saturation (if possible).
- Transverse 2D T2w image with slice thickness ≤3mm and in-plane resolution ≤1mm.
- Post-contrast 3D T1w IR FSPGR images with slice thickness and in-plane resolution ≤1mm.
- Selected sites also performed dynamic susceptibility contrast perfusion imaging: transverse gradient echo (GE) echo planar imaging (EPI) perfusion with slice thickness ≤5mm (no gap), an in-plane resolution of ≤3mm, repetition time <2000ms, 50 phases (100s) with a scan delay of 20s after injection of 10mmol Gd at 4-5ml/s followed by 25ml NaCl. A contrast preload bolus of 0.05 Gd mmol/kg body weight was given prior to the 3D FLAIR acquisition. In sites not performing perfusion imaging, the full contrast bolus was given prior to the 2D T2w image acquisition.

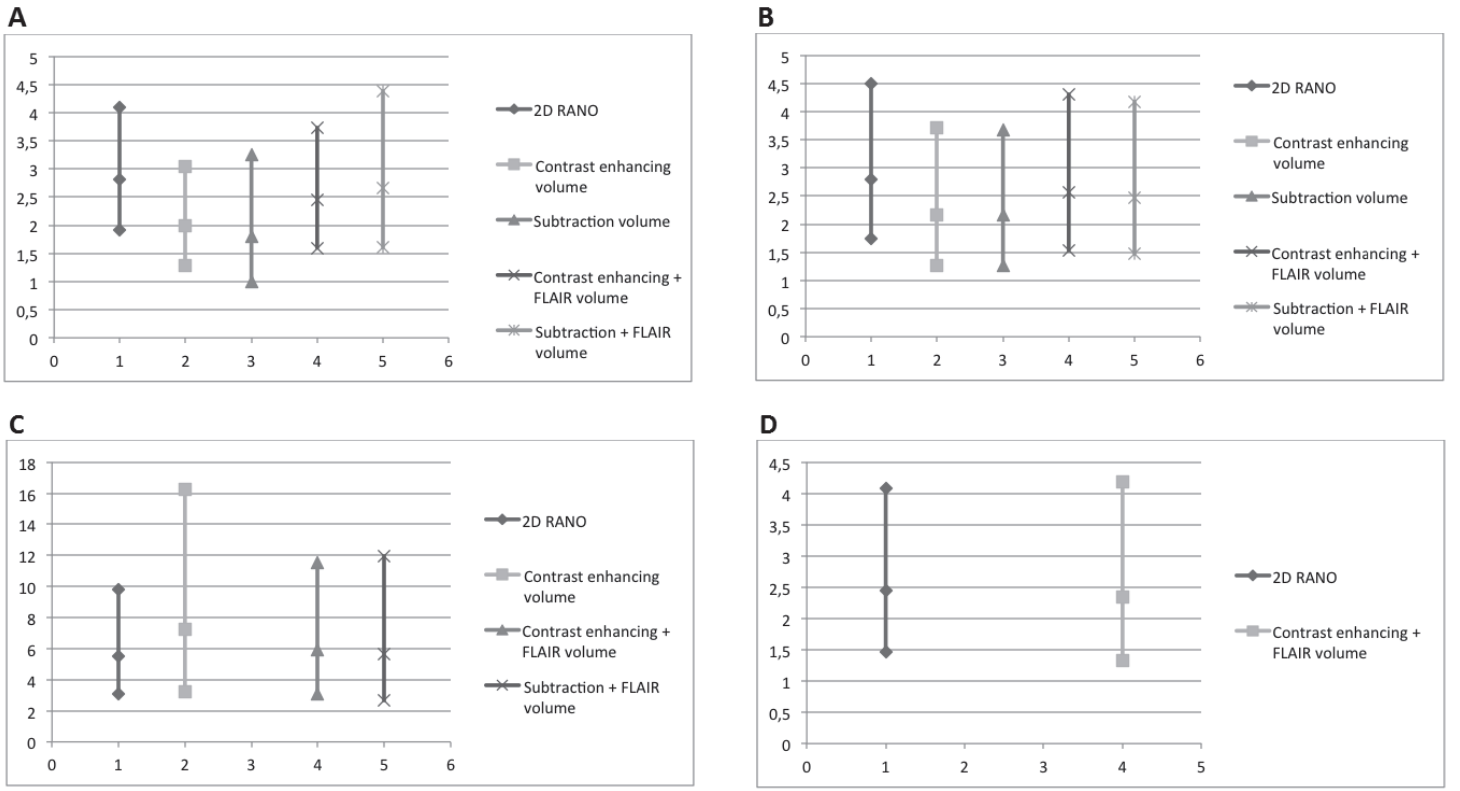


**Figure S1.** All patients together, hazard ratios and their 95% confidence intervals at first (A) and second (B) follow-up (as depicted in Table 1 in the manuscript). Bevacizumab-treated patients only, hazard ratios and their 95% confidence intervals at first (C) and second (B) follow-up (as depicted in Table 2 in the manuscript).

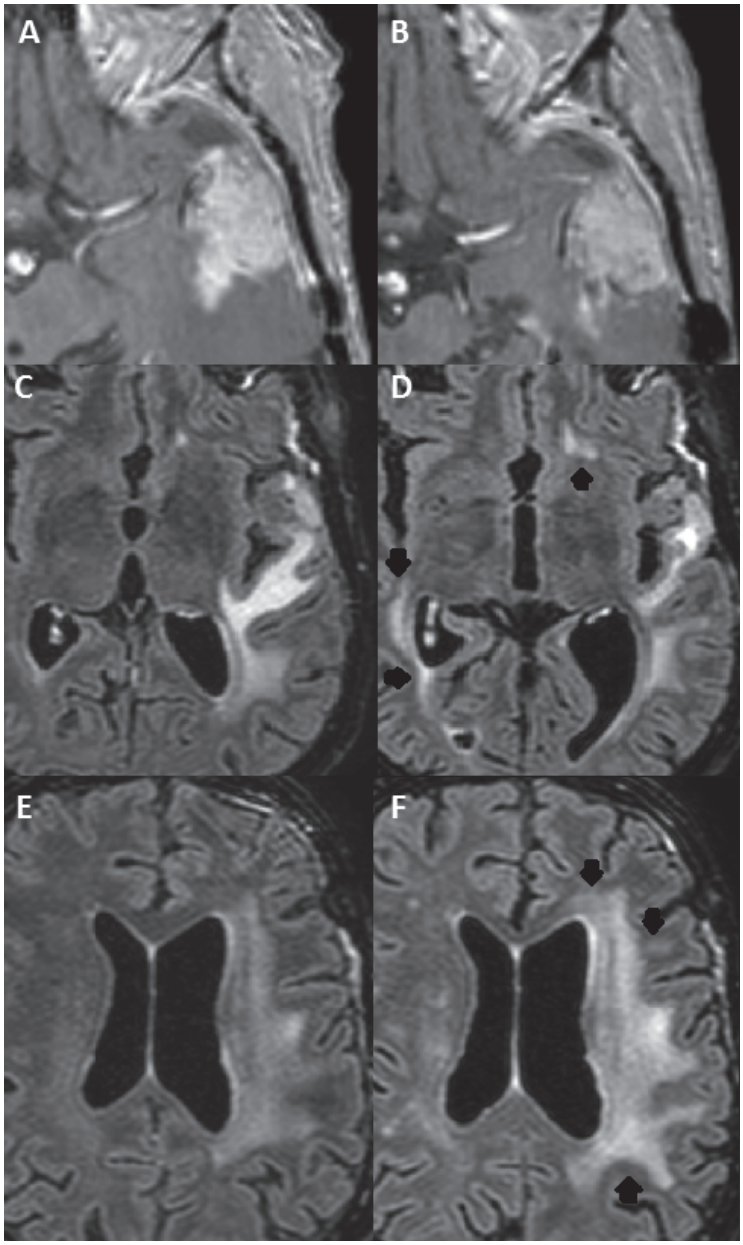


**Figure S2.** Discrepant case 1. Patient treated with bevacizumab and lomustine, scored as no progressive disease (PD) with 2D RANO (method 1) and contrast enhancing volume (method 2), but as PD with contrast-enhancing plus FLAIR volume (method 4). Enhancing lesion in left temporal lobe at baseline (**A**) and first follow-up (**B**) shows decreasing enhancement (decrease in volume of 13.23%) and increasing non-enhancing/FLAIR area at baseline (**C** and **E**) and first follow-up (**D** and **F**) at two different levels (increase in volume of 30.94%). The threshold for PD based on T2w/FLAIR volume increase is set at 25%. Black arrows indicate increasing FLAIR abnormalities.

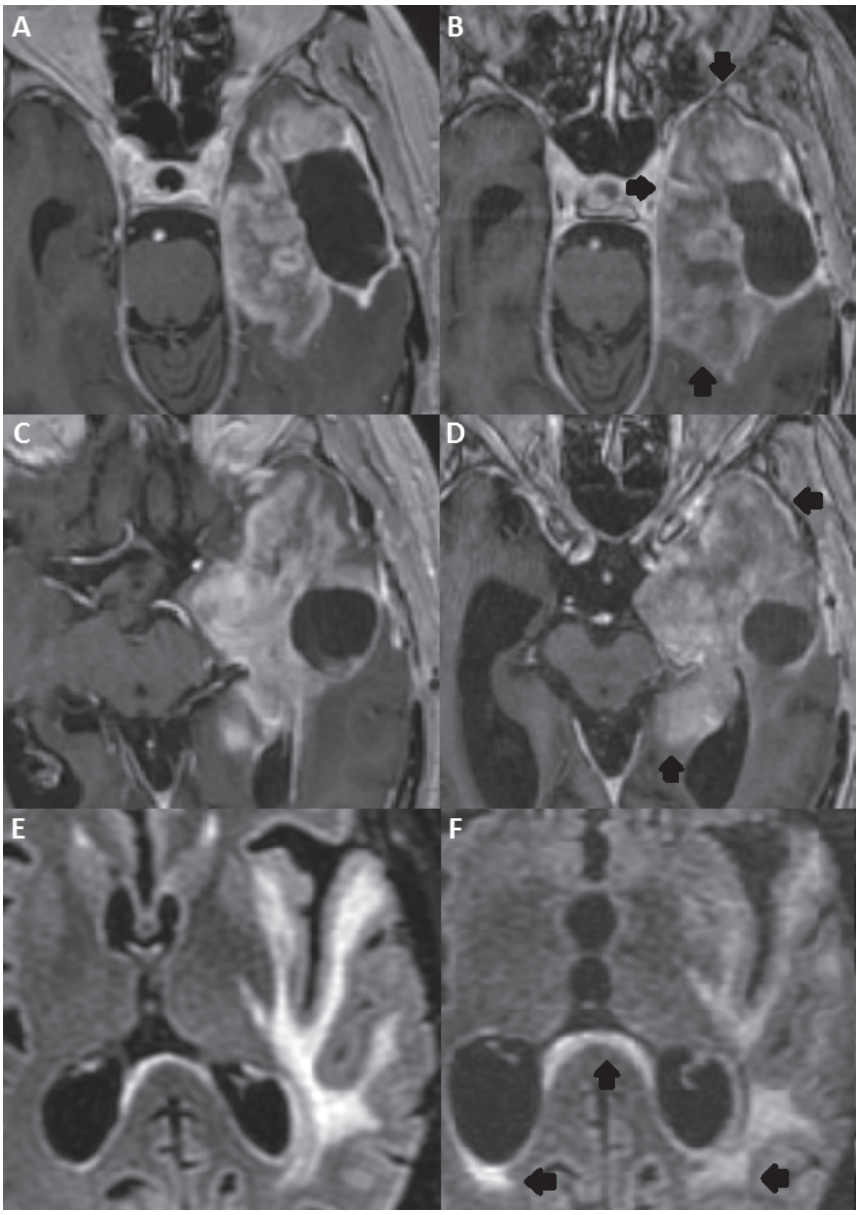


**Figure S3.** Discrepant case 2. Patient treated with lomustine, scored as progressive disease (PD) with 2D RANO (method 1), but as non PD with contrast enhancing volume (method 2) and contrast-enhancing plus FLAIR volume (method 4). Enhancing lesion in the left temporal lobe at baseline (A) and first follow-up (B) with limited increase in volume (increase 3.39%) and non-enhancing/FLAIR area (increase 6.0%) at baseline (C and E) and first follow-up (D and F) at two different levels. Note the differences in angulation between the different time points and the poor quality due to motion artifacts in the scans made at first follow-up. Black arrows indicate increasing enhancement and FLAIR abnormalities.

**Table S1.** Concordances between method 1 (2D RANO) and the volumetric methods, i.e. method 2 (contrast enhancing volume), method 3 (subtraction volume), method 4 (contrast enhancing + FLAIR volume), and method 5 (subtraction + FLAIR volume) at first follow-up in all patients together and in the bevacizumab-treated groups. In case of non-concordance, the presence of progressive disease (PD) was more frequently observed with method 1 than with the volumetric methods (2-5).

| First follow-up | Comparison | Total number of patients | Number of concordant cases | PD established with method1 | PD established with method 2/3/4/5 |
|---|---|---|---|---|---|
| **All patients** | Method 1 vs 2 | 121 | 101 (83.5%) | 16 (13.2%) | 4 (3.3%) |
| | Method 1 vs 3 | 86 | 76 (87.4%) | 9 (10.3%) | 1 (1.1%) |
| | Method 1 vs 4 | 109 | 91 (83.5%) | 10 (9.2%) | 8 (7.3%) |
| | Method 1 vs 5 | 89 | 75 (84.3%) | 9 (10.1%) | 5 (5.6%) |
| **Bevacizumab treated patients** | Method 1 vs 2 | 85 | 70 (82.4%) | 12 (14.1%) | 3 (3.5%) |
| | Method 1 vs 4 | 74 | 61 (82.4%) | 6 (8.1%) | 7 (9.5%) |
| | Method 1 vs 5 | 64 | 52 (81.3%) | 7 (10.9%) | 5 (7.8%) |

# Chapter 3.3

## The impact of different volumetric threshold to determine progressive disease in patients with recurrent glioblastoma treated with bevacizumab

Renske Gahrmann
Marion Smits
René Vernhout
Walter Taal
Giorgios Kapsas
Jan Cees de Groot
Monique Hanse
Maaike Vos
Laurens Beerepoot
Jan Buter
Zwenneke Flach
Bronno van der Holt
Martin van den Bent

*SUBMITTED*

## ABSTRACT

Background. We previously demonstrated that treatment assessment by volumetry using a 40% increase threshold for calling progression in recurrent glioblastoma treated with bevacizumab did not improve survival prediction compared to standard 2D methods. However, the optimal volumetric threshold for determining progressive disease (PD) has not been defined. We investigated a range of thresholds for enhancing and non-enhancing tumor volume increase in association with overall survival (OS).

Materials and Methods. First recurrent glioblastoma patients treated with bevacizumab and/or lomustine were included from the phase II BELOB and phase III EORTC26101 trials. Enhancing and non-enhancing tumor volumes were measured at baseline, first (6 weeks) and second (12 weeks) follow-up on 3D T1w post-contrast and T2w-FLAIR images. Hazard ratios (HRs) for the appearance of new lesions and several thresholds for tumor volume increase were calculated using cox regression analysis. Results were corrected in a multivariate analysis for well-established prognostic factors.

Results. At first follow-up, 15 patients had a new lesion associated with a significantly worse OS (3.2 versus 11.2 months, HR=7.03, p<.001). At first follow-up (n=138), lowering the threshold of enhancing volume increase from ≥40% to ≥20% increased the HR (from HR=1.77, p=.010 to HR=5.55, p=.001), while only categorizing an additional 5 patients as PD. At second follow-up (n=94), lowering the threshold from ≥40% to ≥0% also increased the HR (from HR=3.02, p=.001 to HR=9.00, p<.001). Assessing the additional effect of measuring non-enhancing volume at first follow-up (n=89), the highest HR was found with ≥25% increase in volume (HR=3.25, p=.008).

Conclusion. Early appearing new lesions were associated with poor OS. Lowering the volumetric threshold for PD at both first and second follow-up improved survival prediction. However, the additional number of patients categorized as PD by lowering the threshold was very low. The per-RANO added change in non-enhancing volumes to the analyses was of limited value even in the bevacizumab-treated group.

## INTRODUCTION

Glioblastoma is the most common glioma in adults with an incidence of 0.6-3.7 per 100,000 persons per year. It has the worst survival rate of all gliomas with a 5-year survival of approximately 10% despite intensive surgical, radiotherapy and chemotherapy treatment[1]. Recurrent glioblastoma are often treated with chemotherapy and/or angiogenesis inhibitors. Recently, the United States Food and Drug Administration has given full approval for use of bevacizumab (Avastin®) in glioblastoma[2,3]. Angiogenesis inhibitors normalize the tumor vasculature, leading to a decrease in tumor enhancement on T1-weighted post-contrast images even in the absence of a true reduction of tumor activity.

The Response Assessment in Neuro-Oncology (RANO) criteria[4] expanded on the earlier MacDonald criteria[5] by incorporating non-enhancing abnormalities into treatment response assessment. According to the RANO criteria, progressive disease (PD) is defined as ≥25% increase in the sum of products of perpendicular diameters of enhancing lesions, significant increase in non-enhancing lesions, appearance of new lesions, or clear progression of non-measurable lesions. Steroid dosage and clinical status are also taken into account. The threshold of ≥25% increase was obtained from the World Health Organization response criteria[6] and is originally based on breast cancer assessment on mammogram[7].

Because of their irregular shape in three dimensions and the common presence of necrotic areas, it has been postulated that volumetric assessment of glioblastoma will improve response evaluation and survival prediction. In addition, volumetric methods can help quantify changes in non-enhancing abnormalities, which are currently assessed only qualitatively with the RANO criteria. On the other hand, upon comparing 1D, 2D, and volumetric measures, high concordance between methods has been found, questioning the added value of the more demanding volumetric assessment[8-10]. All these studies extrapolated the RANO-based ≥25% increase in 2D areas to a ≥40% increase in volume ($4/3\pi r^3$), assuming a sphere-shaped tumor equally increasing in all directions[11], which foregoes the potential increased sensitivity of volumetric assessment. Some authors have used different volumetric cut-off values for PD, such as ≥25%[12], ≥15%[13], and ≥5%[14], suggesting that using lower thresholds could lead to a better survival prediction. Previously, a ≥25% increase of non-enhancing volumes has been proposed as the threshold to establish PD[10,15].

We aimed to determine whether lowering the volumetric threshold for PD in both enhancing tumor and non-enhancing abnormalities improves survival prediction and whether there is a preferred moment for first follow-up. We also evaluated the significance of new lesions for the diagnosis of progression.

## METHODS

### Patients

Included in this analysis were patients with first recurrence of glioblastoma treated in the phase II BELOB trial (n=148; eligible patients) and the patients treated with lomustine at our institution in the subsequent phase III EORTC26101 trial (n=35)[16,17]. Patients from the BELOB trial were randomized to three different treatment arms: lomustine (n=46), bevacizumab (n=50), or both (n=52); patients from the EORTC26101 trial were randomized to lomustine or bevacizumab plus lomustine. The 35 patients from the EORTC26101 trial were all treated with lomustine in the same way as in the BELOB trial with similar follow-up measures, and were added to obtain a balanced representation of lomustine and bevacizumab-treated patients. Patients were recruited between December 2009 and October 2011 and between October 2011 and October 2015 for respectively the BELOB trial and EORTC26101 trial. Patients had received no prior treatment with Vascular Endothelial Growth Factor (VEGF) inhibitors or nitrosoureas, were at least 18 years of age and had given informed consent according to national guidelines. Further study and patient details can be found in Taal et al. 2014 and Wick et al. 2016. The study endpoint in the current analysis was overall survival (OS), measured from the moment of follow-up (either first of second) to death from any cause.

Standardized MRI scans were performed at 6-week intervals and included pre- and post-contrast 3D T1-weighted (T1w) inversion recovery (IR) fast spin gradient recalled echo (FSPGR) and 3D T2-weighted (T2w) Fluid Attenuation Inversion Recovery (FLAIR) imaging, all with a slice thickness and in-plan resolution ≤1mm. Scans from baseline, first, and second follow-up were included in this analysis.

### Data processing

Semi-automated segmentation techniques were used to obtain total enhancing and total non-enhancing volumes from respectively 3D T1w post-contrast and 3D FLAIR-images. The BELOB-trial scans were segmented by R.G. in Brainlab iPlan 4.0 Cranial and the EORTC26101 scans were segmented by G.K. and R.G. using ITK-SNAP[18]. Areas of necrosis, pre-contrast T1w hyperintensity, blood vessels, and dura were excluded. New enhancing and non-enhancing lesions were scored by R.G. at the time of performing the segmentation. New lesions of any size were included and in case of unclear lesion origin, persistence or increase in size at the next available follow-up was taken into account according to the RANO criteria.

### Statistical analysis

Hazard ratios (HRs), 95% confidence intervals (CI) and p-values were calculated with Cox regression analysis. All results were corrected in a multivariate analysis for World Health Organization (WHO) performance status, steroid use at baseline, number of target lesions (0-1 versus ≥2), enhancing tumor volume at baseline, and predominantly frontal location (if p<.10)[19]. In the multivariate analysis p<.05 was considered significant.

We calculated the association between the appearance of a new lesion at first, i.e. 6 weeks' follow-up with OS. Both enhancing and/or non-enhancing lesions of any size that remained stable or increased at the next follow-up were scored. As the appearance of a new lesion is considered unequivocal PD, these patients were subsequently excluded from the threshold analysis.

Analyses of enhancing and non-enhancing volume thresholds were performed in all treatment groups together, and subsequently in the lomustine-only treated and in the bevacizumab (with/without lomustine) treated groups separately at both first and second follow-up. To determine the association between increasing tumor volume and OS, HRs were calculated in strata of ≥40%, ≥20 – <40%, and ≥0 – <20% increase in enhancing volume and ≥25%, ≥10 – <25%, and ≥0 – <10% increase in non-enhancing volume (from now on referred to as strata 20-40% etc.). The threshold with the highest HR was considered the most predictive for OS. Patients with PD based on increasing enhancing volume were excluded from the non-enhancing volumetric analysis so that the added values of measuring non-enhancing volumes could be determined.

All analyses were performed in SPSS Statistics, version 24 (Copyright IBM Corporation).

## RESULTS

### Patients

Patients without available 3D T1w post-contrast and FLAIR images at relevant time points were excluded from the analyses. Additionally, patients that did not reach first (n=4) or second (n=60) follow-up were excluded from analyses at these time points (see ***Figure 1*** for included patients per analysis).

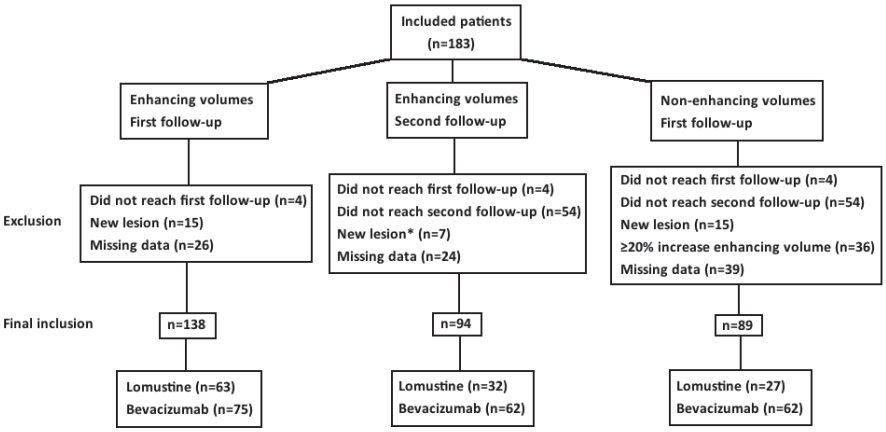


**Figure 1.** Flow diagram of all patients included from the BELOB and EORTC 26101 trials (n=183), reasons for excluding patients (in order) per analysis and number of patients included in the final analyses.

The four patients that did not reach first follow-up within the trial had a median OS of 1.5 months measured from baseline to death. Another 60 patients did not reach second follow-up of which the majority had been randomized to the lomustine-treated group (n=37).

Univariate analyses (Table 1) showed associations between OS and WHO performance status (HR=1.67, p<.001), steroid use at baseline (HR=1.60, p=.002), predominantly frontal location (HR=1.34, p=.061), and enhancing volume at baseline (HR=1.02, p<.001). These variables were therefore included in the multivariate analysis. Number of target lesions and age were not associated (p>.10) with OS.

**Table 1.** Univariate Cox regression analyses of variables with potential influence on survival, Hazard ratios (HRs), 95% confidence intervals (CIs) and p-values for all treatment groups together and bevacizumab- and lomustine-treated patients separately. Overall survival is measured from randomization to death by any cause.

| | **All treatment groups** | | | **Bevacizumab** | | | **Lomustine** | | |
|---|---|---|---|---|---|---|---|---|---|
| **Parameters** | **HR** | **95% CI** | **p-value** | **HR** | **95% CI** | **p-value** | **HR** | **95% CI** | **p-value** |
| WHO performance status | 1.67 | 1.30-2.15 | <.001 | 1.85 | 1.29-2.65 | .001 | 1.49 | 1.01-2.12 | .028 |
| Steroid use | 1.60 | 1.19-2.15 | .002 | 1.52 | 1.02-5.56 | .041 | 1.63 | 1.04-2.55 | .032 |
| Number of target lesions | 1.09 | 0.79-1.52 | .59 | 1.17 | 0.76-1.80 | .48 | 1.07 | 0.63-1.79 | .81 |
| Predominantly frontal location | 1.34 | 0.99-1.83 | .061 | 1.26 | 0.84-1.90 | .26 | 1.54 | 0.95-2.50 | .078 |
| Age | 1.01 | 0.99-1.03 | .16 | 1.01 | 0.99-1.02 | .53 | 1.02 | 0.99-1.04 | .13 |
| Baseline enhancing volume | 1.02 | 1.01-1.03 | <.001 | 1.02 | 1.01-1.04 | .012 | 1.02 | 1.01-1.03 | .009 |

## New lesions

At first follow-up (n=179), a new enhancing and/or non-enhancing lesion appeared in 15 patients (a more detailed description can be found in the ***Supplementary Files. Table S1*** and ***Figure S1***). The univariate HR for OS of the development of new lesions was highly significant (HR=5.27, p<.001) and increased after correction for other variables in a multivariate analysis (HR=7.03, p<.001). The median OS of patients with a new lesion at first follow-up was 2 months versus 8.5 months in patients without a new lesion (***Figure 2***). At second follow-up, 2 additional patients had developed a new lesion (1 enhancing and 1 non-enhancing).

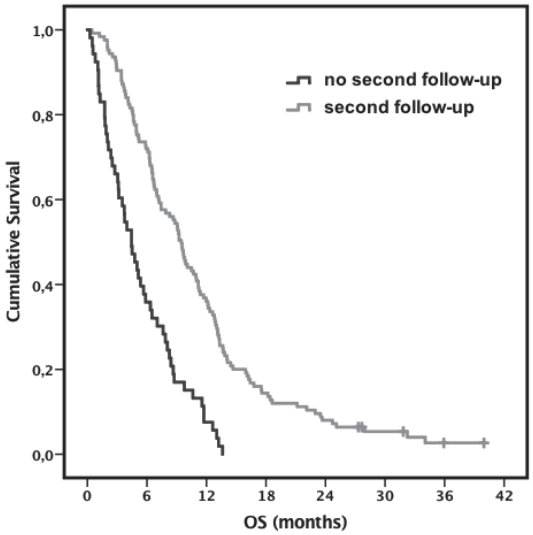


**Figure 2.** Kaplan-Meier curves of patients with and without a new lesion at first follow-up. The median overall survival (measured from first follow-up) was 2 versus 8.5 months, respectively.

## Enhancing lesions

In all treatment groups combined, patients with a ≥ 40% increase in enhancing volume at first or at second follow-up had a significantly worse OS compared to those with less than 40% increase (HR=1.77, p=.010 and HR=3.02, p=.001, respectively) in the multivariate analysis. Within the threshold stratum of 20–40% increase, an additional 5 patients were categorized as PD at first follow-up, and 2 patients at second follow-up. When lowering the threshold to stratum 0-20% increase, 12 and 6 patients were additionally categorized as PD at first and second follow-up respectively. The highest HR at first follow-up was found with stratum 20-40% increase (HR=5.55, p=.001) and at second follow-up with stratum 0-20% increase (HR=9.00, p<.001) (see ***Table 2***).

**Table 2.** Hazard ratios (HRs), 95% confidence intervals (CIs), and p-values for the strata ≥40%, 20-40%, and 0-20% increase in enhancing volume at first and second follow-up in all treatment groups together and in the lomustine-treated group. Patient numbers with enhancing volume increase in the bevacizumab-treated group were insufficient for meaningful analysis.

| Treatment groups | ≥% increase in volume | First follow-up (n=138) | | | | Second follow-up (n=94) | | | |
|---|---|---|---|---|---|---|---|---|---|
| | | n | HR | 95% CI | p-value | n | HR | 95% CI | p-value |
| **All** | 40 | 31 | 1.77 | 1.15-2.72 | .010 | 12 | 3.02 | 1.57-5.79 | .001 |
| | 20-40 | 5 | 5.55 | 2.06-14.91 | .001 | 2 | - | - | - |
| | 0-20 | 12 | 1.01 | 0.54-1.90 | .97 | 6 | 9.00 | 3.32-24.42 | <.001 |
| **Lomustine** | 40 | 30 | 1.76 | 0.99-3.16 | .056 | 8 | 3.63 | 1.33-9.87 | .012 |
| | 20-40 | 4 | - | - | - | 2 | - | - | - |
| | 0-20 | 10 | 0.70 | 0.28-1.78 | .46 | 5 | 10.70 | 3.45-33.17 | <.001 |

In the lomustine-treated group, threshold stratum ≥40% increase and stratum 0-20% increase could be analyzed. HRs were borderline significant at ≥40% (HR=1.76, p=.056) and not significant at stratum of 0-20% increase at first follow-up; at second follow-up the highest significant HR was found with the threshold stratum of 0-20% increase (HR=10.70, p<.001). The number of patients categorized as PD by increase in enhancing volume of strata 20-40% in the lomustine-treated group and ≥0% in the bevacizumab-treated group was insufficient for meaningful analysis.

## Non-enhancing lesions

To determine the added value of measuring non-enhancing volume increase for response assessments, patients with PD based on increasing enhancing volume (at thresholds determined based on the highest HR found) were excluded from the analyses, i.e. stratum 20-40% at first follow-up. In all treatment groups together, the

**Table 3.** Hazard ratios (HRs), 95% confidence intervals (CIs), and p-values for ≥25%, stratum 10-25%, and stratum 0-10% increase in non-enhancing volume at first and second follow-up in all treatment groups together and in the bevacizumab-treated group. Patient number with non-enhancing volume increase in the lomustine-treated group was insufficient for meaningful analysis.

| Treatment groups | ≥% increase in volume | First follow-up (n=89) | | | |
|---|---|---|---|---|---|
| | | n | HR | 95% CI | p-value |
| **All** | 25 | 6 | 3.25 | 1.37-7.70 | .008 |
| | 10-25 | 5 | 1.88 | 0.72-4.86 | .196 |
| | 0-10 | 8 | 0.63 | 0.28-1.39 | .248 |
| **Bevacizumab** | 25 | 5 | 5.04 | 1.80-14.08 | .002 |
| | 10-25 | 2 | - | - | - |
| | 0-10 | 4 | - | - | - |

highest HR was found at a threshold of ≥25% at first follow-up (HR=3.25, p=.008), categorizing 6 additional patients as PD. At the same threshold, the HR was also significant in the bevacizumab-treated group (HR=5.04, p=.002) (see ***Table 3***). The lomustine-treated group could not be analyzed because <5 patients were categorized as PD based on non-enhancing volume increase. Analyses of non-enhancing volumes at second follow-up could not be performed for the same reason.

## DISCUSSION

In this analysis of patients with recurrent glioblastoma, PD was determined based on the appearance of a new lesion, increasing enhancing volume, and increasing non-enhancing volume in association with OS. A new enhancing or non-enhancing lesion of any size at early follow-up was significantly associated with poor OS. When considering patients with increasing enhancing volumes, the majority of patients had an increase of ≥40%. Lowering the threshold to stratum 20-40% increase at first follow-up and to stratum 0-20% increase at second follow-up improved survival prediction, but only a small number of patients were additionally categorized as PD with these lower thresholds.

After excluding all patients with PD based on the appearance of a new lesion or increase in enhancing tumor volume, an increase in non-enhancing volumes of ≥25% was significantly associated with poorer OS. However, only 6 out of 89 patients (5 of whom were treated with bevacizumab) were categorized as PD and thus the added value of considering non-enhancing volumes was limited in this population.

HRs at second follow-up (i.e. after 12 weeks) were higher and more significant than those at first follow-up (i.e. after 6 weeks). This effect can be largely attributed to the lower number of patients included at second follow-up, as many had already reached PD (based on either radiological or clinical parameters) prior to this evaluation point. This complicates the comparison of these two evaluation points. In the lomustine-treated group many patients had reached radiological PD after 6 weeks, while in the bevacizumab-treated group enhancing tumor volumes did not increase much even after 12 weeks follow-up.

While results found in the lomustine-only treated group were similar to those found in all treatment groups together, results from the bevacizumab-treated group are more difficult to interpret as only a small number of patients showed an increase in enhancing tumor volume at 6 and 12-week follow-up. Slightly more bevacizumab-treated patients were categorized as PD when non-enhancing volume increase was taken into account, confirming a possible role for the RANO emphasis on non-enhancing volumes in bevacizumab-treated patients. In previous literature,

an increase in non-enhancing abnormalities has been described as a pattern of progression after anti-angiogenic treatment[20,21], but since our data is limited to the early period of follow-up, we are unable to determine if this patterns of progression is more common in the bevacizumab-treated patients at later stages, and hence what the true value of volumetric assessment of non-enhancing abnormalities is during the entire course of anti-angiogenic treatment.

We measured total volume of either enhancing or non-enhancing lesions, which means that mixed responses were not considered. Mixed response is seen in a subset of patients[22,23], but we postulate that the outcome of these patients is determined by the overall volume increase or by newly appearing lesions. Measuring total non-enhancing volume could also have confounded results, as these volumes include tumor, effects due to earlier treatment, and edema. As bevacizumab is a known edema-relieving agent[24], a decrease in non-enhancing volume in this group is expected at early assessment.

The benchmark for increase in volume was overall survival, considered the gold standard in oncology trials and the ultimate measure of patient benefit. Results were corrected for several known prognostic variables, including baseline enhancing tumor volume[19]. The prognostic significance of the latter was conformed in our dataset. Initial tumor size is also important to take into account when measuring change in size as an increase of ≥25% has a more profound effect in an already large tumor compared to a small tumor. Large tumors are not only associated with a worse OS, but with worse overall clinical condition as well[25].

An important argument in favor of performing volumetric rather than 2D measurement is the lower inter- and intra-rater variability, which has previously been shown with (semi-)automated techniques. Unfortunately, volumetric measurement are still much more difficult to obtain than the commonly used 2D measures, and their added value for response assessment is disputed[8-10]. Despite the unclear added value when it comes to predicting survival, tumor volumes does more accurately reflect the – enhancing – tumor size than 2D measurement. Especially in heterogeneous tumors such as glioblastoma this could be useful. Furthermore, from such a volume of interest, other measures such as Apparent Diffusion Coefficient (ADC) and relative Cerebral Blood Volume (rCBV) can also be determined, facilitating a more integrated approach to tumor assessment, which would potentially improve survival prediction further.

The main limitation of our study is the relatively small sample size of bevacizumab-treated patients showing progression of enhancing lesions at this early assessment time point. Assessment at later time points and/or a larger sample size is desirable to further determine the value of volumetric imaging (i.e. looking at enhancing and non-enhancing volume) in this treatment group.

In conclusion, new lesions, whether enhancing or non-enhancing, appearing early after the start of treatment were clearly associated with poor outcome. While only a small additional number of patients would be categorized as PD with volumetric thresholds lower than the commonly applied 40% increase, survival prediction did improve and therefore lowering the threshold should be considered. We found no added value for measuring non-enhancing volumes in patients treated with lomustine only. In the bevacizumab-treated group early increase in tumor size (either enhancing or non-enhancing) was found to be rare. Here, increasing lesions were also associated with poor outcome, whether enhancing or non-enhancing.

## REFERENCES


1. Stupp R, Hegi ME, Mason WP, et al. Effects of radiotherapy with concomitant and adjuvant temozolomide versus radiotherapy alone on survival in glioblastoma in a randomized phase III study: 5-year analysis of the EORTC-NCIC trial. Lancet Oncol 2009;10(5):459-466.
2. Cohen MH, Shen YL, Keegan P, Pazdur R. FDA drug approval summary: bevacizumab (Avastin) as treatment of recurrent glioblastoma multiforme. Oncologist 2009;14(11):1131-1138.
3. DA Grants Genentech's Avastin Full Approval for Most Aggressive Form of Brain Cancer. Genentech. Accessed December 5. http://www.gene.com/media/press-release/14695/2017-12-05/fda-grants-genentechs-avastin-full-appro.
4. Wen PY, Macdonald DR, Reardon DA, et al. Updated response assessment criteria for high-grade gliomas: response assessment in neuro-oncology working group. J Clin Oncol 2010;28(11):1963-1972.
5. Macdonald DR, Cascino TL, Schold SC Jr, Cairncross JG. Response criteria for phase II studies of supratentorial malignant glioma. J Clin Oncol 1990;8(7):1277-1280.
6. Miller AB, Hoogstraten B, Staquet M, Winkler A. Reporting results of cancer treatment. Cancer 1981;47(1):207-214.
7. Hayward JL, Carbone PP, Heusen JC, et al. Assessment of response to therapy in advanced breast cancer. Br J Cancer 1977;35(3):292-298.
8. Wang MY, Cheng JL, Han YH, Li YL, Dai JP, Shi DP. Measurement of tumor size in adult glioblastoma: classical cross-sectional criteria on 2D MRI or volumetric criteria on high resolution 3D MRI? Eur J Radiol 2012;81(9):2370-2374.
9. Warren KE, Patronas N, Aikin AA, Albert PS, Balis FM. Comparison of one-, two, and three-dimensional measurement of childhood brain tumors. J Natl Cancer Inst 2001;93(18):1401-1405.
10. Gahrmann R, van den Bent MJ, van der Holt B, et al. Comparison of 2D (RANO) and volumetric methods for assessment of recurrent glioblastoma treated with bevacizumab – a report from the BELOB trial. Neuro Oncol 2017;19(6):853-861.
11. Therasse P, Arbuck SG, Eisenhauer EA, et al. New guidelines to evaluate the response to treatment in solid tumors. European Organization for Research and Treatment of Cancer, National Cancer Institute of the United States, National Cancer Institute of Canada. J Natl Cancer Inst 2000;92(3):205-216.
12. Boxerman JL, Zhang Z, Safriel Y, et al. Early post-bevacizumab progression on contrast-enhanced MRI as a prognostic marker for overall survival in recurrent glioblastoma: results from the ACRIN 6677/RTOG 0625 Central Reader Study. Neuro Oncol 2013;15(7):945-954.
13. Radbruch A, Lutz K, Wiestler B, et al. Relevance of T2 signal changes in the assessment of progression of glioblastoma according to the Response Assessment in Neurooncology criteria. Neuro Oncol 2012;14(2):222-229.
14. Gzell CE, Wheeler HR, McCloud P, Kastelan M, Back M. Small increases in enhancement on MRI may predict survival post-radiotherapy in patients with glioblastoma. J Neurooncol 2016;128(1):67-74.
15. Gerstner ER, Chen PJ, Wen PY, Jain RK, Batchelor TT, Sorensen G. Infiltrative patterns of glioblastoma spread detected via diffusion MRI after treatment with cediranib. Neuro Oncol 2010;12(5):466-472.
16. Wick W, Gorlia T, Bendszus M, et al. Lomustine and bevacizumab in progressive glioblastoma. N Engl J Med 2017;377(20):1954-1963.

**17.** Taal W, Oosterkamp HM, Walenkamp AM, et al. Single-agent bevacizumab or lomustine versus a combination of bevacizumab plus lomustine in patients with recurrent glioblastoma (BELOB trial): a randomized controlled phase 2 trial. Lancet Oncol 2014;15(9):943-953.

**18.** Yushkevich PA, Piven J, Hazlett HC, et al. User-guided 3D active contour segmentation of anatomical structures: significantly improved efficiency and reliability. Neuroimage 2006;31(3):1116-1128.

**19.** Gorlia T, Stupp R, Brandes AA, et al. New prognostic factors and calculators for outcome prediction in patients with recurrent glioblastoma: a pooled analysis of EORTC Brain Tumour Group phase I and II clinical trials. Eur J Cancer 2012;48(8):1176-1184.

**20.** Iwamoto FM, Abrey LE, Beal K, et al. Patterns of relapse and prognosis after bevacizumab failure in recurrent glioblastoma. Neurology 2009;73(15):1200-1206.

**21.** Norden AD, Young GS, Setayesh K, et al. Bevacizumab for recurrent malignant gliomas: efficacy, toxicity, and patterns of recurrence. Neurology 2008;70(10):779-787.

**22.** Pope WB, Lai A, Nghiemphu P, Mischel P, Gloughesy TF. MRI in patients with high-grade gliomas treated with bevacizumab and chemotherapy. Neurology 2006;66(8):1258-1260.

**23.** Kreisl TN, Lassman AB, Mischel PS, et al. A pilot study of everolimus and gefitinib in the treatment of recurrent glioblastoma (GBM). J Neurooncol 2009;92(1):99-105.

**24.** Ananthnarayan S, Bahng J, Roring J, et al. Time course of imaging changes of GBM during extended bevacizumab treatment. J Neurooncol 2008;88(3):339-347.

## SUPPLEMENTARY FILES

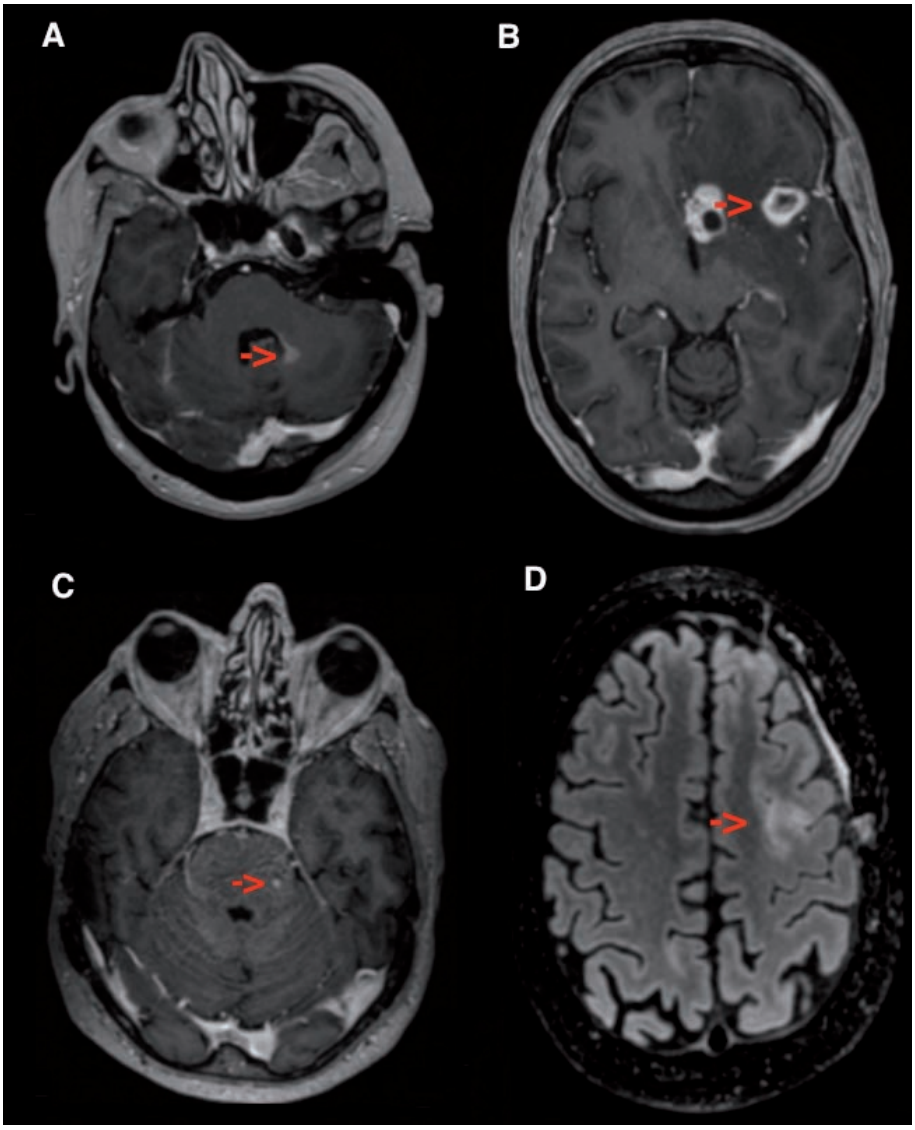


**Figure S1.** Examples of new lesions found at first follow-up. New enhancing lesions found in patients 046 (**A**), 071 (**B**), and 087 (**C**) and a new non-enhancing lesion found in patient 137 (**D**). Additional information on these patients can be found in ***TableS1***.

**Table S1.** Characteristics of all patients with a new lesion at first follow-up (n=15). Enhancing and non-enhancing lesions of any size were included. OS=overall survival.

| Trial | Patient | Treatment | Enhancing or non-enhancing lesion | Volume ($cm^3$) | Max axial diameter (mm) | OS (days) |
|---|---|---|---|---|---|---|
| **BELOB** | 004 | Bevacizumab | Enhancing | 0.773 | 22.1 | 61 |
| | 004 | | Non-enhancing | 0.142 | 11.4 | |
| | 028 | Bevacizumab | Enhancing | 0.019 | 6.73 | 220 |
| | 029 | Lomustine | Non-enhancing | 1.044 | 17.3 | 57 |
| | 046 | Bevacizumab+lomustine | Enhancing | 0.217 | 10.9 | 43 |
| | 071 | Lomustine | Enhancing | 1.388 | 17.7 | 32 |
| | 085 | Lomustine | Enhancing | 0.023 | 4.77 | 35 |
| | 087 | Bevacizumab | Enhancing | 0.016 | 3.10 | 114 |
| | 092 | Bevacizumab | Enhancing | 0.014 | 5.34 | 61 |
| | 100 | Lomustine | Enhancing | 0.022 | 2.58 | 198 |
| | 127 | Bevacizumab | Enhancing | 0.014 | 2.50 | 77 |
| | 137 | Bevacizumab | Non-enhancing | 2.042 | 22.4 | 54 |
| | 151 | Bevacizumab | Non-enhancing | 0.828 | 15.3 | 86 |
| | 151 | | Non-enhancing | 0.328 | 6.60 | |
| **EORTC26101** | 161 | Lomustine | Enhancing | 0.14 | 5.79 | 251 |
| | 180 | Lomustine | Non-enhancing | 14.02 | 62.0 | 39 |
| | 189 | Lomustine | Enhancing | 0.03 | 4.22 | 96 |
| | 189 | | Enhancing | 0.06 | 3.00 | |

# Chapter 3.4

## The value of apparent diffusion coefficient in predicting overall survival after the first course of bevacizumab and lomustine in recurrent glioblastoma

Renske Gahrmann
Alexander Leemans
Bronno van der Holt
René Vernhout
Walter Taal
Jacoline Bromberg
Maaike Vos
Jan Cees de Groot
Monique Hanse
Martin van den Bent
Marion Smits

*SUBMITTED*

## ABSTRACT

Purpose: To investigate the value of apparent diffusion coefficient (ADC) histogram analysis to predict overall survival (OS) after the first treatment course of bevacizumab and/or lomustine in recurrent glioblastoma.

Materials and Methods: Patients (n=148) were included from the board-approved multicenter BELOB-trial and informed consent was acquired. Standardized MRI-scans from baseline and 6-week follow-up were retrospectively analyzed. Volumes of interest (VOIs) of enhancing and non-enhancing lesions were drawn on 3D T1w post-contrast and FLAIR images and co-registered with ADC-maps. Patients with missing MRI-data or small lesions (<0.2cm$^3$) were excluded. Unimodal ADC-histogram parameters were derived per VOI. From exploratory analyses of each histogram parameter performed in all treatment groups together, $ADC_{min}$ was found to be most promising in predicting OS and was further analyzed using cox-regression analysis. The optimum cut-off value for predicting OS was determined in a multivariate analysis.

Results. Change in $ADC_{min}$ in enhancing lesions was analyzed in 108 patients. A decrease of >27.5% resulted in significantly better OS when looking at all treatment arms together (HR=0.572, p=.007), both bevacizumab-treated groups (n=72) (HR=0.452, p=.002), and in the combination-treatment arm (n=38) (HR=0.287, p=.001). After correcting for WHO performance status, corticosteroid use, and baseline enhancing volume, results remained significant: HR=0.482 (p=.001), HR=0.415 (p=.001), and HR=0.250 (p<.001) respectively. No significant differences in OS were found in the monotherapy arms, nor in the non-enhancing lesions.

Conclusion. Decrease in $ADC_{min}$ in enhancing recurrent glioblastoma treated with bevacizumab and lomustine was associated with significantly better OS.

## Advances in knowledge:

- Response in terms of overall survival can be predicted by measuring change in $ADC_{min}$ values from baseline to first follow-up in recurrent glioblastoma treated with bevacizumab combined with lomustine.
- Changes in $ADC_{min}$ were only predictive for response in terms of overall survival in enhancing but not in non-enhancing lesions.

## Implication(s) for patient care:

- Where response in recurrent glioblastoma treated with bevacizumab is difficult to determine on conventional imaging due to issues with pseudo-response, change in $ADC_{min}$ can help to predict response in terms of improved overall survival after the first course of treatment.

## Summary statement:

Change in $ADC_{min}$ values measured in the enhancing portion of recurrent glioblastoma predicts improved overall survival at first follow-up after treatment with bevacizumab and lomustine when using a cut-off percentage change between -5% and -27.5% ($HR_{27.5\%}$=0.250, p<.001).

## INTRODUCTION

Glioblastoma multiforme is the most common malignant primary brain tumor with a 5-year survival rate of only 5% despite intensive treatment[1,2]. Based on the results from two phase-II trials with bevacizumab (Avastin®, Genentech, San Francisco) and irinotecan[3,4], the United States Food and Drug Administration (FDA) approved the use of bevacizumab for second-line treatment in patients with recurrent glioblastoma in 2009. Bevacizumab is an angiogenesis inhibitor that specifically targets Vascular Endothelial Growth Factor (VEGF), resulting in the normalization of tumor blood vessels[5]. This reduces contrast-enhancement, edema, perfusion, and also diffusion[6-9].

Response assessment in glioblastoma is formulated in the Response Assessment in Neuro-Oncology (RANO) criteria, which are based on change in contrast-enhancement and/or non-enhancing abnormalities on T2-weighted (T2w)/Fluid attenuated inversion recovery (FLAIR) magnetic resonance (MR) imaging[10]. Decrease in contrast enhancement and edema in patients treated with bevacizumab may be actual tumor response or pseudo-response (i.e. decrease in vascular permeability only). The RANO do not discern the cause of the decrease and an imaging marker of true tumor response to bevacizumab is at present lacking. With diffusion weighted imaging (DWI), a quantitative measure of the magnitude of diffusion can be obtained, expressed as the apparent diffusion coefficient (ADC). Previous studies using histogram analysis of tumor ADC-values *at baseline* in patients treated with bevacizumab indicate that low values of ADC may be predictive for survival[11,12]. In bevacizumab-treated patients diffusion restriction has been observed *after treatment*, but the exact meaning of this finding is unclear[9,13].

Since not all patients seem to benefit from expensive treatment with bevacizumab, discerning the responders from the non-responders at an early stage is important to save costs and prevent possible side-effects in non-responders[14]. While progressive disease (PD) in bevacizumab-treated patients can be reliably established using the RANO criteria, a distinction between responders and non-responders when there is stable or decreased contrast enhancement is problematic due to the possibility of pseudo-response. The purpose of this study was to assess the value of ADC histogram analysis to predict overall survival (OS) after the first course (i.e. 6 weeks) of bevacizumab to obtain an indication of response at the very early stage after start of treatment.

## METHODS

### Patients

Patients from the Dutch institutional review board-approved BELOB trial (148 eligible patients), which is a phase II randomized controlled trial of first recurrence glioblas-

toma treated with either bevacizumab (Avastin, Roche) (n=50), lomustine (n=46) or a combination of both (n=52), were analyzed (Nederlands Trial Register, www.trialregister.nl, number NTR1929). Patients signed informed consent and were included between December 2009 and October 2011. No prior treatment with angiogenesis inhibitors or nitrosoureas had taken place, instead patients had been treated with surgery, radiotherapy and temozolomide. Details on the in- and exclusion criteria as well as the findings on the primary outcome from the trial are described elsewhere[15]. Earlier radiological analysis in this same patient population[16] did not include analysis of the DWI that were acquired during this study. All patients were above the age of 18, with a mean age of 55.9 years (range 24-77). Outcome measures were 6, 9 and 12-month OS and the proportion of patients with an objective response. In the current analysis OS was measured from first follow-up (i.e. 6 weeks) to death from any cause.

## Data acquisition

Patients were treated in 14 different hospitals with follow-up which included MR scanning at 6-week intervals according to a standardized MR-protocol. Sequences scanned were: pre- and post-contrast 3D inversion recovery (IR) fast spin recovery gradient (FSPGR) T1-weighted (T1w) images with slice thickness and in-plane resolution ≤1mm, 3D T2w-FLAIR with slice thickness and in-plane resolution ≤1mm and fat-saturation, and transverse diffusion weighted images (DWI) with slice thickness of 3mm (no gap), in-plane resolution of 2mm, and b=0 and b=1000 s/mm$^2$. Due to differences in protocol implementation, voxel sizes of the DWI data differed between hospitals, ranging from 0.9x0.9x3.0mm to 2.0x2.0x6.0mm. Additionally, the protocol consisted of transverse 2D T2w, and dynamic susceptibility contrast perfusion imaging (selected sites only), not used for the current study.

## Data post-processing

Enhancing tumor was segmented on T1w post-contrast images, and non-enhancing abnormalities on T2w-FLAIR images in BrainLab's I-Plan 4.0 Cranial using a semi-automated technique. The resulting volumes of interest (VOI) were categorized as enhancing and non-enhancing and assessed separately (***Figure 1***). T2w-FLAIR and DWI images as well as the VOIs were registered to the T1w post-contrast image per time-point with a non-linear registration technique using custom scripts in Matlab (R2014a) and Elastix[17]. During this registration the differences in voxel size and signal-to-noise ratio (SNR) between the different hospitals are taken into account (see ***Supplementary Files A*** for the parameter settings used in Elastix). To obtain a VOI for the non-enhancing lesion only, the enhancing lesion VOI was subtracted from the total non-enhancing VOI. ADC-maps were calculated from the DWI images and unimodal ADC-histogram parameters (mean, median, minimum, maximum, stan-

dard deviation, kurtosis and skewness) were computed from each VOI. A unimodal approach was chosen after visual inspection of histograms from 266 lesions at both baseline and first follow-up, which showed unimodal distribution in respectively 85% and 81% of cases. In case of multiple lesions in a single patient, histogram parameters were combined to obtain a single histogram per enhancing and non-enhancing VOI. VOIs <0.2cm$^3$ were excluded from analysis.

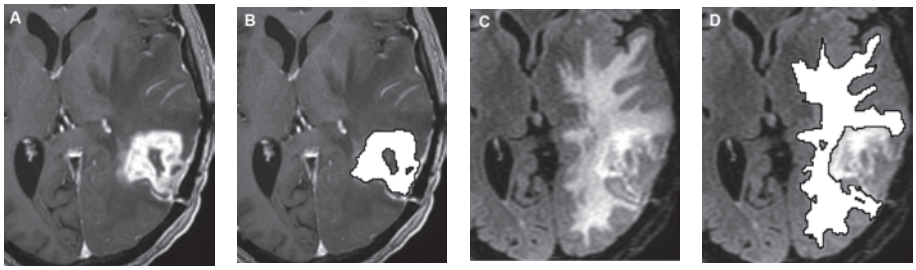


**Figure 1 (A-D):** 3D T1-weighted post-contrast and 3D T2w/FLAIR images without (**A, C**) and with (**B, D**) volumes of interest (VOI) in the same patient. The enhancing VOI was subtracted from the non-enhancing VOI to obtain the truly non-enhancing portion of the tumor.

## Statistical analysis

All statistical analyses were performed using SPSS Statistics for Windows, Version 21.0 (Armonk, NY: IBM Corp. 2012). First, percentage change between baseline and first follow-up (i.e. 6 weeks after start of treatment) was calculated for each ADC histogram parameter. Exploratory analyses were then performed in the entire group of patients to determine which parameter(s) had potential value in establishing differences in OS. For every parameter, the group was dichotomized using its median. With cox regression analysis hazard ratios (HR) were obtained (significance level $p<.05$). Exploratory analyses were not performed in the separate treatment arms to avoid over-fitting, nor were threshold values chosen at this stage.

After determining which parameters were potentially useful in predicting OS, a range of cut-off values for percentage change measured in enhancing and non-enhancing lesions separately were tested in the entire group, in those treated with bevacizumab, and in all treatment arms separately. For the optimal threshold, results were corrected in a multivariate survival analysis (cox regression) for age, WHO performance status, corticosteroid use, and baseline enhancing volume (if $p<.10$ in univariate analysis).

In every patient, baseline and first follow-up scans had been performed in the same hospital on scanners from the same vendor. Four patients were scanned at different scanner field strengths between baseline and first follow-up (i.e. 1.5T and 3.0T). To assess the effect of differences in field strength, an additional analysis was

performed, correcting for differences in ADC values, using a factor of -9.79% to correct the values from the 3.0T scanner[18].

## RESULTS

### Patients

Out of 148 eligible patients, only those patients with 3D T1w post-contrast and/or T2w/FLAIR images were analyzed. In the analysis of enhancing lesions and non-enhancing lesions, respectively 108 and 99 patients were included (see ***Figure 2***).

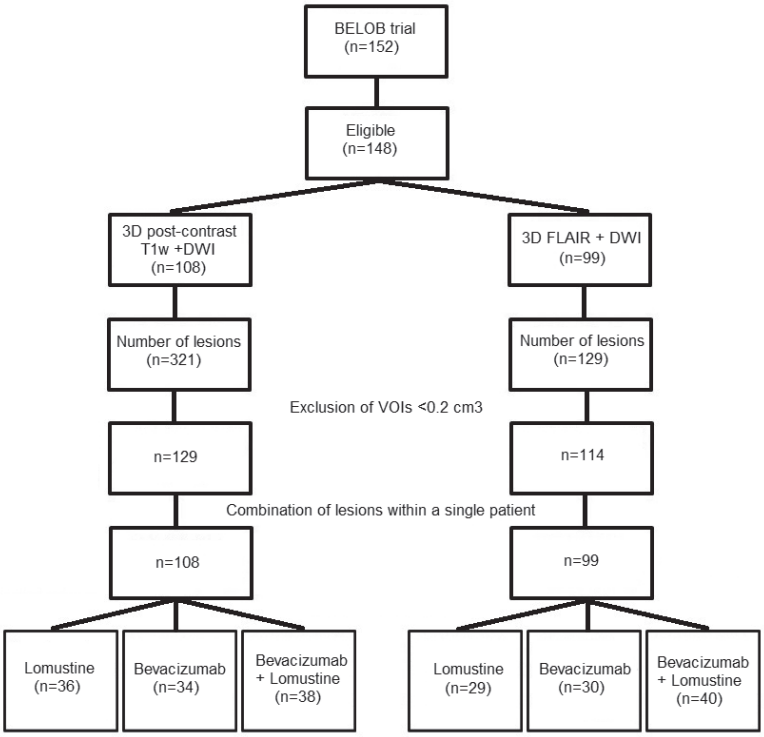


**Figure 2:** Flow diagram showing all patients included in the BELOB trial and those included in the final analyses. Patients with 3D T1weighted post-contrast (T1w+C) and 3D FLAIR scans at both baseline and first follow-up were included. Lesions <0.2cm$^3$ were excluded; if multiple lesions were present within a single patient, these were combined in a single volume of interest.

### Histogram analysis

In the exploratory analysis, only skewness ($ADC_{skew}$) and minimum ADC ($ADC_{min}$) showed promise in predicting OS. Further exploration of the $ADC_{skew}$ data showed inconsistent

findings due to multiple outliers. $ADC_{min}$ did show consistent significant results and further cut-off values for percentage decrease of this parameter were tested (5%, 10%, 15%, 20%, 22.5%, 25%, 27.5%, 30%, and 32.5%) in enhancing and non-enhancing lesions separately (***Supplementary Files: Table S1*** and ***Table S2***). ***Figure 3*** shows an example of $ADC_{min}$ histograms at baseline and first follow-up. Other histogram parameters explored did not show meaningful correlations with OS (data not shown).

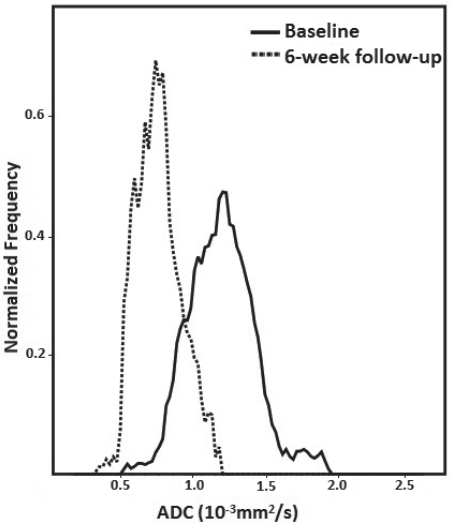


**Figure 3:** Apparent diffusion coefficient (ADC) histogram at baseline (**bold line**) and first follow-up at 6 weeks (**dotted line**) in an enhancing lesion of a patient treated with bevacizumab plus lomustine. Percentage change in $ADC_{min}$ was -33.64% and the OS 13.3 months.

In enhancing VOIs (n=108), when assessing all treatment groups combined stratification of patients based on a decrease in $ADC_{min}$ of 20% to 30% showed a significant difference in OS, with the most significant HR found with 27.5% decrease (HR=0.572, 95% CI 0.38-0.86, p=.007). This result remained significant after correcting for WHO performance status, corticosteroid use, and baseline enhancing volume (HR=0.482, 95% CI 0.32-0.74, p=.001), see ***Table 1***. In both bevacizumab-treated groups combined (n=72) stratification of patients based on decrease in $ADC_{min}$ of 10% to 30% showed a significant difference in OS. The most significant HR was found with 27.5% decrease (HR=0.452, 95% CI 0.27-0.75, p=.003), which after correcting for covariates remained significant (HR=0.415, 95% CI 0.25-0.70, p=.001), see ***Table 2***. Upon further dividing the bevacizumab-treated groups into the bevacizumab-only and combined treatment arms, the significant differences were shown to originate from the combined treatment arm (n=38): stratification of patients based on decrease in $ADC_{min}$ of 5% to 27.5% showed a significant difference in OS in this patient group. The most significant HR was again found with 27.5% decrease (HR=0.287, 95% CI 0.34-0.60, p=.001). Results remained significant after correcting for corticosteroid use (HR=0.250, 95% CI 0.12-0.54, p<.001), see ***Table 3***. The mean OS measured

**Table 1:** Univariate and multivariate assessment of the predictive value of >27.5% decrease in $ADC_{min}$ in enhancing lesions in all treatment groups together (n=108)

| All patients (n=108) | | | | | | |
|---|---|---|---|---|---|---|
| **Variables** | **Univariate** | | | **Multivariate** | | |
| | **Hazard Ratio** | **95% CI** | **p-value** | **Hazard Ratio** | **95% CI** | **P-value** |
| >27.5% decrease in $ADC_{min}$* | 0.572 | 0.38-0.86 | .007 | 0.482 | 0.32-0.74 | .001 |
| Age | 1.003 | 0.99-1.02 | .713 | | | |
| WHO performance status | 1.446 | 1.02-2.05 | .039 | 1.424 | 0.94-2.16 | .096 |
| Corticosteroid use | 1.551 | 1.05-2.28 | .026 | 1.010 | 0.62-1.64 | .968 |
| Baseline enhancing volume | 1.022 | 1.01-1.04 | .006 | 1.026 | 1.01-1.04 | .003 |

**$ADC_{min}$ = minimum apparent diffusion coefficient; WHO = world health organization; CI=confidence interval*

**Table 2:** Univariate and multivariate assessment of the predictive value of >27.5% decrease in $ADC_{min}$ in enhancing lesions in both bevacizumab-treated groups (n=72)

| Both bevacizumab-treated groups (n=72) | | | | | | |
|---|---|---|---|---|---|---|
| **Variables** | **Univariate** | | | **Multivariate** | | |
| | **Hazard Ratio** | **95% CI** | **p-value** | **Hazard Ratio** | **95% CI** | **p-value** |
| >27.5% decrease in $ADC_{min}$* | 0.452 | 0.27-0.75 | .002 | 0.415 | 0.25-0.70 | .001 |
| Age | 1.005 | 0.99-1.03 | .611 | | | |
| WHO performance status | 1.456 | 0.94-2.25 | .090 | 1.417 | 0.85-2.36 | .181 |
| Corticosteroid use | 1.677 | 1.04-2.69 | .033 | 1.213 | 0.69-2.14 | .503 |
| Baseline enhancing volume | 1.021 | 1.00-1.04 | .038 | 1.017 | 0.99-1.04 | .118 |

**$ADC_{min}$ = minimum apparent diffusion coefficient; WHO = world health organization; CI=confidence interval*

**Table 3:** Univariate and multivariate assessment of the predictive value of >27.5% decrease in $ADC_{min}$ in enhancing lesions in the combined treatment arm (i.e. lomustine and bevacizumab) (n=38).

| Bevacizumab + lomustine (n=38) | | | | | | |
|---|---|---|---|---|---|---|
| **Variables** | **Univariate** | | | **Multivariate** | | |
| | **Hazard Ratio** | **95% CI** | **p-value** | **Hazard Ratio** | **95% CI** | **p-value** |
| >27.5% decrease in $ADC_{min}$* | 0.287 | 0.14-0.60 | .001 | 0.250 | 0.12-0.54 | <.001 |
| Age | 1.003 | 0.98-1.03 | .836 | | | |
| WHO performance status | 1.329 | 0.74-2.40 | .344 | | | |
| Corticosteroid use | 1.807 | 0.92-3.55 | .085 | 2.139 | 1.07-4.29 | .033 |
| Baseline enhancing volume | 1.015 | 0.99-1.04 | .264 | | | |

**$ADC_{min}$ = minimum apparent diffusion coefficient; WHO = world health organization; CI=confidence interval*

from first follow-up was 15.2 months in patients with a decrease in $ADC_{min}$ ≥27.5% (n=24), versus 6.8 months in those with a decrease of $ADC_{min}$ <27.5% (n=14). In the bevacizumab or the lomustine monotherapy group, no significant differences in OS were seen at any of the cut-off values. After correction for differences in scanner field strength between baseline and follow-up in four patients, stratification of patients based on the $ADC_{min}$ percentage change in the enhancing lesions was unchanged. Kaplan-Meier curves of all patients together, both bevacizumab-treated groups, and the bevacizumab-treated groups separately using 27.5% decrease in $ADC_{min}$ as a cut-off value are shown in ***Figure 4***.

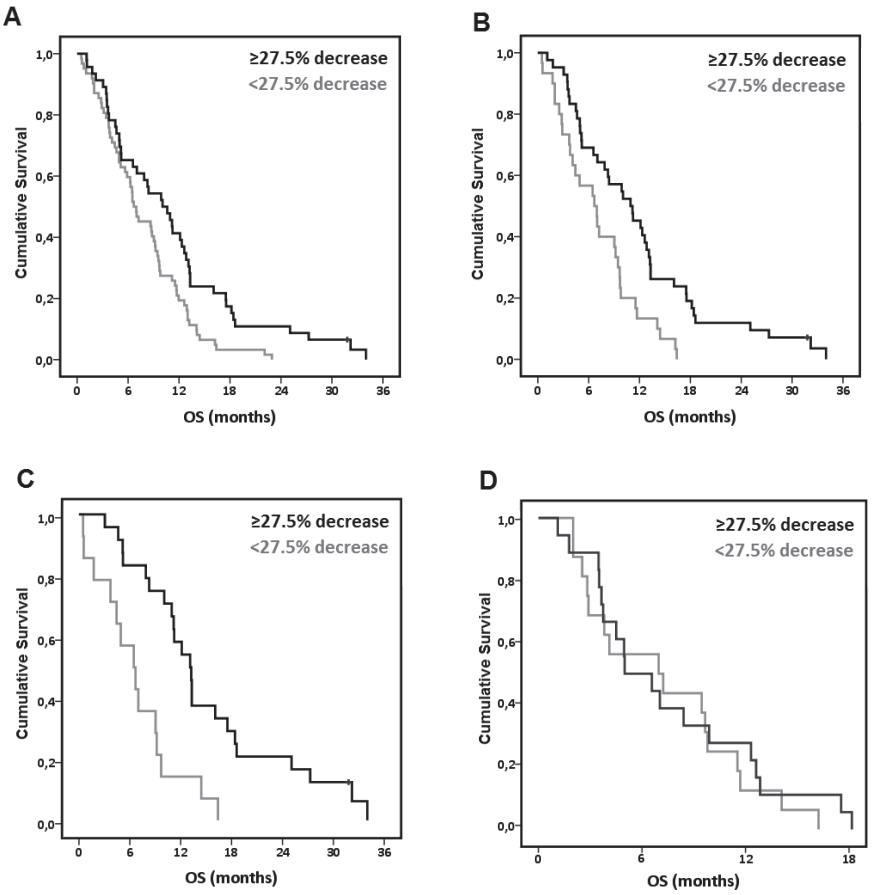


**Figure 4 (A-D):** Kaplan-Meier with 27.5% decrease of minimum apparent diffusion coefficient ($ADC_{min}$) as a cut-off value in enhancing lesions (data from table 1), for all treatment groups together (**A**), for both bevacizumab-treated (bevacizumab monotherapy and bevacizumab plus lomustine combined treatment) groups (**B**), for the bevacizumab plus lomustine group (**C**), and the bevacizumab monotherapy group (**D**).

In non-enhancing lesions (n=99) (***Supplementary Files: Table S2***) there were no significant differences in OS after stratification of patients based on any of the $ADC_{min}$ percentage change values.

## DISCUSSION

In the context of the phase II BELOB-trial, we found that patients treated with bevacizumab and lomustine for recurrent glioblastoma had a significantly better OS, i.e. an indication of response, when there was a decrease of $ADC_{min}$ in enhancing lesions after the first course of treatment than in those who didn't show such a decrease. The optimum cut-off value for establishing response was 27.5% decrease in $ADC_{min}$. In patients treated with bevacizumab or lomustine monotherapy, or in non-enhancing lesions, an association between ADC changes and OS was not seen.

The significant difference in OS based on $ADC_{min}$ was seen when patients from all treatment arms were combined as well as when all bevacizumab-treated patients were considered. These findings seemed to be driven by the combined treatment arm, as no significant effects were found in the monotherapy groups. Considering the BELOB-trial survival data, published previously[15], patients treated with bevacizumab plus lomustine showed a better OS then those treated with bevacizumab or lomustine alone. This result was however not reproduced in the subsequent phase III trial EORTC 26101[19], possibly indicating differences between patient samples. We must therefore consider the possibility that our results are specific to the BELOB-trial population. However, the observed changes could also indicate true tumor response in a subset receiving combination treatment. Our results will need to be externally validated in order to generalize these. It should be noted that while exploratory analyses were performed in the same population as the test population, they were performed within the entire patient group without optimization for a specific treatment arm nor was a specific threshold value established at this stage.

Because of tumor heterogeneity, changes in diffusion may differ between tumor regions[20]. Measures such as $ADC_{mean}$ and $ADC_{median}$ are therefore less insightful when considering lesions as a whole. Aside from $ADC_{min}$, skewness also showed promise, but in our analysis there were so many outliers in the $ADC_{skew}$ data that this parameter was considered unreliable.

A comparison between our study and previous studies is problematic, because of differences in patient populations (with varying number of recurrences or inclusion of grade III glioma), post-processing methods, treatment (bevacizumab monotherapy and/or combined therapy groups), and measured time-points (pretreatment-only; different follow-up). In a recent publication, Ellingson et al. conclude that *pre-*

*treatment* diffusion histogram analysis can be predictive in recurrent GBM treated with angiogenesis inhibitor monotherapy[21]. Here, we focused on determining the response *after* treatment, which is known to be problematic in the context of anti-angiogenic agents due to issues with pseudo-response. We specifically looked at the first moment of follow-up after start of treatment, assessing *change* in ADC from baseline to first follow-up, considering an early response assessment most relevant for treatment decisions. There are a few other studies assessing changes from baseline to first follow-up. These measured volumes of foci with low ADC values within T2w/FLAIR abnormalities[22-24], sometimes by means of a graded functional diffusion map (fDM)[25]. In these studies, low $ADC_{min}$ at baseline and larger volumes of areas with low ADC values predicted a worse outcome.

Low ADC is hypothesized to reflect regions of high cellularity within the tumor[25], which is consistent with worse outcome as established in previous studies[22-24]. Our seemingly contradictory results can be explained in light of the changes occurring after bevacizumab-treatment specifically. Anti-angiogenic treatment normalizes tumor vasculature leading to a decrease in enhancement, perfusion, and ADC[7-9]. Diffusion restriction could be the result of hypoxia, but could also be due to a reduction in blood volume. The decrease in ADC in those treated with both bevacizumab and chemotherapy may thus reflect a strong anti-angiogenic treatment induced anti-tumoral effect, resulting in better OS as an indication of treatment response. In patients not treated with bevacizumab, diffusion restriction likely corresponds with hypercellularity[26], thus showing a negative impact on survival.

ADC changes in non-enhancing lesions were not predictive of OS. The T2w/FLAIR abnormalities in recurrent glioblastoma are generally a combination of non-enhancing tumor, edema, and treatment effects. Given the heterogeneity of the T2w/FLAIR abnormalities it is possible that differential effects were obscured.

Aside from the need to validate our findings in a different cohort, other limitations are the retrospective nature of the study, and the fact that these patients were all derived from a phase II trial.

In conclusion, we found that decreasing $ADC_{min}$ in enhancing tumor from baseline to first follow-up in patients with recurrent glioblastoma treated with bevacizumab and lomustine predicted OS using a cut-off percentage change between 5 and 27.5% with a significantly better OS found in those with decreasing $ADC_{min}$. These results indicate that the assessment of ADC may have a role in predicting response after the first course of combined bevacizumab and lomustine treatment, but given the fact that findings are derived from data acquired in the context of a phase II trial, external validation in a wider cohort is required before these can be generalized to all patients treated with bevacizumab in combination with lomustine.

## REFERENCES


1. Stupp RH, Mason ME, van den Bent MJ, et al. Effects of radiotherapy with concomitant and adjuvant temozolomide versus radiotherapy alone on survival in glioblastoma in a randomized phase III study: 5-year analysis of the EORTC-NCIC trial. Lancet Oncol 2009;10(5):459-466
2. Ostrom QT, Gittleman H, Fulop J, et al. CBTRUS statistical report: primary brain and central nervous system tumors diagnosed in the United States in 2008-2012. Neuro Oncol 2015;17 Suppl 4:iv1-iv62.
3. Friedman HS, Petros WP, Friedman AH, et al. Irinotecan therapy in adults with recurrent or progressive malignant glioma. J Clin Oncol 1999;17(5):1516-1525.
4. Kreisl TN, Kim L, Moore K, et al. Phase II trial of single-agent bevacizumab followed by bevacizumab plus irinotecan at tumor progression in recurrent glioblastoma. J Clin Oncol 2009;27(5):740-745.
5. Jain JK. Normalization of tumor vasculature: an emerging concept in antiangiogenic therapy. Science 2005;307(5706):58-62.
6. Pope WB, Lai A, Nghiemphu P, Mischel P, Cloughesy TF. MRI in patients with high-grade gliomas treated with bevacizumab and chemotherapy. Neurology 2006;66(8):1258-1260.
7. Sawlani RN, Raizer J, Horowitz SW, et al. Glioblastoma: a method for predicting response to antiangiogenic chemotherapy by using MR perfusion imaging – pilot study. Radiology 2010;255(2): 622-628.
8. Jain R, Scarpace LM, Ellika S, et al. Imaging response criteria for recurrent gliomas treated with bevacizumab: role of diffusion weighted imaging as an imaging biomarker. J Neurooncol 2010; 96(3):423-431.
9. Rieger J, Bähr O, Müller K, Franz K, Steinbach J, Hattingen E. Bevacizumab-induced diffusion-restricted lesions in malignant glioma patients. J Neurooncol 2010;99(1):49-56.
10. Wen PY, Macdonald DR, Reardon DA, et al. Updated response assessment criteria for high-grade gliomas: response assessment in neuro-oncology working group. J Clin Oncol 2010;28(11):1963-1972.
11. Pope WB, Kim HJ, Huo J, et al. Recurrent glioblastoma multiforme: ADC histogram analysis predicts response to bevacizumab treatment. Radiology 2009;252(1):182-189.
12. Ellingson BM, Sahebjam S, Kim HJ, et al. Pretreatment ADC histogram analysis is a predictive imaging biomarker for bevacizumab treatment but not chemotherapy in recurrent glioblastoma. AJNR Am J Neuroradiol 2014;35(4):673-679.
13. Pope WB, Young JR, Ellingson BM. Advances in MRI assessment of gliomas and response to anti-VEGF therapy. Curr Neurol Neurosci Rep 2011;11(3):336-344.
14. Norden AD, Young GS, Setayesh K, et al. Bevacizumab for recurrent malignant gliomas: efficacy, toxicity, and patterns of recurrence. Neurology 2008;70(10):779-787.
15. Taal W, Oosterkamp HM, Walenkamp AM, et al. Single-agent bevacizumab or lomustine versus a combination of bevacizumab plus lomustine in patients with recurrent glioblastoma (BELOB trial): a randomized controlled phase 2 trial. Lancet Oncol 2014;15(9):943-953.
16. Gahrmann R, van den Bent MJ, van der Holt B, et al. Comparison of 2D (RANO) and volumetric methods for assessment of recurrent glioblastoma treated with bevacizumab – a report from the BELOB trial. Neuro Oncol 2017;19(6):853-861.
17. Klein S, Staring M, Murphy K, Viergever MA, Pluim JP. Elastix: a toolbox for intensity-based medical image registration. IEEE Trans Med Imaging 2010;29(1):196-205.

**18.** Huisman TA, Loenneker T, Barta G, et al. Quantitative diffusion tensor MR imaging of the brain: field strength related variance of apparent diffusion coefficient (ADC) and fractional anisotropy (FA) scalars. Eur Radiol 2006;16(8):1651-1658.

**19.** Wick W, Brandes AA, Gorlia A, et al. EORTC 26101 phase III trial exploring the combination of bevacizumab and lomustine in patients with first progression of a glioblastoma. J Clin Oncol 2016; 34:15_suppl.2001.

**20.** Moffat BA, Chenevert TL, Lawrence TS, et al. Functional diffusion map: a noninvasive MRI biomarker for early stratification of clinical brain tumor response. Proc Natl Acad Sci U S A 2005; 102(15):5524-5529.

**21.** Ellingson BM, Gerstner E, Smits M, et al. Diffusion MRI phenotypes predict overall survival benefit from anti-VEGF monotherapy in recurrent glioblastoma: converging evidence from phase II trials. Clinical Cancer research 2017; DOI 10.1158/1078-0432.CCR-16-2844 [Epub ahead of print].

**22.** Hwang EJ, Cha Y, Lee AL, et al. Early response evaluation for recurrent high grade gliomas treated with bevacizumab: a volumetric analysis using diffusion-weighted imaging. J neurooncol 2013; 112(3):427-435.

**23.** Gerstner ER, Chen PJ, Wen PY, Jain RK, Batchelor TT, Sorensen G. Infiltrative patterns of glioblastoma spread detected via diffusion MRI after treatment with cediranib. Neuro Oncol 2010;12(5): 466-472.

**24.** Zhang M, Gulotta B, Thomas A, et al. Large-volume low apparent diffusion coefficient lesions predict poor survival in bevacizumab-treated glioblastoma patients. Neuro Oncol 2016;18(5): 735-743.

**25.** Ellingson BM, Cloughesy TF, Lai A, et al. Graded diffusion map-defined characteristics of apparent diffusion coefficients predict overall survival in recurrent glioblastoma treated with bevacizumab. Neuro Oncol 2011;13(10):1151-1161.

**26.** Sugahara T, Korogi Y, Kochi M, et al. Usefulness of diffusion-weighted MRI with echo-planar technique in the evaluation of cellularity in gliomas. J Magn Reson Imaging 1999;9(1):53-60.

## SUPPLEMENTARY FILES

### **A**: Parameter settings used in Elastix

**Parameter settings "rigid" component**
(FixedInternalImagePixelType "float")
(MovingInternalImagePixelType "float")
(FixedImageDimension 3)
(MovingImageDimension 3)
(UseDirectionCosines "true")
(Registration "MultiResolutionRegistration")
(Interpolator "BSplineInterpolator")
(ResampleInterpolator "FinalBSplineInterpolator")
(Resampler "DefaultResampler")
(FixedImagePyramid
"FixedSmoothingImagePyramid")
(MovingImagePyramid
"MovingSmoothingImagePyramid")
(Optimizer "AdaptiveStochasticGradientDescent")
(Transform "AffineDTITransform")
(Metric "AdvancedMattesMutualInformation")
(AutomaticScalesEstimation "true")
(AutomaticTransformInitialization "true")
(HowToCombineTransforms "Compose")
(NumberOfHistogramBins 32)
(ErodeMask "false")
(Scales 1.0e+03 1.0e+03 1.0e+03 3.0e+038 3.0e+038
3.0e+038 3.0e+038 3.0e+038 3.0e+038 -1 -1 -1)
(NumberOfResolutions 2)
(MaximumNumberOfIterations 3000)
(NumberOfSpatialSamples 10000)
(CheckNumberOfSamples "false")
(NewSamplesEveryIteration "true")
(ImageSampler "RandomCoordinate")
(BSplineInterpolationOrder 1)
(FinalBSplineInterpolationOrder 1)
(DefaultPixelValue 0)
(WriteResultImage "true")
(ResultImagePixelType "float")
(ResultImageFormat "nii")
(MaximumNumberOfSamplingAttempts 100)

**Parameter settings "affine" component**
(FixedInternalImagePixelType "float")
(MovingInternalImagePixelType "float")
(FixedImageDimension 3)
(MovingImageDimension 3)
(UseDirectionCosines "true")
(Registration "MultiResolutionRegistration")
(Interpolator "BSplineInterpolator")
(ResampleInterpolator "FinalBSplineInterpolator")
(Resampler "DefaultResampler")
(FixedImagePyramid
"FixedRecursiveImagePyramid")
(MovingImagePyramid
"MovingRecursiveImagePyramid")
(Optimizer "AdaptiveStochasticGradientDescent")
(Transform "AffineDTITransform")
(Metric "AdvancedMattesMutualInformation")
(AutomaticScalesEstimation "true")
(AutomaticTransformInitialization "true")
(HowToCombineTransforms "Compose")
(NumberOfHistogramBins 64)
(ErodeMask "false")
(Scales -1 -1 -1 1.0e+6 1.0e+6 1.0e+6 1.0e+6
1.0e+6 1.0e+6 -1 -1 -1)
(NumberOfResolutions 1)
(MaximumNumberOfIterations 2000)
(NumberOfSpatialSamples 10000)
(CheckNumberOfSamples "false")
(NewSamplesEveryIteration "true")
(ImageSampler "RandomCoordinate")
(BSplineInterpolationOrder 1)
(FinalBSplineInterpolationOrder 1)
(DefaultPixelValue 0)
(WriteResultImage "true")
(ResultImagePixelType "float")
(ResultImageFormat "nii")
(MaximumNumberOfSamplingAttempts 100)

**Parameter settings “b-spline” component**
(FixedInternalImagePixelType “float”)
(MovingInternalImagePixelType “float”)
(FixedImageDimension 3)
(MovingImageDimension 3)
(UseDirectionCosines “true”)
(Registration “MultiResolutionRegistration”)
(Interpolator “BSplineInterpolator”)
(ResampleInterpolator “FinalBSplineInterpolator”)
(Resampler “DefaultResampler”)
(FixedImagePyramid “FixedSmoothingImagePyramid”)
(MovingImagePyramid “MovingSmoothingImagePyramid”)
(Optimizer “AdaptiveStochasticGradientDescent”)
(Transform “BSplineTransform”)
(Metric “AdvancedMattesMutualInformation”)
(FinalGridSpacingInPhysicalUnits 30 30 30)
(MovingImageDerivativeScales 0.0 1.0 0.0)
(HowToCombineTransforms “Compose”)
(NumberOfHistogramBins 32)
(ErodeMask “false”)
(NumberOfResolutions 1)
(MaximumNumberOfIterations 5000)
(NumberOfSpatialSamples 10000)
(CheckNumberOfSamples “false”)
(NewSamplesEveryIteration “true”)
(ImageSampler “RandomCoordinate”)
(BSplineInterpolationOrder 1)
(FinalBSplineInterpolationOrder 1)
(DefaultPixelValue 0)
(WriteResultImage “true”)
(ResultImagePixelType “float”)
(ResultImageFormat “nii”)
(MaximumNumberOfSamplingAttempts 5)

**Table S1:** Findings in all enhancing lesions (n=108) for all treatment groups together, both bevacizumab-treated groups together, and the bevacizumab-treated groups separately (i.e. bevacizumab + lomustine and bevacizumab-only). Hazard ratio's (HRs), 95% confidence intervals (CI) and p-values per percentage decrease in $ADC_{min}$ at first follow-up.

| Treatment | All treatment groups (n=108) | | | Both bevacizumab-treated groups (n=72) | | | Bevacizumab + lomustine (n=38) | | | Bevacizumab-only (34) | | | Lomustine-only (n=36) | | |
|---|---|---|---|---|---|---|---|---|---|---|---|---|---|---|---|
| $ADC_{min}$ % decrease | HR | 95% CI | p-value | HR | 95% CI | p-value | HR | 95% CI | p-value | HR | 95% CI | p-value | HR | 95% CI | p-value |
| **5** | 0.781 | 0.52-1.17 | .230 | 0.609 | 0.36-1.05 | .074 | 0.361 | 0.16-0.81 | .013 | 1.110 | 0.52-2.36 | .787 | 1.653 | 0.84-3.26 | .147 |
| **10** | 0.731 | 0.49-1.09 | .122 | 0.571 | 0.34-0.96 | .038 | 0.386 | 0.18-0.82 | .014 | 0.956 | 0.47-1.94 | .901 | 1.627 | 0.82-3.23 | .165 |
| **15** | 0.725 | 0.49-1.08 | .112 | 0.571 | 0.34-0.96 | .038 | 0.386 | 0.18-0.82 | .014 | 0.956 | 0.47-1.94 | .901 | 1.900 | 0.91-3.95 | .086 |
| **20** | 0.647 | 0.43-0.97 | .032 | 0.528 | 0.32-0.88 | .016 | 0.356 | 0.17-0.75 | .007 | 0.917 | 0.46-1.84 | .807 | 1.583 | 0.73-3.44 | .246 |
| **22.5** | 0.641 | 0.43-.095 | .027 | 0.528 | 0.32-0.88 | .016 | 0.356 | 0.17-0.75 | .007 | 0.917 | 0.46-1.84 | .807 | 2.350 | 0.88-6.30 | .089 |
| **25** | 0.597 | 0.40-0.89 | .011 | 0.482 | 0.29-0.80 | .006 | 0.329 | 0.16-0.69 | .003 | 0.820 | 0.41-1.65 | .577 | 2.772 | 0.94-8.17 | .064 |
| **27.5** | 0.572 | 0.38-0.86 | .007 | 0.452 | 0.27-0.75 | .003 | 0.287 | 0.34-0.60 | .001 | 0.820 | 0.41-1.65 | .577 | 2.772 | 0.94-8.17 | .064 |
| **30** | 0.664 | 0.48-0.99 | .040 | 0.585 | 0.36-0.95 | .032 | 0.531 | 0.27-1.05 | .070 | 0.754 | 0.38-1.52 | .429 | 2.772 | 0.94-8.17 | .064 |
| **32.5** | 0.746 | 0.50-1.12 | .147 | 0.698 | 0.44-1.12 | .135 | 0.663 | 0.34-1.30 | .230 | 0.901 | 0.45-1.81 | .768 | 2.772 | 0.94-8.17 | .064 |

$ADC_{min}$ = minimum apparent diffusion coefficient

**Table S2:** Findings in all non-enhancing lesions (n=99). Results from all treatment groups together, both bevacizumab-treated groups together, and the three separate treatment arms, i.e. bevacizumab + lomustine, bevacizumab-only and lomustine-only. Hazard ratio's (HR) and their 95% confidence intervals (CI) with corresponding p-values per percentage decrease in $ADC_{min}$ at first follow-up.

| Treatment | All treatment groups (n=99) | | | Both bevacizumab-treated groups (n=70) | | | Bevacizumab + lomustine (n=40) | | | Bevacizumab-only (30) | | | Lomustine-only (n=29) | | |
|---|---|---|---|---|---|---|---|---|---|---|---|---|---|---|---|
| $ADC_{min}$ % decrease | HR | 95% CI | p-value | HR | 95% CI | p-value | HR | 95% CI | p-value | HR | 95% CI | p-value | HR | 95% CI | p-value |
| **5** | 0.737 | 0.49-1.11 | 0.145 | 0.685 | 0.41-1.14 | 0.143 | 0.571 | 0.29-1.13 | 0.106 | 0.852 | 0.39-1.85 | 0.686 | 1.289 | 0.61-2.74 | 0.511 |
| **10** | 0.727 | 0.49-1.09 | 0.121 | 0.675 | 0.42-1.09 | 0.110 | 0.681 | 0.36-1.30 | 0.243 | 0.631 | 0.30-1.32 | 0.223 | 1.734 | 0.76-3.98 | 0.195 |
| **15** | 0.818 | 0.54-1.24 | 0.339 | 0.767 | 0.48-1.24 | 0.279 | 0.776 | 0.41-1.48 | 0.441 | 0.616 | 0.29-1.31 | 0.207 | 2.093 | 0.86-5.08 | 0.102 |
| **20** | 0.841 | 0.54-1.32 | 0.448 | 0.795 | 0.48-1.33 | .0380 | 0.855 | 0.43-1.68 | 0.650 | 0.865 | 0.30-1.55 | 0.365 | 2.207 | 0.82-5.98 | 0.119 |
| **22.5** | 0.775 | 0.48-1.24 | 0.291 | 0.699 | 0.41-1.20 | 0.197 | 0.814 | 0.41-1.63 | 0.560 | 0.567 | 0.22-1.50 | 0.252 | 2.207 | 0.82-5.98 | 0.119 |
| **25** | 1.120 | 0.65-1.92 | 0.680 | 1.116 | 0.61-2.06 | 0.724 | 1.214 | 0.55-2.68 | 0.630 | 1.067 | 0.40-2.86 | 0.897 | 1.725 | 0.51-5.87 | 0.383 |
| **27.5** | 1.418 | 0.81-2.48 | 0.218 | 1.452 | 0.77-2.74 | 0.248 | 1.780 | 0.77-4.12 | 0.176 | 1.067 | 0.40-2.86 | 0.897 | 1.725 | 0.51-5.87 | 0.383 |
| **30** | 1.342 | 0.73-2.47 | 0.343 | 1.312 | 0.65-2.67 | 0.453 | 1.509 | 0.62-3.66 | 0.363 | 1.315 | 0.38-4.50 | 0.663 | 1.725 | 0.51-5.87 | 0.383 |
| **32.5** | 1.250 | 0.65-2.42 | 0.506 | 1.165 | 0.53-2.57 | 0.704 | 1.199 | 0.42-3.42 | 0.734 | 1.315 | 0.38-4.50 | 0.663 | 1.725 | 0.51-5.87 | 0.383 |

$ADC_{min}$ = minimum apparent diffusion coefficient

# Chapter 4

## General discussion

In this thesis I investigated the value of several specific Magnetic Resonance Imaging (MRI) techniques in patients with recurrent glioblastoma treated with bevacizumab. In these patients, a phenomenon known as pseudo-response complicates treatment response assessment. I investigated a variety of methods for measuring treatment response in this patient group. Additionally, I investigated growth patterns in newly diagnosed non-enhancing low-grade glioma using Diffusion Tensor Imaging (DTI).

## MAIN FINDINGS

### Conventional MRI techniques

The appearance of new lesions in recurrent glioblastoma patients on T1-weighted post-contrast images or T2-weighted/FLuid Attenuated Inversion Recovery (FLAIR) images (i.e. enhancing or non-enhancing lesions) early after the start of treatment clearly is associated with poor overall survival (OS) with a mean OS of just 3.2 months for those with a new lesion compared to 11.2 months in those without a new lesion at 6 weeks follow-up. We can therefore conclude that the appearance of a new lesion is a strong predictor for OS. This effect is independent of treatment.

We compared the 2D Response Assessment in Neuro-Oncology (RANO) criteria with various volumetric methods: contrast-enhancing volume only (measured on either T1w post-contrast images or subtraction images) and contrast-enhancing volume plus non-enhancing volume (the latter measured on FLAIR images). The RANO criteria are the current method of choice for assessing treatment response in glioblastoma. According to the RANO criteria, progressive disease (PD) is defined as any of the following: ≥25% increase in the sum of perpendicular diameters of enhancing lesions or a significant increase in T2w/FLAIR non-enhancing lesions compared to baseline or best response scan after start of treatment, the appearance of new lesions, clear progression of non-measurable lesions, or clinical deterioration. Steroid dosage is also taken into account[1]. While the enhancing lesions are measured in 2D, the T2w/FLAIR non-enhancing lesions are not quantified. By measuring not only contrast-enhancing volume, but also non-enhancing volumes we hypothesized that survival prediction based on change in tumor size would improve.

Especially in patients treated with bevacizumab we hoped to find an improvement in survival prediction using volumetric measurements of non-enhancing lesions. Bevacizumab directly influences tumor vasculature (i.e. abnormal vasculature) by decreasing the permeability of the vessel wall, which may lead to a decrease in contrast-enhancement on T1-weighted post-contrast images. Since tumor activity has not decreased but is only masked, this effect is known as pseudo-response. Bevacizumab also alleviates edema and by doing so, decreases non-enhancing abnormalities on T2w/FLAIR images. At progression, an increase in non-enhancing tumor has been described (gliomatosis cerebri), but whether this pattern of progression occurs more often in patients treated with bevacizumab has been questioned[2-5].

We assessed both lomustine-only treated and bevacizumab-treated (with and without lomustine) patients and found that determining PD with volumetric methods did not significantly improve survival prediction at 6 and 12 weeks follow-up in any of the treatment groups and nor did subtraction techniques improve survival

prediction. Since volumetric assessment is more time-consuming, these findings support the use of 2D evaluation.

However, the threshold set for volumetric PD was ≥40% for enhancing tumor volume[6-8] and ≥25% for non-enhancing volume[9]. To see whether different thresholds would lead to different results, we tested lower thresholds at both 6 and 12 weeks follow-up. We found that lowering the thresholds improved prediction and that this result persisted after removing patients with high percentages of increase in tumor size from the analysis. Despite the better survival prediction found with these lower thresholds, the number of additional patients categorized as progressors was quite low. This was especially the case in the bevacizumab-treated group in which only a small number of patients had increasing enhancing and/or non-enhancing tumor volume.

## Diffusion Weighted Imaging

We also explored whether Apparent Diffusion Coefficient (ADC) histogram analysis would allow better outcome assessment. Some promising results for treatment response assessment were observed in patients treated with both bevacizumab and lomustine. In this group, a decrease in histogram derived minimum ADC values ($ADC_{min}$) from the enhancing tumor volume from baseline to first follow-up significantly improved survival. Those with a decrease in $ADC_{min}$ of >27.5% had a mean OS of 15.2 months versus 6.8 months in those without this decrease. This effect was however not found in the bevacizumab-only and lomustine-only treatment arms, nor were significant results found when analyzing histograms from non-enhancing volumes.

## Diffusion Tensor Imaging

A different diffusion technique is diffusion tensor imaging (DTI), which can be used to determine directionality of diffusion of water molecules. Where in DWI only the presence of diffusion restriction is measured (by measuring diffusion in 3 directions), many different directions of diffusion are measured with DTI. Subsequently, the general direction of diffusion within a voxel can be calculated. Directionality in the brain is strongest in white matter where diffusion occurs along white matter tracts (high anisotropic values) and lowest in the ventricles (high isotropic values). Disturbances in white matter architecture by a tumor are made apparent using DTI. A tumor can grow by infiltrating white matter tracts by pushing into them or growing alongside the fiber bundles.

DTI derived isotropic (*p*) and anisotropic (*q*) maps have previously been used by Price et al.[10] to discern different molecular subtypes of glioblastoma (i.e. *IDH*-mutated versus *IDH* wild-type) based on different patterns of growth into/along white matter tracts. The authors reconfirmed that Isocitrate dehydrogenase (*IDH*) mutated glioblastomas grow less invasively than *IDH* wild-type tumors and that this is associated with patient prognosis. We used the same technique in pretreated non-

enhancing (presumed low-grade) gliomas to discern *IDH*-mutated and *IDH* wild-type tumors as well. We also looked at 1p19q codeleted versus non-codeleted tumors (i.e. molecular oligodendrogliomas versus astrocytomas) to see if there were differences in growth patterns between these molecular subtypes. Only 4 patients with an *IDH*-WT tumor were available for this analysis, but these all showed different growth patterns. These same 4 growth patterns were also found in the *IDH*-mutated group. 1p19q codeleted and non-codeleted tumors were more evenly distributed, but no significant differences in growth patterns were found here either.

## METHODOLOGICAL CONSIDERATIONS

All four chapters on the BELOB-trial have their focus on finding a better method for treatment response assessment in bevacizumab-treated recurrent glioblastoma. Effectiveness of treatment can be determined by correlating this with the golden endpoint for oncology trials: overall survival (OS). To predict OS, a cox regression analysis can be performed in which hazard ratios (HRs) are calculated for those with and without progressive disease (PD) as determined per method. The evaluation method leading to the highest HR at a given time-point is the best method for predicting OS and most likely to reflect benefit in a phase III trial with OS as the primary endpoint. When interpreting these results, it is important to consider the number of patients that are categorized as progressors with a particular method and the overlap in confidence intervals between methods. This places results in a broader perspective (shown in ***chapter 3.2***).

Different methods, such as DWI and perfusion imaging, can potentially provide other markers for treatment response in bevacizumab-treated patients. Regarding the results we found, it is important to note that our research took place within the context of a clinical trial and thus results are not directly generalizable to all patients with recurrent glioblastoma treated with other agents. This means that aside from validation in a different and larger cohort of patients, positive findings in our analysis would need to be confirmed in independent datasets and preferably in 'real life' clinical setting as well.

We also assessed non-enhancing glioma growth patterns with DTI. We reproduced a *p/q* mapping technique that was previously found successful for discerning molecular subtypes of glioblastoma[10,11]. The methodology included the drawing of volumes of interest (VOIs) on both the *p* and *q* maps and subsequently overlaying the two in order to detect mismatch. Mismatch was determined if the *p*-VOI exceeded the *q*-VOI by >0.5cm, although in the 2017 publication by Price, a cut-off of 1.0cm was

used. Three different patterns of mismatch were described: a minimally invasive pattern, a localized pattern, and a diffuse pattern.

Reproducing the exact methodology proved difficult: drawing a volume of interest (VOI) on the *q*-map was unreliable as many variations were possible within a single patient (***Figure 1***). Instead we overlaid the *p*-VOI on the *q*-map and scored where the *p*-VOI overlapped high intensity areas on the *q*-map (i.e. white matter tracts), basically measuring the invasiveness of the tumor into white matter tracts. However, the three categories described by Price et al. did not adequately define the patterns we encountered and we instead used 5 different categories. One of the reasons for doing so, is that we found that some tumors would expand into white matter tracts, while others would follow the tracts in a more infiltrative fashion.

Because of the many possible variations in delineation of the *q*-VOI, as well as the different patterns of infiltrative growth encountered, we were unable to reproduce the exact method used by Price. Possibly, our different patient characteristics, i.e. glioblastoma versus non-enhancing gliomas, are to blame. However, when evaluating the specific problems we encountered, we find that the technique itself is not reliable and/or robust enough for application. The lack of positive results and in particular the four different patterns found in the *IDH*-WT patients was unexpected given the highly positive results found by Price in glioblastomas. The difficulties we encountered reproducing the method were reflected in the low interrater agreement of 62.7%. In fact, the troubles we encountered using this technique could have obscured possible actual differences in growth patterns between the molecular subtypes of gliomas in our cohort.

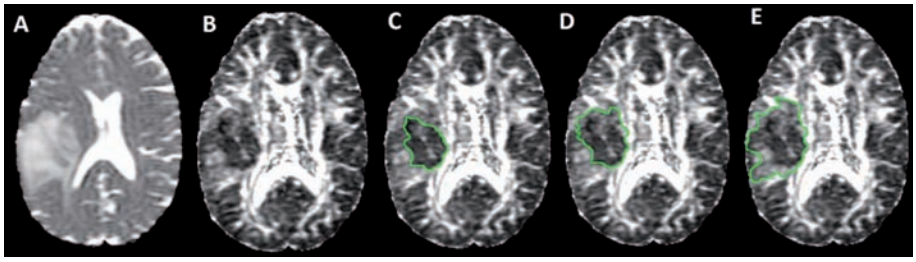


**Figure 1.** DTI-derived isotropic map (**A**), anisotropic map (**B**), and three possible volume of interest (VOI) drawings (**C**, **D**, **E**).

## Clinical Implications and future directions

The association between the appearance of new lesions and survival has direct clinical implications. The association found was independent of treatment. We found that the negative impact of a new lesion on overall survival is stronger than that of increasing tumor volume. We scored and measured both enhancing and

non-enhancing new lesions of any size that persisted or increased in volume at the subsequent follow-up scan (i.e. 6 weeks later). While the appearance of a new lesion is already included in the definition of 'progressive disease' as described in the RANO criteria, we find that more emphasis on the appearance of new lesions is needed.

(Semi)-automated volumetric tumor measures have lower intra- and interrater variability than manual measures, including 2D measures[7,12]. Heterogeneous tumors with lots of necrosis, as is the case in glioblastoma, are more difficult to measure in an axial plane and the axial plane itself is influenced by head position and slice alignment. These are strong arguments for using volumetric instead of 2D measurements. However, volumetric methods are time-consuming for various reasons: I) it takes time to send the MRI-sequence to a dedicated work-station with software for volumetric segmentation and then it takes time to send the information back to the main system, and II) an segmentation by (semi)-automated techniques is based on algorithms that often include non-tumorous areas into the volume of interest (VOI). Examples are the inclusion of blood vessels and dura into an enhancing VOI and the inclusion of the cortical ribbon into a non-enhancing VOI. This means that manual work is needed to check the VOIs and to adjust them where necessary, which is time-consuming.

Only if (semi)-automated techniques became more readily available and faster than is currently the case, would we advise volumetric methods over 2D measures. At present there is no reason to switch to volumetric methods.

When it comes to the thresholds currently in use for determining PD, we see no reason to lower them at this time as the number of patients additionally categorized as progressors is quite low in our study cohort.

In recurrent glioblastoma patients treated with bevacizumab, only a few have increasing enhancing (and non-enhancing) tumor volumes at first follow-up, despite the absence of true anti-tumor activity of this agent. More advanced methods for measuring treatment outcome should therefore be considered, unless bevacizumab is only considered as a steroid-like drug. For instance, change in $ADC_{min}$ in enhancing tumor in recurrent glioblastoma treated with both bevacizumab and lomustine is a very promising predictor for overall survival. There was a clear difference in survival between those with a decrease in $ADC_{min}$ and those without. As mentioned before, these results will need to be validated in a different and larger cohort.

Since we were unable to discern different molecular subtypes of non-enhancing gliomas using *p/q*-mapping based on different growth patterns and because of the difficulties we encountered when using this technique, we currently do not recommend using this technique in non-enhancing gliomas.

Other techniques that could be used to look at white matter changes due to tumor infiltration are tractography, FA-skeletons, and fiber density mapping. In

tractography, the orientation of diffusion is determined for every voxel individually, after which the voxels are linked together to visualize diffusion occurring along white matter tracts[13,14]. White matter tracts can also be made visible by setting a threshold above which diffusion is considered anisotropic (generally FA is used) for the whole brain. A 'skeleton' of white matter tracts appears, commonly referred to as a FA-skeleton[15]. In both tractography and FA-skeleton techniques, a threshold is needed to prevents tracts from being 'drawn' outside the white matter. The chosen threshold affects the results. Fiber density mapping is a postprocessing method that includes the reconstruction of all fiber paths in the brain and calculations of fiber density values per voxel while also using measures from adjacent voxels. It is an additional measure to FA-skeleton maps and tractography and can help quantify the extent of destruction of white matter[16]. While the extent of destruction and the type of white matter damage can be determined using these techniques, it is unclear if they can be used to determine growth patterns and if results can provide information on the molecular subtype of the tumor. Instead of looking at affected white matter, one could also look at a variety of parameters to see which correlate with molecular tumor subtypes. This method is known as radiogenomics and it has the ability to look at very large datasets and numerous parameters from different MRI sequences (and other imaging methods) from which a predictive model can be calculated.

## CONCLUSIONS

There is currently no reason to change the 2D treatment response measures to volumetric measures in recurrent glioblastoma, nor is there a reason to adjust thresholds for measuring progressive disease. More attention to early appearing new lesions is justified to optimize survival prediction and deciding on the continuation of treatment within the currently used 2D RANO criteria.

Measuring change in minimum ADC measured in enhancing tumor from baseline to first follow-up is a promising tool for determining treatment response in recurrent glioblastoma treated with both bevacizumab and lomustine.

Possible differences in growth-patterns between different molecular subtypes of non-enhancing glioma cannot be discerned using DTI-derived isotropic and anisotropic maps as described by Price et al.

## REFERENCES


1. Wen PY, MacDonald DR, Reardon DA, et al. Updated response assessment criteria for high-grade gliomas: response assessment in neuro-oncology working group. Journal of Clinical Oncology 2010;28(11):1963-1972.
2. Iwamoto FM, Abrey LE, Beal K, et al. Patterns of relapse and prognosis after bevacizumab failure in recurrent glioblastoma. Neurology 2009;73(15):1200-1206.
3. Norden AD, Young GS, Setayesh K, et al. Bevacizumab for recurrent malignant gliomas: efficacy, toxicity, and patterns of recurrence. Neurology 2008;70(10):779-787.
4. Radbruch A, Lutz K, Wiestler B, et al. Relevance of T2 signal changes in the assessment of progression of glioblastoma according to the Response Assessment in Neurooncology criteria. Neuro Oncol 2012;14(2):222-229.
5. Wick W, Wick A, Weiler M, Weller M. Patterns of progression in malignant glioma following anti-VEGF therapy: perceptions and evidence. Curr Neurol Neurosci Rep 2011;11(3):305-312.
6. Pichler J, Pachinger C, Pelz M, et al. MRI assessment of relapsed glioblastoma during treatment with bevacizumab: volumetric measurement of enhanced and FLAIR lesions for evaluation of response and progression – a pilot study. Eur J Radiol. 2013;82(5):240-245.
7. Chow DS, Qi J, Miloushev VZ, et al. Semiautomated volumetric measurement on postcontrast MR imaging for analysis of recurrent and residual disease in glioblastoma multiforme. AJNR Am J Neuroradiol. 2014;35(3):498-503.
8. Wang MY, Cheng JL, Han YH, et al. Measurement of tumor size in adult glioblastoma: classical cross-sectional criteria on 2D MRI or volumetric criteria on high resolution 3D MRI? Eur J Radiol. 2012;81(9):2370-2374.
9. Gerstner ER, Chen PJ, Wen PY, et al. Infiltrative patterns of glioblastoma spread detected via diffusion MRI after treatment with cediranib. Neuro Oncol. 2010;12(5):466-472.
10. Price SJ, Allinson K, Liu H, et al. Less invasive phenotype found in isocitrate dehydrogenase-mutated glioblastomas than in isocitrate dehydrogenase wild-type glioblastomas: a diffusion-tensor imaging study. Radiology 2017;283(1):215-221.
11. Price SJ, Jena R, Burnet NG, et al. Improved delineation of glioma margins and regions of infiltration with the use of diffusion tensor imaging: an image-guided biopsy study. AJNR Am J Neuroradiol 2006;27(9):1969-1974.
12. Sorensen AG, Patel S, Harmath C, et al. Comparison of diameter and perimeter methods for tumor volume calculation. J Clin Oncol 2001;19(2):551-557.
13. Stadlbauer A, Nimsky C, Buslei R, et al. Diffusion tensor imaging and optimized fiber tracking in glioma patients: histopathologic evaluation of tumor-invaded white matter structures. Neuroimage 2007;34(3):949-956.
14. Bucci M, Madelli ML, Berman JI, et al. Quantifying diffusion MRI tractography of the corticospinal tract in brain tumors with deterministic and probabilistic methods. Neuroimage Clin 2013;3:p.361-368.
15. Miller P, Coope D, Thompson G, Jackson A, Herholz K. Quantitative evaluation of white matter tract DTI parameter changes in gliomas using nonlinear registration. Neuroimage 2012;60(4): 2309-2315.
16. Stadlbauer A, Buchfelder M, Salomonowitz E, Ganslandt O. Fiber density mapping of gliomas: histopathologic evaluation of a diffusion-tensor imaging data processing method. Radiology 2010; 257(3):846-853.

# Chapter 5

## Summary / Samenvatting

## SUMMARY

Gliomas encompass a spectrum of primary brain tumors with different prognoses based on the exact tumor type. Originally, patient prognosis was determined by the histological tumor grade. Grade I and II gliomas are considered low-grade and bear a better prognosis than high-grade (III and IV) gliomas. However, categorizing gliomas based on molecular characteristics instead of histology has been shown to significantly improve survival prediction. The most important molecular markers in glioma are of the chromosome armes 1p and 19q and the isocitrate dehydrogenase gene 1 and 2 (*IDH*) status.

IDH mutated (*IDHmt*) gliomas bear in general a better prognosis than *IDH* wild-type (*IDHwt*) gliomas and if a codeletion of 1p19q is present (i.e. oligodendroglioma) the prognosis is better as well. An association between these molecular characteristics and specific MRI measures has previously been described. In ***Chapter 2*** we investigated whether *IDHmt* could be predicted using imaging in 'presumed low-grade' gliomas, which show no enhancement on a T1-weighted image after the administration of intravenous contrast. Using a technique called Diffusion Tensor Imaging (DTI) we aimed to determine the molecular status of the tumor. Where invasive growth in *IDHwt* compared to *IDHmt* grade IV gliomas (i.e. glioblastoma) had previously been described, we found no such results in the presumed low-grade gliomas and were therefore unable to determine molecular status based on imaging alone.

Glioblastoma are grade IV gliomas that have a 5-year survival rate of approximately 10%. Initial treatment includes surgery, chemotherapy and radiotherapy. Further treatment can consist of re-surgery and different types of chemotherapy. Recently, the US Food and Drug Administration (FDA) approved bevacizumab (Avastin) for use in glioblastoma. Bevacizumab is an angiogenesis inhibitor and inhibits Vascular Endothelial Growth Factor (VEGF). VEGF is produced in high quantities by glioblastoma and induces angiogenesis resulting in an abnormal tumor vasculature with 'leaky' blood vessels. The abnormal blood vessels will partially normalize when VEGF signaling is inhibited resulting in a decrease of the abnormal leakiness.

The results of bevacizumab-treatment can be demonstrated on MRI. After administration of intravenous contrast, the tumor will 'enhance' due to the contrast-agent leaking out of the abnormal blood vessels. Since bevacizumab normalizes the vasculature, the enhancement of the tumor decreases and edema diminishes. Despite these changes on MRI suggestive of a decrease in tumor activity, the tumor activity may not have changed at all and these bevacizumab-induced changes on MRI imaging have been called 'pseudo-response' to reflect that. The main focus of the research presented in this thesis is on finding new and better ways to determine

treatment response in patients with recurrent glioblastoma treated with or without bevacizumab.

In ***chapter 3.2*** conventional 2D tumor measurements are compared with semi-automated volumetric methods. While measurements in tumor volume very accurately reflect changes, they didn't improve survival prediction. However, since we used volumetric thresholds set for determining progressive disease (PD) that are a direct extension of 2D thresholds, we considered that using different thresholds might improve survival prediction. In order to find the optimal threshold we looked at both enhancing tumor portion and non-enhancing abnormalities (including tumor, radiation effects and edema). The results, shown in ***chapter 3.3***, include that early increase in enhancing (and non-enhancing) volumes is rare in patients treated with bevacizumab, but that lowering thresholds did improve survival prediction. In contrast, the occurrence of a new lesion early after the start of treatment was strongly associated with poor overall survival.

In addition to measuring tumor volumes, we also used a more advanced MRI method to determine treatment response in ***chapter 3.4***. With Diffusion Weighted Imaging (DWI), the degree of movement of water molecules within a voxel can be measured. Enhancing portions of glioblastoma in patients treated with both bevacizumab and lomustine showed a clear decrease in minimal Apparent Diffusion Coefficient ($ADC_{min}$) in a subset of patients. These patients had a significantly better overall survival compared to patients without a decrease in $ADC_{min}$, making DWI a possible alternative for determining treatment response in this treatment group.

Other challenges in treatment response assessment come from radiotherapy treatment and include a phenomenon known as pseudo-progression. Gliomas (especially high-grade) and other intra-cranial tumors such as meningiomas and metastases are treated with radiotherapy. In ***chapter 3.1***, different MRI and nuclear imaging techniques are discussed that play an important role in post-radiotherapy treatment response assessment.

## SAMENVATTING

De meest voorkomende primaire hersentumoren zijn gliomen. De term glioom omvat een heel spectrum aan subtypen. Vroeger werd de prognose bij deze patiënten bepaald door de histologische tumorgradering waarbij laaggradige gliomen (graad I en II) een betere prognose hebben dan hooggradige gliomen (graad III en IV). Er is echter gebleken dat het indelen van gliomen op basis van moleculaire eigenschappen tot een veel betere voorspelling van de overleving leidt. De belangrijkste moleculaire eigenschappen bepalend voor de prognose zijn verlies van de chromosoomarmen 1p en 19q, en de status van het gen dat codeerd voor isocitraat dehydrogenase 1 of 2 (*IDH*).

*IDH* gemuteerde (*IDHmt*) gliomen hebben een betere prognose dan *IDH* wild-type (*IDHwt*) gliomen. Een *IDHmt* tumor met codeletie van de chromosoomarmen 1p en 19q (diagnostisch voor een oligodendroglioom) heeft een betere prognose. In eerder onderzoek is er een associatie gevonden tussen deze moleculaire tumoreigenschappen en specifieke MRI-kenmerken. In ***Hoofdstuk 2*** hebben we onderzocht of we *IDH* mutaties konden voorspellen met MRI bij 'waarschijnlijk laaggradige gliomen', welke zich kenmerken door een gebrek aan aankleuring na toediening van intraveneus contrast. Met een techniek genaamd Diffusion Tensor Imaging (DTI) hebben we geprobeerd de moleculaire status van de tumor te bepalen. Gezien de associatie gevonden in eerder onderzoek in een populatie van patiënten met hooggradige gliomen (graad IV), hoopten we vergelijkbare uitkomsten te genereren. Wij vonden echter geen associatie en hebben daarom moeten concluderen dat deze methode niet geschikt is als niet-invasieve methode voor het bepalen van moleculaire status.

Glioblastomen zijn graad IV gliomen met een 5-jaars overleving van ca. 10%. De behandeling bestaat uit chirurgische resectie, chemotherapie en radiotherapie. De tumor recidiveert altijd en wordt vervolgens opnieuw behandeld. Opties zijn o.a. re-resectie en chemotherapie. Sinds kort heeft de Amerikaanse Food and Drug Administration (FDA) gebruik van het middel bevacizumab (Avastin®) goedgekeurd voor gebruik bij patiënten met een eerste recidief glioblastoom. Bevacizumab remt Vascular Endothelial Growth Factor (VEGF) wat in grote hoeveelheden geproduceerd wordt door het glioblastoom. VEGF induceert nieuwe, maar abnormale, lekkende bloedvaten in de tumor waardoor de tumor op de MRI scan 'aankleurt' na toediening van intraveneus contrast. Bevacizumab normaliseert de bloedvaten waardoor de tumor niet of minder aankleurt en ook het oedeem (zwelling) rondom de tumor neemt af. Echter, ondanks deze verbeteringen van de MR afwijkingen is de tumor vaak onveranderd aanwezig en deze door bevacizumab geïnduceerde veranderingen zijn als 'pseudo-response' betiteld. Het grootste deel van mijn onderzoek is gericht

op het vinden van een goede manier om behandelrespons te meten bij patiënten met een eerste recidief glioblastoom behandeld met bevacizumab en/of lomustine.

In **Hoofdstuk 3.2** hebben we 2D metingen vergeleken met volumemetingen. Ondanks dat volumemetingen een betere weerspiegeling zijn van de tumoromvang, verbeterde de overlevingsvoorspelling niet wanneer er volumes in plaats van 2D metingen werden uitgevoerd. We hebben echter hiervoor afkapwaarden gebruikt die zijn afgeleid van de 2D afkapwaarden voor het bepalen van tumorprogressie, mogelijk zijn andere afkapwaarden beter in staat de overleving te voorspellen. Daarom hebben we verschillende afkapwaarden getest voor zowel volumes aankleurende tumor en niet-aankleurende afwijkingen (bestaande uit tumor, bestralingseffecten en oedeem). De resultaten worden uiteengezet in ***Hoofdstuk 3.3***. Een vroege toename in volume bij patiënten behandeld met bevacizumab bleek zeldzaam, maar het verlagen van de afkapwaarden verbeterde wel de overlevingsvoorspelling. Daarnaast vonden we dat het ontstaan van nieuwe afwijkingen na het starten van behandeling geassocieerd was met een significant slechtere overleving.

Ook hebben we een meer geavanceerde MRI methode gebruikt om behandelrespons te meten. In ***Hoofdstuk 3.4*** gebruiken we Diffusion Weighted Imaging (DWI) om de bewegingsvrijheid van watermoleculen te meten binnen een voxel. Bij een subset van de patiënten die zijn behandeld met de combinatie bevacizumab and lomustine bleek binnen het aankleurende deel van het glioblastoom er een duidelijke afname in minimale Apparent Diffusion Coëfficiënt ($ADC_{min}$) te zien. Deze patiënten bleken een significant betere overleving te hebben en het meten van $ADC_{min}$ zou derhalve als alternatief kunnen dienen bij het meten van behandelrespons.

Andere uitdagingen bij het meten van behandelrespons worden behandeld in ***Hoofdstuk 3.1***. Een belangrijke behandeling bij patiënten met hooggradige gliomen, maar ook meningiomen en metastasen, is radiotherapie. Naast tumorrespons op de radiotherapie kan er ook een fenomeen optreden bekend als pseudoprogressie. In dit hoofdstuk bespreken we verschillende MRI en nucleaire beeldvormende technieken bruikbaar bij het meten van behandelrespons na radiotherapie.

# Chapter 6

Dankwoord
List of publications
List of presentations
PhD portfolio
About the Author

## DANKWOORD

Ongeveer 4 jaar geleden kreeg ik de mogelijkheid aangeboden om aan een promotietraject te werken. Eigenlijk was het mijn bedoeling om naast de opleiding Radiologie ook wat onderzoek te doen, maar ik begreep al snel van mijn promotoren dat er zeker genoeg werk te doen was om een heel promotietraject mee te vullen. Ik hoefde er niet lang over na te denken en heb gelijk toegezegd.

Mijn grootste dank gaat uit naar Marion Smits: van co-promotor gepromoveerd naar promotor! Niet alleen heb je mij de mogelijkheid geboden om een keuze-onderzoek uit te voeren tijdens mijn opleiding geneeskunde, maar daarna ook nog eens de mogelijkheid geboden om een promotie-onderzoek te doen. Al die jaren heb ik enorm veel van jou geleerd en stond je altijd klaar om me te steunen en bij te sturen waar nodig. Ook tijdens verblijf in het buitenland gingen onze afspraken gewoon verder, maar dan via Skype. Ik kan me geen betere supervisor bedenken.

Mijn tweede promotor vanuit de Neuro-Onoclogy, Martin van den Bent, wiens nuchtere en doelgerichte blik het onderzoek de nodige klinische richting gaf. Je was altijd bereikbaar voor overleg en erg betrokken bij het onderzoek. Ik vond het een voorrecht om met jou samen te mogen werken.

Dank aan mijn commissieleden. De kleine commissie, Aad van der Lugt, Linda Jacobi-Postma en Adam Waldman, bedankt voor het lezen, beoordelen (en, ook niet onbelangrijk, het goedkeuren) van mijn proefschrift. En de grotere commissie, Jacoline Bromberg, Wiro Niessen en Sieger Leenstra, voor het deelnemen aan mijn verdediging.

Ook wil ik mijn (co-)opleiders Winnifred van Lankeren, Gabriel Krestin en Paul Lohle bedanken voor hun flexibiliteit met betrekking tot mijn opleiding Radiologie. Toen ik aan mijn onderzoek begon, had ik net 2 jaar van de opleiding Radiologie afgerond en zou ik eigenlijk naar het Elisabeth-Tweesteden ziekenhuis in Tilburg gaan ter uitwisseling. Door mijn promotietraject ben ik ruim 3.5 jaar later dan gepland naar Tilburg gegaan voor mijn 3$^{e}$ opleidingsjaar om daarna mijn opleiding weer te vervolgen in het Erasmus MC in Rotterdam.

Room 2513 originals en nieuwe roommates: Rebecca, Rozanna, Taihra, Anouk, Rinske, Carolina, Fatih, Kars en Dianne. Bedankt voor jullie continue gezelligheid en steun waardoor het werken in de toren altijd leuk was. Zeker in december met de top2000 en de kerstlampjes aan was het nooit een straf om naar werk te komen. Ook buiten

het werk hebben we veel mooie dingen samen meegemaakt zoals congresbezoeken, de Efteling, baby-bezoeken en natuurlijk op bezoek bij Rozanna in Edinburgh!

Rebecca, ik heb niet voor niets gevraagd of je mijn paranimf wilde zijn. De afgelopen jaren was jij er altijd zowel op werk als bij onze vele uitjes. Je bent een hele goede vriendin van me geowrden en ik ben altijd blij als we samen op pad zijn.

Rozanna, jij was een van mijn muziek-buddies op de kamer. Het was altijd gezellig als jij er was en ondanks dat ik het je volledig gun dat je het geluk in Schotland hebt gevonden, had ik je liever hier in buurt gehouden. Door de jaren heen ben je een van mijn beste vriendinnen geworden en ik ben daarom ook erg bij dat je nog regelmatig deze kant op reist. En ook ik kom zeker binnenkort weer naar Edinburgh!

Naast mijn roommates en supervisoren hebben er natuurlijk nog veel meer mensen ondersteuning geboden tijdens mijn promotie: in het bijzonder Laurens en Mart. Ik heb jullie vele mailtjes gestuurd met vragen om hulp als ik het niet alleen af kon. En jullie stonden altijd klaar om te helpen.

Mijn co-auteurs, met in het bijzonder Sebastian en Maarten, wil ik bedanken voor de fijne samenwerking. Ronnie, jou wil ik graag bedanken voor alle nuttige commentaren die je mij hebt toegestuurd.

Juan Antonio and Alexandra, I would very much like to thank you both for helping out with my hEPI pilot project.

My Borrel buddies: Rozanna, Rebecca, Ewoud, Hakim, Marcel, Mattias, Joost and Gabriela. Throughout the years we have organized many succesful ‘borrels’, I would say.

Olga en Roos, mijn beste vriendinnen en metalbuddies, heel erg bedankt voor alle leuke momenten de afgelopen jaren. Ik kan altijd op jullie rekenen en we hebben altijd zoveel lol samen. En eigenlijk vallen Alex, Tai-Pau en Oscar als mede-Wackengangers natuurlijk ook onder metalbuddies tegenwoordig!

Lieve Anouk, wij gaan al jaren dezelfde richting op en dat maakt dat we altijd samen in onbegrijpelijk radiologische taal kunnen praten terwijl iedereen om ons heen zich afvraagt of het wel goed met ons gaat. Je bent een van mijn beste vriendinnen en wie weet worden we ooit nog eens directe collega’s.

Pauline, we kennen elkaar al sinds de brugklas en zijn daarmee al zolang goede vriendinnen. Ik vind het jammer dat je tegenwoordig zo'n stuk bij ons vandaan woont, maar ik gun het je van harte. Dank je wel dat ik af en toe bij jou kon uitblussen.

Iedereen van de Osse groep: het is altijd gezellig om samen op pad te zijn, thema-oudjaarsavonden te vieren en jaarlijks een weekend met zijn allen in een villa te spenderen.

Dennis en Gabriella (en DJ), we zien elkaar regelmatig en het is altijd supergezellig. Altijd als onze speelgoed-magneetballetjes in de kast zie liggen waar DJ zo graag mee speelt, denk ik aan jullie.

Aan Pat's Horsewives, we hebben jarenlang zo'n leuke les samen gehad. Ik vind het zo jammer dat dit niet houdbaar was op de lange termijn. Gelukkig gaan we nog samen op buitenrit naar de Drunense duinen: ik zie nog Roos op het Ravelijnpaard steigeren in de duinen. Het was echt zo gaaf om dat samen mee te maken.

Mijn tweede paranimf, mijn zusje Ninke: bedankt dat je mij wilt komen ondersteunen tijdens deze laatste fase van mijn promotie ondanks alle drukte thuis met 2 kleine meiden. Het was voor mij niet meer dan vanzelfsprekend om jou hiervoor te vragen, je bent mijn lieve zusje. Ondanks dat je als dierenarts hele andere ziekten en problemen tegenkomt dan ik als 'mensen'-arts, blijken er toch altijd opvallend veel overeenkomsten te zijn.

Lieve pap en mam, jullie hebben mij al die jaren gesteund en mij alle mogelijkheden gegeven om tot dit punt in mijn leven te komen. Jullie hebben mij het zelfvertrouwen gegeven waardoor ik nooit getwijfeld heb of ik wel arts kon worden, of radioloog, of mijn PhD zou kunnen voltooien. Ik heb teveel aan jullie te danken om alles hier op te schrijven, maar zal volstaan door te zeggen dat ik heel veel van jullie hou.

Ook van jou oma, heb ik veel geleerd en ik vind het fantastisch dat je altijd enthousiast en geïnteresseerd bent in alles wat ik doe. Je bent een top-oma!

Mijn schoonfamilie, Jan, Janet, Ilse en Joyce, wat fijn dat we het zo goed met elkaar kunnen vinden. Ilse, als ik weer naar Chicago ga, ga je vast weer mee toch?

En 'last but not least', Alex, je bent er altijd voor mij en zoals je zelf ook vaak zegt: ik heb je nodig. Dank je wel dat ik (bijna) nooit hoef te koken en dat je altijd tijd voor me maakt. We hebben zo onderhand al veel samen meegemaakt en ik ben ervan overtuigd dat we ook in de toekomst nog veel avonturen zullen beleven samen (zolang Poezeltje maar geen grasspriet inhaleert).

# LIST OF PUBLICATIONS

## Book Chapter

**Gahrmann R**, Arbizu J, Morales Lozano MI, Laprie A, Smits M. Imaging and Interventional Radiology for Radiation Oncology. Chapter 26: Response evaluation and follow-up by imaging in brain tumors. Springer Nature. *Not yet published*.

## Papers

**Gahrmann R**, van den Bent MJ, van der Holt B, Vernhout RM, Taal W, Vos M, de Groot JC, Beerepoot LV, Buter J, Flach ZH, Hanse M, Jasperse B, Smits M. Comparison of 2D (RANO) and volumetric methods for assessment of recurrent glioblastoma treated with bevacizumab – a report from the BELOB trial. Neuro Oncol (2017) 19(6):853-861.

**Gahrmann R**, Spoor JKH, Wijnenga MMJ, Leenstra S, Vincent AJPE, de Groot M, French PJ, van den Bent MJ, Smits M. Growth patterns of non-enhancing glioma assessed on DTI-derived isotropic and anisotropic maps are not associated with IDH mutation or 1p19q codeletion status. *Submitted*.

**Gahrmann R**, Smits M, van der Holt B, Vernhout RM, Taal W, de Groot JC, Hanse MCJ, Vos MJ, Beerepoot LV, Buter J, Flach ZH, Kapsas G, van den Bent MJ. The impact of volumetric thresholds to determine progressive disease in patients with recurrent glioblastoma treated with bevacizumab. *Ready for submission*.

**Gahrmann R**, Leemans A, van der Holt B, Vernhout RM, Taal W, Bromberg JEC, Vos MJ, de Groot JC, Hanse MCJ, van den Bent MJ, Smits M. The value of apparent diffusion coefficient in predicting response after the first course of treatment with bevacizumab and lomustine in recurrent glioblastoma. *Submitted*.

## Co-author papers

Wijnenga MMJ, French PJ, Dubbink HJ, Dinjens WNM, Atmodimedjo PN, Kros JM, Smits M, **Gahrmann R**, Rutten GJ, Verheul JB, Fleischeuer R, Dirven CMF, Vincent AJPE, van den Bent MJ. The impact of surgery in molecularly defined low-grade glioma: an integrated clinical, radiological and molecular analysis. Neuro Oncol 2018;20(1):103-112.

Ellingson BM, Gerstner ER, Smits M, Huang RY, Colen R, Abrey LE, Aftab DT, Schwab GM, Hessel C, Harris RJ, Chakoyan A, **Gahrmann R**, Pope WB, Leu K, Raymond C, Woodworth DC, de Groot J, Wen PY, Batchelor TT, van den Bent MJ, Cloughesy TF. Diffusion MRI is a predictive imaging biomarker of survival benefit from anti-VEGD monotherapy in recurrent glioblastoma: combined evidence from phase II trials. Clin Cancer Res 2017;23(19):5745-5756.

## LIST OF PRESENTATIONS

**Gahrmann R**, Burke M, Fernandez B, van den Bent MJ, Smits M. Clinical implementation of hybrid echo-planar perfusion imaging (hEPI) for the assessment of glioma. *ESMRMB 2015, Edinburgh.*

**Gahrmann R**, Burke M, Fernandez B, van den Bent MJ, Smits M. Clinical implementation of hybrid echo-planar perfusion imaging (hEPI) for the assessment of glioma. *Radiologendagen 2015, Rotterdam.*

**Gahrmann R**, Burke M, Fernandez B, van den Bent MJ, Smits M. Clinical implementation of hybrid echo-planar perfusion imaging (hEPI) for the assessment of glioma. *ONWAR annual meeting 2015, Zeist.*

**Gahrmann R**, van den Bent MJ, van der Holt B, Vernhout RM, Taal W, Taphoorn MJB, de Groot JC, Beerepoot LV, Jasperse B, Smits M. Radiological response assessment in the era of bevacizumab: RANO or volumetry? A report from the BELOB trial. *EANO, 2016, Mannheim.*

**Gahrmann R**, van den Bent MJ, van der Holt B, Vernhout RM, Taal W, Taphoorn MJB, de Groot JC, Beerepoot LV, Buter J, Flach Z, Hanse M, Jasperse B, Smits M. Radiological response assessment in the era of bevacizumab: RANO or volumetry? A report from the BELOB trial. *ESMRMB, 2016, Vienna.*

*Accepted application for Student Support Program: the ESMRMB will waive the registration fee and additionally provide a contribution to hotel and travel expenses of EUR 200.*

**Gahrmann R**, van den Bent MJ, van der Holt B, Vernhout RM, Taal W, Taphoorn MJB, de Groot JC, Beerepoot LV, Buter J, Flach Z, Hanse M, Jasperse B, Smits M. Radiological response assessment in the era of bevacizumab: RANO or volumetry? A report from the BELOB trial. *ONWAR annual meeting 2016, Zeist.*

**Gahrmann R**, Spoor JKH, Vincent AJPE, Leenstra S, de Groot M, Wijnenga MMJ, French PJ, van den Bent MJ, Smits M. Groeipatronen van niet-aankleurende gliomen gemeten op DTI-afgeleide isotrope en anisotrope maps zijn niet geassocieerd met IDH en 1p19q codeletie status. *LWNO 2017, Utrecht.*

**Gahrmann R**, van den Bent MJ, van der Holt B, Vernhout RM, Taal W, de Groot JC, Vos M, Buter J, Flach HZ, Hanse M, Smits M. Establishing the optimal volumetric threshold for determining progressive disease in patients with recurrent glioblastoma. *RSNA 2017, Chicago.*

*Accepted application for Student Travel Award for young investigators. Top-rated scientific abstract to receive a $500 stipend to attend the 2017 Annual Meeting.*

**Gahrmann R**, Spoor JKH, Wijnenga MMJ, Leenstra S, Vincent AJPE, de Groot M, French PJ, van den Bent MJ, Smits M. Growth patterns of non-enhancing glioma assessed on DTI- derived isotropic and anisotropic maps are not associated with IDH and 1p19q codeletion status. *ISMRM Benelux, Antwerpen.*

**Gahrmann R**, Spoor JKH, Wijnenga MMJ, Leenstra S, Vincent AJPE, de Groot M, French PJ, van den Bent MJ, Smits M. Growth patterns of non-enhancing glioma assessed on DTI-derived isotropic and anisotropic maps are not associated with IDH and 1p19q codeletion status. *Joint Annual Meeting ISMRM-ESMRMB 2018, Paris.*

*Accepted application for Trainee (Educational) Stipend of US$50.00 cash plus waived six-day registration rate of US$475.00.*

# PhD PORTFOLIO

| | |
|---|---|
| Name PhD Candidate | Renske Gahrmann |
| Erasmus MC Departments | Radiology and Nuclear Medicine<br>Cancer Institute (Neuro-Oncology) |
| Research School | Graduate School of Neurosciences Amsterdam Rotterdam (ONWAR) |

| PhD Training | Location | Year | ECTS |
|---|---|---|---|
| ***Courses ONWAR*** | | | |
| Introductory course for PhD students | Amsterdam/NL | 2014 | 0.9 |
| Quantitative Methods | Amsterdam/NL | 2015 | 3.6 |
| Functional Neuro-anatomy | Amsterdam/NL | 2015 | 1.4 |
| Cognitive Neuroscience | Amsterdam/NL | 2015 | 1.1 |
| Annual Meeting | Zeist/NL | 2015 | 0.9 |
| Annual Meeting | Zeist/NL | 2016 | 0.9 |
| ***Courses Other*** | | | |
| OpenClinica | Rotterdam/NL | 2014 | 0.3 |
| Research Integrity Course | Rotterdam/NL | 2015 | 0.3 |
| ESMRMB School of MRI: Clinical fMRI and DTI - Theory and Practice | Basel/CH | 2015 | 0.7 |
| BSL/AED providor course, European Resuscitation Council | Rotterdam/NL | 2015 | 0.3 |
| Biostatistical Methods I: Basic Principles A (NIHES) | Rotterdam/NL | 2015 | 2.0 |
| One-day course on Neuro-Oncology | Utrecht/NL | 2015 | 0.3 |
| CEL Symposium: reproducibility, credibility, and validity | Rotterdam/NL | 2016 | 0.3 |
| ISMRM Workshop: Breaking the barriers of diffusion MRI | Lisbon/PT | 2016 | 1.1 |
| BROK | Rotterdam/NL | 2016 | 1.5 |
| 26th Annual Late Summer CT and MRI course on Neuroradiology | Maastricht/NL | 2017 | 0.3 |
| ***Conferences and Meetings*** | | | |
| Radiologendagen | Den Bosch/NL | 2014 | 0.6 |
| Symposium: Technological Breakthroughs in brain tumor treatment | Rotterdam/NL | 2014 | 0.15 |
| ISMRM Benelux | Ghent/BE | 2015 | 0.3 |
| Radiologendagen | Rotterdam/NL | 2015 | 0.7 |
| ESMRMB | Edinburgh/UK | 2015 | 0.9 |

| PhD Training | Location | Year | ECTS |
|---|---|---|---|
| ISMRM Benelux | Eindhoven/NL | 2016 | 0.3 |
| ESMRMB | Vienna/AT | 2016 | 1.0 |
| EANO | Mannheim/DE | 2016 | 1.6 |
| ISMRM Benelux | Tilburg/NL | 2017 | 0.3 |
| Regionale refereeravond Radiologie | Rotterdam/NL | 2017 | 0.07 |
| Endovascular thrombectomy in acute ischemic stroke | Rotterdam/NL | 2017 | 0.1 |
| LWNO | Utrecht/NL | 2017 | 0.4 |
| RSNA | Chicago/US | 2017 | 1.9 |
| ISMRM Benelux | Antwerpen/BE | 2018 | 0.4 |
| ISMRM-ESMRMB Joint Annual Meeting | Paris/FR | 2018 | 1.9 |
| Monthly research meetings in neuro-oncology | Rotterdam/NL | 2016-2018 | 0.3 |
| ***Teaching*** | | | |
| Training and supervision of medical students in semi-automated tumor segmentation | | 2014-2018 | 0.6 |
| and attendance of monthly joint meetings on neuro-imaging (BIGR, KNICR, AMBER and ART) | | 2015-2016 | 1.6 |
| Organization and attendance of monthly neuro-imaging meetings (AMBER) | | 2015-2017 | 3.0 |
| Organization and attendance of monthly neuro-oncology meetings | | 2016-2018 | 1.8 |
| Organization ‘meet the experts in MRI’ ESMRMB 2015 | | 2015 | 0.3 |
| | | **TOTAL** | **34.12** |

## ABOUT THE AUTHOR

Renske Gahrmann was born on December 28, 1985 in Leidschendam, The Netherlands. In 2004, she finished her secondary education at the Coornhert Gymnasium in Gouda. Renske then enrolled in medical school at the Erasmus Medical Center in Rotterdam. During these years Renske worked on a Master's project at the department of Radiology supervised by Prof. Dr. Marion Smits and completed a three-months long internship at the same department. In 2012 she started the residency program for Radiology at the Erasmus Medical Center and completed 2 years (of a 5 year program) before starting her PhD research. Her PhD thesis, 'MRI based response assessment and diagnostics in glioma', was supervised by Prof. Dr. Marion Smits and Prof. Dr. Martin van den Bent and was completed in 2019. During the final year of her PhD research, Renske continued with the residency program in Elisabeth-Tweesteden Hospital in Tilburg. Renske currently lives in Dordrecht with her partner Alex and will be continuing the residency program in the Erasmus Medical Center with special focus on Neuro, Head and Neck Radiology.